이학박사 학위논문

Texture analysis on the fluence map of intensity modulated beams to evaluate the plan delivery accuracy for quality assurance of patient treatment plans

세기변조 방사선치료 빔의 플루언스 분포도 질감분석을 통한 환자치료계획 정도관리 예측에 관한 연구

2016 년 2 월

서울대학교 대학원

방사선응용생명과학 협동과정

박 소 연

A thesis of the Degree of Doctor of Philosophy

세기변조 방사선치료 빔의 플루언스 분포도 질감분석을 통한 환자치료계획 정도관리 예측에 관한 연구

Texture analysis on the fluence map of intensity modulated beams to evaluate the plan delivery accuracy for quality assurance of patient treatment plans

February 2016

The Department of Interdisciplinary program in Radiation Applied Life Science,
Seoul National University
College of Medicine
So-Yeon Park

ABSTRACT

Purpose: The goal of this study is to evaluate the plan delivery accuracy of volumetric modulated arc therapy (VMAT) using texture analysis on the fluence map of VMAT.

Methods: Twenty prostate and twenty head-and-neck (H&N) VMAT plans from Trilogy™ with Millennium™ multi-leaf collimators (MLCs) (Varian Medical Systems, Palo Alto, CA, USA) were selected. Fluence maps were generated for each VMAT plan (1) by integrating spatial MU distributions defined by MLC apertures at each control point (CP), (2) by doubling the values (MUs) of pixels representing MLC tips, and (3) by taking summations of segments in sequential groups of CPs. A total of 6 textural features, which were *angular second moment* (*ASM*), *inverse difference moment* (*IDM*), *contrast*, *variance*, *correlation*, and *entropy*, were calculated from each fluence map generated from 20 prostate and 20 H&N VMAT plans. For each textural feature, the particular displacement distances (d) were 1, 5, and 10. To investigate the plan deliverability of each VMAT plan, gamma passing rates of pre-treatment quality assurance (QA), differences in modulating parameters such as MLC position, gantry angle, and monitoring unit (MU) between VMAT plans and dynamic log files registered by the linac control system during delivery, and differences in dose-volumetric parameters between VMAT plans and reconstructed plans using dynamic log files were acquired. To test the performance of textural features as indicators of modulation degree of VMAT plans, Spearman's rank correlation coefficients (r_s) for the plan

deliverability were calculated. For comparison purposes, conventional modulation indices for VMAT, i.e., the modulation complexity score for VMAT (MCS_v), the leaf travel modulation complexity score (LTMCS), and the modulation index supporting station parameter optimized radiation therapy (MI_{SPORT}) were calculated; their correlations were analyzed using the same method.

For the same 20 prostate and 20 H&N patients from Trilogy™ with Millennium™ MLCs, VMAT plans were generated using TrueBeam™ with high-definition MLC (Varian Medical Systems, Palo Alto, CA, USA). Gamma passing rates of pre-treatment QA, differences in modulating parameters, and differences in dose-volumetric parameters were acquired. To compare the performances between the two MLC systems, fluence maps and a total of 6 textural features were calculated at different displacement distances (d) of 1, 2, 3, 5, and 10. Then, their correlations were analyzed using the same method.

Results: In this study for the single fluence maps calculated using integrating spatial MU distributions defined by MLC apertures at each CP, there was no particular textural feature that consistently exhibited the best correlation for every type of plan deliverability. Taken together, the results for *contrast* (d = 1) and *variance* (d = 1) for Trilogy™ and *variance* (d = 1) for TrueBeam™ showed good correlations with every type of plan deliverability. These textural features showed consistently better performances than the conventional modulation indices, except for one case, namely, the modulating parameter differences. The r_s values of *contrast* (d = 1) for Trilogy™ for the

global gamma passing rates with criteria of 2%/2 mm, 2%/1 mm, and 1%/2 mm were 0.536, 0.473, and 0.718, respectively. The values of *variance* (d = 1) for Trilogy™ were 0.551, 0.481, and 0.688, respectively. The values of *variance* (d = 1) for TrueBeam™ were 0.662, 0.740, and 0.660, respectively. In the case of local gamma passing rates, the r_s values of *contrast* (d = 1) for Trilogy™ were 0.547, 0.578, and 0.620, respectively. Those of *variance* (d = 1) for Trilogy™ were 0.519, 0.527, and 0.569, respectively. Those of *variance* (d = 1) for TrueBeam™ were 0.403, 0.616, and 0.443, respectively. Every r_s value in these cases was statistically significant ($p < 0.004$). The values of r_s of *contrast* (d = 1) and *variance* (d = 1) for Trilogy™ and *variance* (d = 1) for TrueBeam™ with MLC errors were -0.863, -0.828, and -0.822, respectively, with statistical significance ($p < 0.001$). These results most frequently showed r_s values with statistical significance for the dose-volumetric differences.

In this study, using fluence maps calculated by doubling the values (MUs) of pixels representing MLC tips, the r_s values of *contrast* (d = 1) with edge-enhancement for Trilogy™ for global gamma passing rates of 2%/2 mm, 2%/1 mm, and 1%/2 mm were 0.546 ($p < 0.001$), 0.487 ($p = 0.001$), and 0.744 ($p < 0.001$), respectively. Those of *contrast* (d = 10) with edge-enhancement for TrueBeam™ were 0.705, 0.703, and 0.701, respectively (all with $p < 0.001$). The r_s values of *contrast* (d = 1) with edge-enhancement for Trilogy™ for local gamma passing rates of 2%/2 mm, 2%/1 mm, and 1%/2 mm were 0.588, 0.644, and 0.640, respectively (all with $p < 0.001$). Those of *contrast* (d = 10) with edge-enhancement for TrueBeam™ were 0.459 ($p < 0.001$), 0.700

($p < 0.001$), and 0.522 ($p = 0.001$), respectively. The r_s values of *contrast* (d = 1) for Trilogy™ for MLC and gantry angle errors were -0.853 and 0.655, respectively (all with $p < 0.001$). Those of *contrast* (d = 10) for TrueBeam™ were -0.722 ($p < 0.001$) and 0.333 ($p = 0.036$), respectively. *Contrast* (d = 1) for Trilogy™ and *contrast* (d = 10) for TrueBeam™ showed statistically significant r_s values in 11 and 4 dose-volumetric parameter differences, respectively, from a total of 35 cases. These contrasts showed generally better correlations with plan delivery accuracy than either (as previously suggested) textural features with non-edge-enhanced fluence maps or conventional modulation indices.

In this study of fluence maps calculated using summations of segments at sequential groups of control points, the values of r_s of *contrast* (d = 10) with 10 segments for Trilogy™ to both global and local gamma passing rates at 1%/2 mm were 0.692 ($p < 0.001$) and 0.798 ($p < 0.001$), respectively. The results showed r_s values of -0.895 ($p < 0.001$) and 0.727 ($p < 0.001$) for multi-leaf collimator positional errors and gantry angle errors during delivery, respectively. The number of statistically significant r_s values ($p < 0.05$) for the changes in dose-volumetric parameters during delivery was 14 from a total of 35 tested parameters. The values of r_s of *contrast* (d = 10) with 20 segments for TrueBeam™ for both global and local gamma passing rates of 1%/2 mm were 0.839 ($p < 0.001$) and 0.738 ($p < 0.001$), respectively. The results showed r_s values of -0.881 ($p < 0.001$) and 0.569 ($p < 0.001$) for multi-leaf collimator positional errors and gantry angle errors during delivery, respectively. The number of statistically significant r_s values ($p < 0.05$) for the

changes in dose-volumetric parameters during delivery was 8 among a total of 35 tested parameters.

Conclusions: *Contrast* (d = 10) with 10 segments calculated from segmental fluence maps of VMAT plans for Trilogy™ and *contrast* (d = 10) with 20 segments calculated from segmental fluence maps of VMAT plans for TrueBeam™ showed good correlations with the plan deliverability, indicating that they could be used as indicators for assessing the delivery accuracy of VMAT plans.

Keywords: Texture analysis, Fluence map, Volumetric modulated arc therapy, Degree of modulation, Modulation index, MLC system

Student number: 2012-30574

CONTENTS

LIST OF TABLES

LIST OF FIGURES

INTRODUCTION

Using technological improvements in radiation therapy, such as the advent of intensity modulated radiation therapy (IMRT) and volumetric modulated arc therapy (VMAT), it has become possible to deliver a prescription dose capable of controlling tumor volume while simultaneously minimizing the dose to the surrounding normal tissues.[1-6] The key feature of both VMAT and IMRT is the modulation of photon beam intensity.[2, 3] VMAT modulates the beam intensity by modulating three parameters simultaneously: multi-leaf collimator (MLC) movements, gantry rotation speed, and dose-rate at each control point (CP); whereas IMRT modulates only MLC movement.[2, 3] Although the beam intensity modulation of IMRT and VMAT make possible the delivery of a conformal dose to the target while sparing organs at risk (OAR), excessive modulation may result in the delivery of dose distributions to the patient that are different from the intended calculated dose distributions.[2, 5, 7-18] This issue is caused by increased uncertainties in the mechanical components of the linac caused by excessive movement and inaccurate dose calculations for small or irregular fields applied by the treatment planning systems (TPSs), the significance of which increases as the degree of modulation increases.[18] Therefore, excessive modulation of IMRT and VMAT may reduce the treatment efficacy and (potentially) cause severe complications for the patient. For this reason, pretreatment quality assurance (QA) for each patient treated with IMRT or VMAT is strongly recommended (and is routinely performed in the clinic) to identify undeliverable plans

before treatment.[2, 5] Studies have also been performed on the modulation index, which evaluates the degree of modulation of IMRT or VMAT plans to identify excessively modulated plans at the planning level.[7-20] The modulation index is more beneficial than pretreatment QA, as it can lead to early detection of undeliverable plans, resulting in saving those resources needed to perform pretreatment QA. Various studies on the modulation index have been performed for IMRT;[7, 10-13, 15-20] however, similar studies have been less frequent for VMAT.[8, 9, 14] Nicolini *et al.* previously demonstrated the robustness of gantry speed and dose-rate modulations of RapidArc (Varian Medical Systems, Palo Alto, CA, USA), a form of VMAT, using dynamic log files recorded by the linac control system.[14] Masi *et al.* applied the concept of the modulation complexity score (MCS), originally proposed by McNiven *et al.*,[11] to VMAT by proposing the modulation complexity score for VMAT (MCS_v) and the leaf travel modulation complexity score (LTMCS).[9] These indices evaluate the MLC motion variability and MLC aperture variability. Li and Xing proposed a modulation index for VMAT to support the concept of station parameter optimized radiation therapy (SPORT) introduced by the authors, which is an evaluation tool for MLC modulation weighted by segmental monitor units (MUs) for gantry angle.[8]

Unlike feasibility studies on modulation indices for VMAT,[8, 9, 14] in this study, we focused on the fluence maps generated by VMAT plans. We performed texture analysis on the fluence maps to assess the degree of modulation of VMAT plans. Texture analysis has been widely applied in the medical imaging field for the identification of tumors, automatic organ

contouring, and various other applications.[21-23] Recently, textural features of a parotid gland injury induced by radiation therapy for head and neck (H&N) cancer were analyzed to obtain a predictor of parotid shrinkage due to radiation therapy.[24, 25] Another study analyzed textural features to predict tumor recurrence after stereotactic ablative radiotherapy (SABR) for lung cancer.[26] In this study, we analyzed second-order statistical textural features of fluence maps generated from prostate and H&N VMAT plans based on the gray level co-occurrence matrix (GLCM) under the assumption that the fluence maps of highly modulated VMAT plans might have different textural features than those of less modulated plans. In a feasibility study, a single fluence map was generated by integration of all MUs shaped by MLC apertures (MU maps) at each CP to quantify the modulation degree of VMAT.

Although we can demonstrate strong correlations of textural features calculated from a single fluence map with the discrepancy between plan and delivery in the feasibility study, several small or irregular fields at different CPs could be smeared out when fluence maps were generated by the integration of differently shaped MU maps. For example, if several small fields with the same MU, which could cause discrepancy between plan and delivery, are contained in a VMAT plan at different CPs, and if those small fields create a single large field when they are integrated, the small fields cannot be identified in a fluence map generated by the integration of every MU map. If we can distinguish every small field in a fluence map, textural features calculated using said fluence map might be better able to quantify the modulation degree of VMAT.

In this study, we attempted to distinguish all of the small fields in the fluence map of a VMAT plan so as to calculate textural features while considering every aperture at each CP using two methodologies for generating the fluence maps. In the first method, which considered every small field in a fluence map, we enhanced the values of edges shaped by MLCs at each CP in a fluence map. We tested the performance of the textural features (calculated using edge-enhanced fluence maps) using correlation analysis, and compared the results both to the indices suggested in our feasibility study and to the conventional set of modulation indices suggested for VMAT.[8, 9, 27, 28] However, the fluence maps with edge-enhancement were generated by artificially doubling the values (MUs) on the MLC tips at each CP. This technique could result in image distortion of edge-enhanced fluence maps in extreme situations. In the second technique, considering every small field in a fluence map and no image distortion, we generated various fluence maps with various numbers of segments from 5 to 356 for each VMAT plan and calculated textural features from the fluence maps. Correlation analysis of the textural features with the plan delivery accuracy was performed to compare the performance of each textural feature calculated to various segmental fluence maps. We investigated which textural feature showed the highest correlation with the plan delivery accuracy so as to suggest a textural feature as a modulation index for VMAT.

The plan deliverability was investigated by 1) performing pretreatment QA with a 2D detector array, 2) comparing modulating parameters from the original VMAT plans to those from the dynamic log files recorded by the

linac system during actual delivery, and 3) comparing dose-volumetric parameters from the original VMAT plans to those from the plans reconstructed from dynamic log files. Next, correlations of the textural features extracted from the fluence maps with the plan deliverability were investigated using the Spearman's rank correlation coefficients (r_s). For comparison purposes, the correlations of the conventional modulation indices [such as MCS_v, LTMCS, and modulation index suggested by Li and Xing (MI_{SPORT})] with the plan deliverability were also analyzed.[8, 9] The receiver operating characteristic (ROC) curves were analyzed to investigate the sensitivity and specificity of the textural features and the conventional modulation indices.

MATERIALS AND METHODS

II.A. VMAT plans for prostate and H&N cancer

After approval from an institutional review board (IRB, Seoul National University Hospital Human Research Protection Program Center), among patients previously treated with VMAT technique in our institution, 20 patients with prostate cancer and 20 patients with H&N cancer were chosen retrospectively for this study (IRB No. H-1512-113-729). Every VMAT plan using Trilogy^{TM} with Millennium^{TM} MLC (Varian Medical Systems, Palo Alto, CA, USA) and TrueBeam^{TM} with High-definition MLC (Varian Medical Systems, Palo Alto, CA, USA) was generated in the Eclipse system (Varian Medical Systems, Palo Alto, CA, USA) with the progressive resolution optimizer 3 (PRO3, ver. 10, Varian Medical Systems, Palo Alto, CA, USA). The dose distributions were calculated using the anisotropic analytic algorithm (AAA, ver.10, Varian Medical Systems, Palo Alto, CA, USA) with a calculation grid of 2.5 mm. For the planning and delivery, 2 full arcs using 2 different MLC systems were used. The prostate VMAT plans consisted of a primary plan with a prescription dose of 50.4 Gy for both prostate and seminal vesicles as a target volume and a boost plan with a prescription dose of 30.6 Gy for the prostate as a target volume. Only primary plans were analyzed for this study. The H&N VMAT plans were generated with simultaneously integrated boost (SIB) technique with a total of 3 target volumes (target 1, target 2 and target 3). The prescription doses for the target volumes of prostate VMAT plans, target 1, target 2 and target 3 of H&N VMAT plans were 81 Gy

(1.8 Gy/fraction), 67.5 Gy (2.25 Gy/fraction), 54 Gy (1.8 Gy/fraction) and 48 Gy (1.6 Gy/fraction), respectively.

II.B. Generation of fluence maps

II.B.1. Generation of a single fluence map

Each VMAT plan was exported in DICOM format (DICOM-RT files) from the Eclipse system. The information on MLC positions and corresponding MUs at each CP were extracted from the DICOM-RT files. By integrating spatial MU distributions defined by MLC apertures at each CP, a fluence map for each VMAT plan was generated with an in-house program written in Matlab (ver. 8.1, Mathworks Inc., Natick, MA, USA). Although the widths of Millennium^{TM} MLC were 5 mm and 10 mm and the widths of High-definition MLC were 2.5 mm and 5 mm, the resolution of the fluence map was set to be 1 mm in this study for the consideration of MLC movement with fine resolution. The MUs of H&N VMAT plans were generally larger than those of prostate VMAT plans in this study. Since the magnitude of MUs in the fluence map influence map the size of the GLCM, the fluence maps were normalized such that each pixel in the fluence map (*i.e.* beamlet) had a gray level ranging from 0 to 127 in order to eliminate the effect of MU differences on textural features. In other words, the number of quantized gray levels (N_g) of each fluence map was 128.

II.B.2. Fluence map with edge-enhancement

When integrating MU maps, the values (MUs) of pixels (size of 1 mm × 1

mm) representing MLC tips were doubled (edge-enhancement of fluence map). The goal of this was to distinguish individual small fields at different CPs contained in a single VMAT plan. Unlike IMRT, MLCs of VMAT moves in and out continuously during beam delivery,[29] therefore, if we enhance the edges of MU maps parallel to the direction of MLC movement, excessively high values would be assigned at that region in a fluence map. Since this could be a disturbance factor of texture analysis, and small (or irregular) fields could be identified without edge-enhancement of this region, the edges parallel to the MLC moving direction were not enhanced, but the edges perpendicular to the direction of MLC movement (*i.e.* MLC tip) were enhanced. Consequently, the edge-enhanced fluence maps showed a lot of short discrete lines perpendicular to the direction of MLC movement, in contrast to the relatively smoother fluence maps without edge-enhancement.

II.B.3. Segmental fluence maps

Since PRO3 uses a total of 178 CPs per each full arc and all VMAT plans in this study used 2 full arcs for 2 different MLC systems, a total of 356 MU maps were generated for each VMAT plan.[29] Fluence maps for each VMAT plan were generated by integration of sequences of 5, 10, 20, 45, 90, 178 and 356 MU maps. Since the total number of CPs per arc, 178, is not divisible by 5, 10, 20, 45 and 90, the remaining MU maps after division of 178 were included in the last fluence map under the assumption that the results would not be significantly affected. Various numbers of fluence maps were generated for each VMAT plan according to the number of CPs integrated.

For example, 2 fluence maps per VMAT plan were generated in the case of integration of 178 MU maps, while 70 fluence maps per VMAT plan were generated for the integration of 5 MU maps. The fluence maps generated with 356 segments were identical to those analyzed in the feasibility study by the authors, and data from those fluence maps are also presented in this study for comparison purposes.[28] Since the value of the maximum MU in the fluence map varied, each fluence map was normalized such that the maximum value would be 127 to eliminate the effect of MU differences on the values of textural features in the same way.

II.C. Textural features from fluence maps

II.C.1. Generation of GLCM

A 2D matrix indicating the intensity relationships between pairs of pixels in the image, known as a GLCM, where the number of rows and columns is the same as N_g, was generated for each fluence map.[24] Since there were numerous beamlets with values of 0 in the fluence maps due to not being irradiated during VMAT delivery, a region of interest (ROI) was defined as an area which only included beamlets having values larger than 1. When generating the GLCM, values of 1, 5 and 10 for Trilogy™ and values of 1, 2, 3, 5 and 10 for TrueBeam™ were chosen as particular displacement distances (d) and for each value of d, values of 0°, 45°, 90° and 135° were chosen as angles (θ) indicating search directions of the intensity relationship in the fluence map. An example of the generation of a GLCM with d and θ values is shown in Fig. 1.

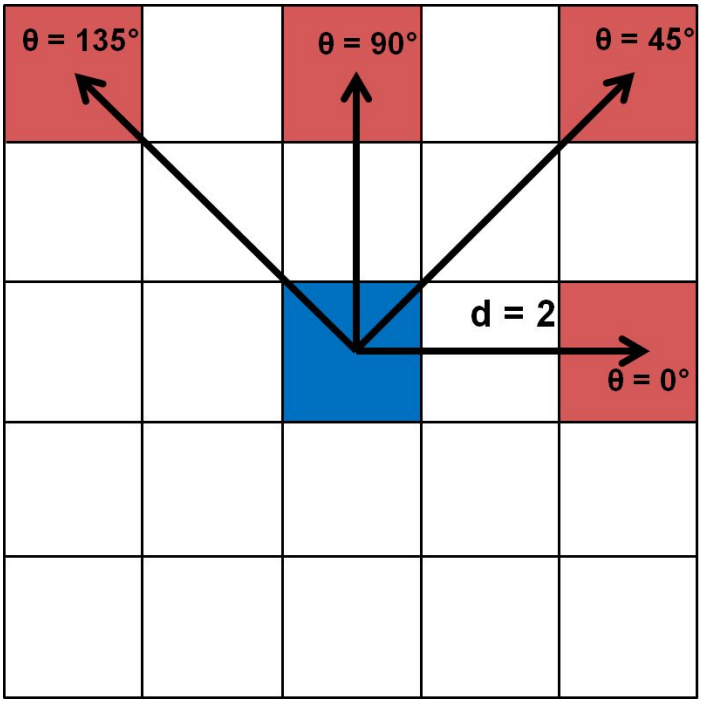

FIG. 1. An example to show determination of the matrix elements of gray level co-occurrence matrix (GLCM) with particular displacement distance (d) and angles (θ) is shown. In this case, the value of d was chosen as 2 while the values of θ were chosen as 0°, 45°, 90° and 135°.

The choice of values of 1, 5 and 10 for Trilogy™ as particular displacement distances means the relationships between pairs of pixels in the fluence map were investigated at the distance of 1 mm, 5 mm and 10 mm ($\sqrt{2}$ mm, $5\sqrt{2}$ mm and $10\sqrt{2}$ mm for diagonal direction) the resolution of fluence map was 1 mm in this study. The value of 1 mm was chosen to coincide with the resolution of the fluence map, while the values of 5 mm and 10 mm were chosen to coincide with the width of the Millennium™ MLC. The particular displacement distances should be used only as an integer and one of the widths of High-definition MLC was 2.5 mm. For that reason, values of 2 and 3 were additionally selected while value of 1, 5 and 10 were chosen for TrueBeam™ to compare with the same particular displacement distances for Trilogy™. With these combinations of *d* and θ, the matrix element *p(i,j)* of the gray level co-occurrence matrix, which indicates the intensity relationships between pairs of pixels in the 2D image, was defined as follows:

$$\boldsymbol{p(i,j)} = \frac{\boldsymbol{C(i,j)}}{\sum_{\boldsymbol{i=0}}^{\boldsymbol{Ng-1}} \sum_{\boldsymbol{j=0}}^{\boldsymbol{Ng-1}} \boldsymbol{C(i,j)}} \quad (1)$$

where *C(i,j)* is the number of occurrences of gray levels *i* and *j* within a window of *d* and θ. Therefore, a total of 12 GLCMs were generated for each fluence map.

The means (μ) and standard deviations (σ) for the columns and rows were defined as follows:[24]

$$\boldsymbol{\mu_x} = \sum_{\boldsymbol{i=0}}^{\boldsymbol{N_g-1}} \sum_{\boldsymbol{j=0}}^{\boldsymbol{N_g-1}} \boldsymbol{i \cdot p(i,j)} \quad (2)$$

$$\boldsymbol{\mu_y} = \sum_{\boldsymbol{i=0}}^{\boldsymbol{N_g-1}} \sum_{\boldsymbol{j=0}}^{\boldsymbol{N_g-1}} \boldsymbol{j \cdot p(i,j)} \quad (3)$$

$$\boldsymbol{\sigma_x = \sum_{i=0}^{N_g-1}\sum_{j=0}^{N_g-1}(i-\mu_x)^2 \cdot p(i,j)} \quad (4)$$

$$\boldsymbol{\sigma_y = \sum_{i=0}^{N_g-1}\sum_{j=0}^{N_g-1}(j-\mu_y)^2 \cdot p(i,j)} \quad (5)$$

II.C.2. Textural features

A total of 6 textural features were calculated based on the acquired GLCM to evaluate the degree of modulation of VMAT plans. The calculated textural features were *angular second moment* (*ASM*, also known as energy), *inverse difference moment* (*IDM*), *contrast*, *variance*, *correlation* and *entropy*.

The *ASM,* which is a measure of homogeneity of a fluence map, was calculated as follows:[30]

$$\boldsymbol{ASM = \sum_{i=0}^{N_g-1}\sum_{j=0}^{N_g-1} p(i,j)^2} \quad (6)$$

The *IDM* measures the local homogeneity of a fluence map.[24, 25] We calculated *IDM* as follows:

$$\boldsymbol{IDM = \sum_{i=0}^{N_g-1}\sum_{j=0}^{N_g-1} \frac{1}{1+|i-j|} p(i,j)} \quad (7)$$

The *contrast* which is a measure of the local variations in a fluence map was calculated as follows:

$$\boldsymbol{Contrast = \sum_{i=0}^{N_g-1}\sum_{j=0}^{N_g-1} p(i,j) \cdot |i-j|^2} \quad (8)$$

The *variance* measures the inhomogeneity in a fluence map. We calculated variance as follows:

$$\boldsymbol{Variance = \sum_{i=0}^{N_g-1}\sum_{j=0}^{N_g-1}(i-u_x)^2 \cdot p(i,j) + \sum_{i=0}^{N_g-1}\sum_{j=0}^{N_g-1}(j-u_y)^2 \cdot p(i,j)} \quad (9)$$

The *correlation* is a measure of the linear dependency of gray levels. We calculated correlation as follows:

$$\boldsymbol{Correlation} = \frac{\sum_{i=0}^{N_g-1}\sum_{j=0}^{N_g-1}(i-u_x)\cdot(i-u_y)\cdot p(i,j)}{\sigma_x\sigma_y} \quad (10)$$

The *entropy,* which is a measure of a randomness of a fluence map, was calculated as follows:

$$\boldsymbol{Entropy} = -\sum_{i=0}^{N_g-1}\sum_{j=0}^{N_g-1} p(i,j)\cdot log(p(i,j)) \quad (11)$$

For each value of *d*, a total of 4 textural features according to the value of θ (0°, 45°, 90° and 135°) were calculated. Those 4 textural features were averaged for each value of *d*, thus a total of 18 textual features were calculated for each VMAT plan in the case of a single fluence map and edge-enhanced fluence map for Trilogy™ (a total of 30 textural features for TrueBeam™). For segmental fluence maps, since a total of 3 values of *d* were used to calculate each type of textural feature, and the tested number of segments to generate the fluence map was seven (5, 10, 20, 45, 90, 178 and 356 segments), a total of 126 textural features were calculated (7 types of segment numbers × 6 types of textural features × 3 values of *d*) for Trilogy™ (a total of 210 textural features for TrueBeam™). Tendencies of changes in each textural feature according to the degree of modulation with simple fluence maps are shown in Fig. 2.

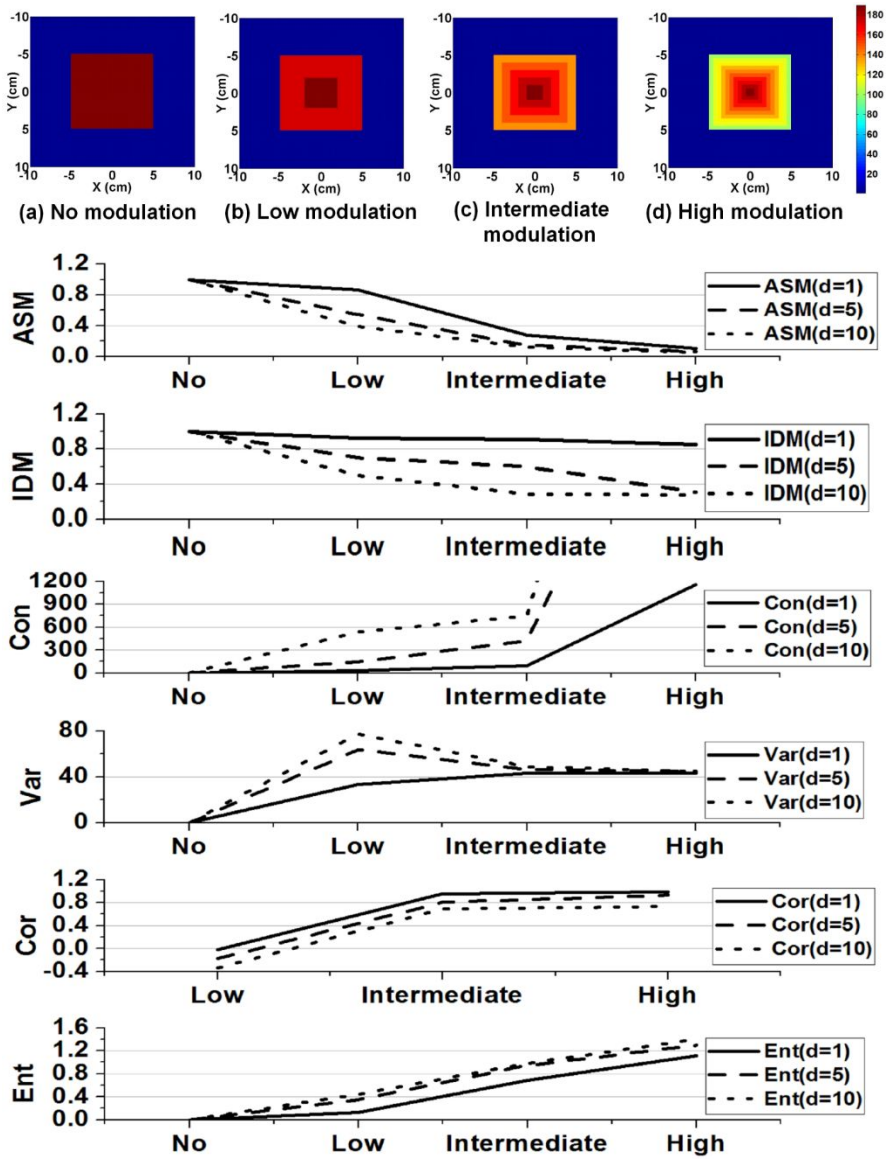

FIG. 2. Tendencies of changes in each textural feature according to the degree of modulation with simple fluence maps are shown. The changes in values of angular second moment (ASM), inverse difference moment (IDM), contrast (Con), variance (Var), correlation (Cor) and entropy (Ent) are shown for each value of particular displacement distance (1, 5 and 10).

II.D. Plan deliverability of VMAT

II.D.1. 2D pretreatment QA

2D dose distributions of each VMAT plan were acquired with a MapCHECK2 detector array (Sun Nuclear Corporation, Melbourne, FL, USA). The MapCHECK2 was inserted into a MapPHAN (Sun Nuclear Corporation, Melbourne, FL, USA) when performing pretreatment QA. Rather than taking CT images of the MapCHECK2 inserted into the MapPHAN, a virtual water phantom was generated in the Eclipse system and used for the calculation of reference 2D dose distributions. Since the physical thickness of the MapCHECK2 system is different from the radiological thickness of water due to it having a different electron density than that of water, the CT number of the virtual water phantom was assigned as 455 instead of 0 following manufacturer recommendations. Using the virtual water phantom, the dose distributions of each VMAT plan were calculated with a calculation grid of 1 mm. Before delivering pretreatment QA plans, the relative responses of each detector in the MapCHECK2, as well as the absolute response of the detector to the known dose was calibrated. The absolute dose of Trilogy was also calibrated according to the American Association of Physicists in Medicine (AAPM) Task Group 51 (TG-51) protocol.[31] After calibration, both global and local gamma evaluations were performed with SNC patient software (ver. 6.1.2, Sun Nuclear Corporation , Melbourne, FL, USA). Gamma criteria of 2%/2 mm, 2%/1 mm and 1%/2 mm were used with 10% as a threshold value for the ROI. We adopted a threshold value of 10% as that value is typically sited in the literature.[32-34]

Additionally, Gafchromic® EBT3 film (Ashland ISP Advanced. Materials, NJ) which is high spatial resolutions 2D detector were used for another pre-treatment QA. Very high spatial resolution allows for better verification in using small width of MLC. Among patients verified with MapCHECH2 in this study, 5 patients with prostate cancer and 5 patients with H&N cancer which had similar value of gamma passing rates between Trilogy™ and TrueBeamTM in all gamma criteria were selected for this pre-treatment QA. The films were positioned between two 5-cm solid water phantoms at a source-to-axis distance of 100 cm during pretreatment QA plans delivery. For absolute dose measurement with film, Gafchromic® EBT3 films were calibrated, based on the fading time of 24 h in Trilogy. The dose distributions of each VMAT plan were calculated with a calculation grid of 1 mm using CT image of 10-cm solid water phantom. Global gamma evaluations were performed with gamma criteria of 2%/2 mm, 2%/1 mm and 1%/2 mm and a threshold value of 10% for the ROI with Verisoft® software.

II.D.2. Differences in modulating parameters between VMAT plans and machine log files

A machine log file is a record of actual information of modulating parameters such as MLC positions, gantry angles and MU. For the Varian's linac systems, different recording systems are used. A dynamic log file, which is a record generated by the linac control system of modulating parameters such as gantry angles and MUs at each CP, was acquired during delivery of pretreatment QA. A DynaLog file, which is a record of MLC positions every

50 ms during delivery, was also acquired. These 2 machine log files were obtained from Trilogy™ with Millennium™ MLC. A trajectory file, which is generated in a binary format including modulating parameter with an update rate of 20 ms instead of the 50 ms for DynLog file, were acquired from TrueBeam™ STx with High-definition MLC. A DICOM-RT format file based on the machine log file information was generated by combining the two log files with an in-house program written in Matlab (ver. 8.1, Mathworks Inc., Natick, MA, USA). The MLC positions, gantry angles and MUs from the VMAT plans were compared to those from the DICOM-RT format log files at each CP and the differences were averaged for each VMAT plan.

II.D.3. Differences in dose-volumetric parameters between VMAT plans and reconstructed VMAT plans with DICOM-RT format log files

The DICOM-RT format log files were imported to the Eclipse system and the dose distributions in patient CT images were calculated with a calculation grid of 2.5 mm. For the target volume, dose-volumetric parameters such as dose received by 95% of the target volume ($D_{95\%}$), $D_{5\%}$, the minimum dose, the maximum dose and mean dose were compared between the VMAT plans and the reconstructed VMAT plans with log files. For organs at risk (OARs) in the prostate VMAT plans, $D_{20\%}$ of the rectal wall and bladder, $D_{50\%}$ of the femoral head and mean dose to the rectal wall, bladder and femoral head were compared. For the H&N VMAT plans, the maximum dose to the spinal cord, brain stem, each lens, optic chiasm and each optic nerve, as well as mean dose to each parotid gland were compared.

II.E. Data analysis

The correlations between the values of textural features and the plan deliverability (pretreatment QA results, modulating parameter differences and the dose-volumetric parameter differences) were analyzed using Spearman's rank correlation coefficients (r_s) with corresponding p values. For comparison purposes, the conventional modulation indices (MCS_v, LTMCS and MI_{SPORT}) were calculated and the correlations to the plan deliverability were analyzed for each VMAT plan. The sample sizes for the correlation analysis of pretreatment QA and modulating parameter differences were both 40, and included both prostate and H&N VMAT plans. In the case of dose-volumetric parameter differences, the sample size was 20 since the OARs were different between prostate and H&N VMAT plans.

To compare the textural features to the conventional modulation indices in t erms of the sensitivity and the specificity as an indicator of modulation degree for VMAT plans, ROC curves and the area under the curve (AUC) were acq uired.

RESULTS

III.A. Textural features and conventional modulation indices

III.A.1. Textural features calculated from a single fluenece map and conventional modulation indices

For Trilogy™, calculated values of textural features for a single fluence map according to *d* values of 1, 5 and 10, and also conventional modulation indices are shown in Table 1. In the same way, calculated values of textural features for a single fluence map according to *d* values of 1, 2, 3, 5 and 10, and also conventional modulation indices for TrueBeam™ are shown in Table 2.

TABLE 1. Textural features calculated from a single fluenece map and conventional modulation indices for Trilogy™

Textural features									
	$d = 1$			$d = 5$			$d = 10$		
	Prostate	H&N	p	Prostate	H&N	p	Prostate	H&N	p
ASM ($\times 10^{-3}$)	1.71 ± 0.27	1.08 ± 0.25	< 0.001	2.20 ± 0.48	0.84 ± 0.25	< 0.001	3.03 ± 0.64	0.99 ± 0.45	< 0.001
IDM	0.27 ± 0.02	0.32 ± 0.02	< 0.001	0.11 ± 0.01	0.16 ± 0.02	< 0.001	0.08 ± 0.01	0.12 ± 0.01	< 0.001
Contrast	252.86 ± 63.90	108.62 ± 49.02	< 0.001	1149.75 ± 245.04	380.63 ± 153.17	< 0.001	2096.51 ± 451.88	607.10 ± 249.72	< 0.001
Variance	50.31 ± 3.75	39.72 ± 6.65	< 0.001	51.23 ± 3.98	40.90 ± 7.07	< 0.001	50.96 ± 4.83	41.35 ± 7.13	< 0.001
Correlation	0.90 ± 0.02	0.93 ± 0.01	< 0.001	0.59 ± 0.05	0.79 ± 0.04	< 0.001	0.30 ± 0.14	0.69 ± 0.06	< 0.001
Entropy	2.92 ± 0.06	3.18 ± 0.09	< 0.001	2.86 ± 0.08	3.30 ± 0.11	< 0.001	2.71 ± 0.10	3.28 ± 0.14	< 0.001

Conventional modulation indices			
	Prostate	H&N	p
MCS_v	0.59 ± 0.07	0.51 ± 0.07	< 0.001
LTMCS	0.39 ± 0.06	0.23 ± 0.06	< 0.001
MI_{SPORT}	4250 ± 645	17132 ± 3054	< 0.001

Abbreviations: d = particular displacement distance, Prostate = volumetric modulated arc therapy plans for prostate cancer, H&N = volumetric modulated arc therapy plans for head and neck cancer, ASM = angular second moment, IDM = inverse difference moment, MCS_v = modulation complexity score for VMAT, LTMCS = leaf travel modulation complexity score, MI_{SPORT} = modulation index supporting station parameter optimized radiation therapy, H&N = head and neck

TABLE 2. Textural features calculated from a single fluenece map and conventional modulation indices for TrueBeam™

Textural features															
	d = 1			*d* =2			*d* = 3			*d* = 5			*d* = 10		
	Prostate	H&N	*p*	Prostate	H&N	*p*	Prostate	H&N	*p*	Prostate	H&N	*p*	Prostate	H&N	*p*
ASM ($\times 10^{-3}$)	1.37 ± 0.20	1.07 ± 0.22	< 0.001	1.15 ± 0.16	0.81 ± 0.18	< 0.001	1.18 ± 0.19	0.75 ± 0.17	< 0.001	1.34 ± 0.26	0.74 ± 0.16	< 0.001	1.79 ± 0.56	0.83 ± 0.19	< 0.001
IDM	0.33 ± 0.02	0.32 ± 0.03	< 0.001	0.23 ± 0.02	0.25 ± 0.02	< 0.001	0.18 ± 0.01	0.21 ± 0.02	< 0.001	0.13 ± 0.01	0.18 ± 0.02	< 0.001	0.09 ± 0.01	0.13 ± 0.01	< 0.001
Contrast	118.38 ± 30.27	80.90 ± 34.74	< 0.001	300.79 ± 82.10	136.61 ± 59.46	< 0.001	494.53 ± 124.64	191.32 ± 78.49	< 0.001	831.70 ± 189.12	288.54 ± 106.53	< 0.001	1429.11 ± 273.60	475.47 ± 185.21	< 0.001
Variance	50.93 ± 3.46	35.60 ± 6.34	< 0.001	51.55 ± 3.49	35.93 ± 6.47	< 0.001	52.07 ± 3.53	36.18 ± 6.55	< 0.001	52.73 ± 3.64	36.61 ± 6.71	< 0.001	52.99 ± 3.72	37.33 ± 6.80	< 0.001
Correlation	0.95 ± 0.01	0.94 ± 0.02	< 0.001	0.89 ± 0.03	0.90 ± 0.04	< 0.001	0.82 ± 0.03	0.86 ± 0.05	< 0.001	0.71 ± 0.04	0.80 ± 0.06	< 0.001	0.51 ± 0.06	0.68 ± 0.07	< 0.001
Entropy	3.06 ± 0.04	3.20 ± 0.09	< 0.001	3.12 ± 0.05	3.28 ± 0.09	< 0.001	3.13 ± 0.05	3.32 ± 0.09	< 0.001	3.11 ± 0.06	3.35 ± 0.09	< 0.001	3.03 ± 0.08	3.36 ± 0.09	< 0.001

Conventional modulation indices			
	Prostate	H&N	*p*
MCS_v	0.73 ± 0.08	0.42 ± 0.11	< 0.001
LTMCS	0.49 ± 0.07	0.16 ± 0.07	< 0.001
MI_{SPORT}	1582 ± 266	95492 ± 4036	< 0.001

Abbreviations: d = particular displacement distance, Prostate = volumetric modulated arc therapy plans for prostate cancer, H&N = volumetric modulated arc therapy plans for head and neck cancer, ASM = angular second moment, IDM = inverse difference moment, MCS_v = modulation complexity score for VMAT, LTMCS = leaf travel modulation complexity score, MI_{SPORT} = modulation index supporting station parameter optimized radiation therapy, H&N = head and neck

As shown in Table 1, the values of *contrast* in both prostate and H&N plans and those of *ASM* in prostate plans also increased when the value of *d* was increased. The values of *IDM* and *correlation* in both prostate and H&N plans and *entropy* in prostate plans were decreased as the value of *d* increased. The values of *variance* in both prostate and H&N plans, and *ASM* and *entropy* in H&N plans didn't show noticeable tendencies in comparison with variations in the value of *d*. For the values of textural features shown in Table 2, the values of *contrast* and *variance* in both prostate and H&N plans and those of *entropy* in H&N plans also increased as the value of *d* was increased. The values of *IDM* and *correlation* in both prostate and H&N plans were decreased as the value of *d* increased. The values of *ASM* in both prostate and H&N plans, and *entropy* in prostate plans didn't show noticeable tendencies in comparison with variations in the value of *d*.

For comparison of the values of textural features between Trilogy™ and TrueBeam™, The values of *IDM* and *entropy* in both prostate and H&N plans, and those of *variance* and *correlation* in prostate plans for TrueBeam™ were higher than those for Trilogy™. The values of *ASM* and *contrast* in both prostate and H&N plans and those of *variance* in H&N plans for TrueBeam™ were lower than those for Trilogy™. The values of correlation in H&N plans for TrueBeam™ were similar with those for Trilogy™.

The values of *ASM*, *contrast* and *variance* of prostate plans were higher than those of H&N plans, while those were opposite in *IDM*, *correlation* and *entropy*. Therefore, the fluence maps of prostate plans showed more overall homogeneities but less local homogeneities than those of H&N plans. In

addition, the fluence maps of H&N plans were more random than those of prostate plans. All of the differences in values of textural features between prostate and H&N plans in this study were statistically significant, showing p values less than 0.001.

Both MCS_v and LTMCS, which decrease when the degree of modulation increases, showed lower values in H&N plans than in prostate plans with statistical significance ($p < 0.001$), indicating that the degree of modulation was higher in H&N VMAT plans than in prostate plans.[9] The value of MI_{SPORT}, which increases when the degree of modulation increases, showed the same tendency, with higher values in H&N plans than in prostate plans with statistical significance ($p < 0.001$).[8] This was reasonable as the degree of modulation in H&N VMAT plans is generally higher than that in prostate plans.[32]

III.A.2. Textural features calculated from edge-enhanced fluence map

The fluence maps with and without edge-enhancement of prostate and H&N VMAT plans from Trilogy™ are shown in Fig. 3.

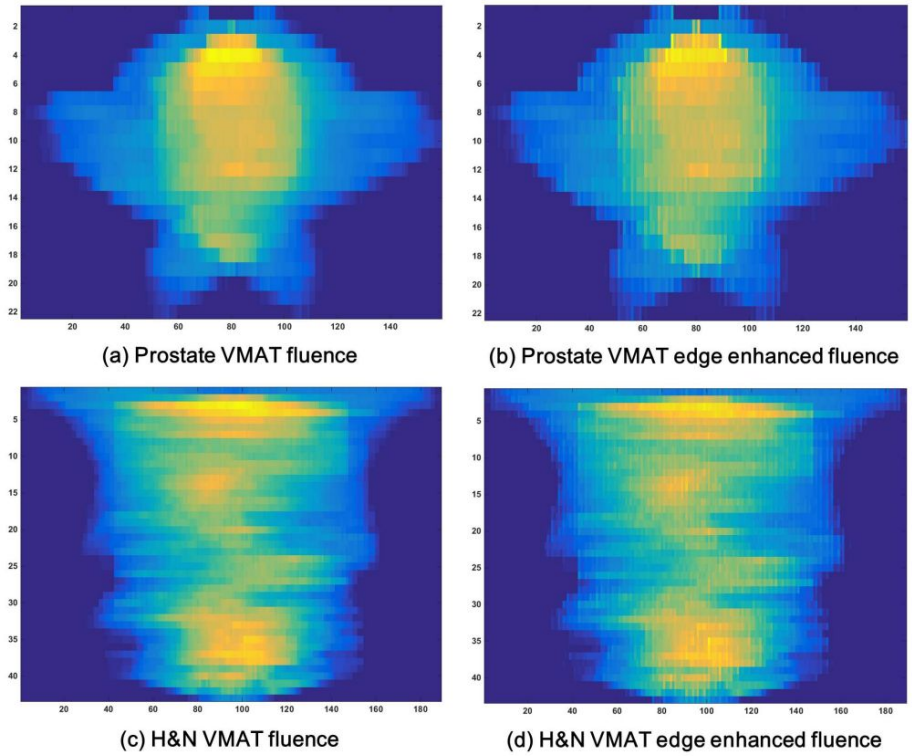

Fig. 3. The fluence maps with non-edge-enhancement of prostate (a) and head and neck (H&N) volumetric modulated arc therapy (VMAT) plans (c) are shown. Those fluence maps were generated by whole integration of every monitor units (MUs) shaped by multi-leaf collimator (MLC) apertures at each control point (CP). The fluence maps with edge-enhancement of prostate (b) and H&N VMAT plans (d) are also shown. For edge-enhancement of fluence maps, when integrating MUs, the values of pixels (size of 1 mm × 1 mm) representing MLC tips were doubled.

The GLCMs generated with edge-enhancement of those prostate and H&N VMAT plans are shown in Fig. 4.

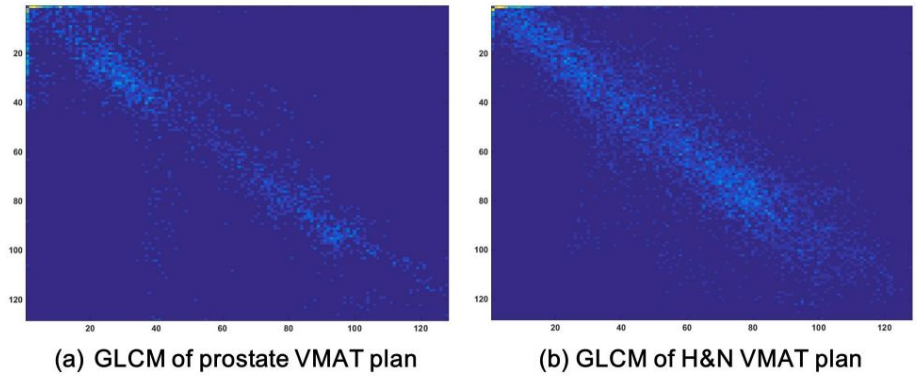

Fig. 4. The gray level co-occurrence (GLCM) matrices generated with edge-enhancement of prostate (a) and H&N VMAT plans (b) are shown. The particular displacement distance (d) was 1 and the searching angles were 0°, 45°, 90° and 135° when generating GLCM from a fluence map.

The textural features of prostate and H&N VMAT plans calculated from the GLCMs, and *p* values showing the statistical significances of their differences are shown in Table 3 and 4 for Trilogy™ and TrueBeam™ respectively.

TABLE 3. Textural features calculated from edge-enhanced fluence maps for Trilogy™

	d = 1			*d* = 5			*d* = 10		
	Prostate	H&N	p	Prostate	H&N	p	Prostate	H&N	p
ASM (×10-3)	1.43 ± 0.17	0.84 ± 0.26	< 0.001	2.18 ± 0.50	0.84 ± 0.27	< 0.001	2.97 ± 0.65	0.99 ± 0.44	< 0.001
IDM	0.24 ± 0.02	0.27 ± 0.03	< 0.001	0.12 ± 0.01	0.17 ± 0.02	< 0.001	0.08 ± 0.01	0.13 ± 0.02	< 0.001
Contrast	264.73 ± 70.21	113.52 ± 51.79	< 0.001	960.75 ± 236.74	341.90 ± 152.29	< 0.001	1737.04 ± 484.32	537.56 ± 239.04	< 0.001
Variance	45.48 ± 4.60	37.48 ± 7.74	0.001	46.41 ± 4.49	38.59 ± 8.08	0.001	46.32 ± 4.64	39.06 ± 8.10	0.002
Correlation	0.87 ± 0.02	0.92 ± 0.02	< 0.001	0.58 ± 0.05	0.79 ± 0.04	< 0.001	0.31 ± 0.13	0.69 ± 0.06	< 0.001
Entropy	2.97 ± 0.06	3.24 ± 0.12	< 0.001	2.88 ± 0.07	3.31 ± 0.12	< 0.001	2.73 ± 0.09	3.29 ± 0.15	< 0.001

Abbreviations: *d* = particular displacement distance, prostate = volumetric modulated arc therapy plans for prostate cancer, H&N = volumetric modulated arc therapy plans for head and neck cancer, ASM = angular second moment, IDM = inverse difference moment

TABLE 4. Textural features calculated from edge-enhanced fluence maps for TrueBeam™

	d = 1			*d* = 5			*d* = 10		
	Prostate	H&N	p	Prostate	H&N	p	Prostate	H&N	p
ASM (×10-3)	1.24 ± 0.23	0.93 ± 0.44	< 0.001	1.42 ± 0.31	0.82 ± 0.31	< 0.001	1.96 ± 0.66	0.91 ± 0.33	< 0.001
IDM	0.30 ± 0.02	0.28 ± 0.04	< 0.001	0.15 ± 0.02	0.19 ± 0.03	< 0.001	0.10 ± 0.01	0.14 ± 0.02	< 0.001
Contrast	135.54 ± 35.05	84.99 ± 40.97	< 0.001	617.43 ± 195.11	251.97 ± 120.87	< 0.001	1022.99 ± 284.56	405.13 ± 209.74	< 0.001
Variance	42.34 ± 5.78	32.23 ± 8.26	0.001	44.16 ± 5.99	33.20 ± 8.62	0.001	44.43 ± 5.88	33.89 ± 8.75	0.002
Correlation	0.92 ± 0.02	0.92 ± 0.03	< 0.001	0.70 ± 0.04	0.79 ± 0.06	< 0.001	0.50 ± 0.06	0.68 ± 0.07	< 0.001
Entropy	3.07 ± 0.06	3.22 ± 0.15	< 0.001	3.10 ± 0.07	3.31 ± 0.14	< 0.001	3.02 ± 0.09	3.32 ± 0.13	< 0.001

Abbreviations: *d* = particular displacement distance, prostate = volumetric modulated arc therapy plans for prostate cancer, H&N = volumetric modulated arc therapy plans for head and neck cancer, ASM = angular second moment, IDM = inverse difference moment

All textural features of prostate VMAT plans were different from those of H&N VMAT plans with statistical significances (all with $p < 0.003$). The values of textural features according to d values of 2 and 3 for TrueBeam™ are not shown since the differences between the those according to d values of 1, 2 and 3 are insignificant in this study. The values of *ASM*, *contrast* and *variance* of prostate VMAT plans were higher than those of H&N VMAT plans, while the values of *IDM*, *correlation* and *entropy* of H&N VMAT plans were higher than those of prostate VMAT plans. This tendency of the values of textural features calculated with edge-enhanced fluence maps was the same as that of the textural features with non-edge-enhanced fluence maps (a single fluence map) in our feasibility study, although the values were different from each other.[28]

III.A.3. Textural features calculated with various conditions

An example of the textural changes in fluence maps of prostate and H&N VMAT plans according to the numbers of segments which were used to generate those fluence maps are shown in Fig. 5.

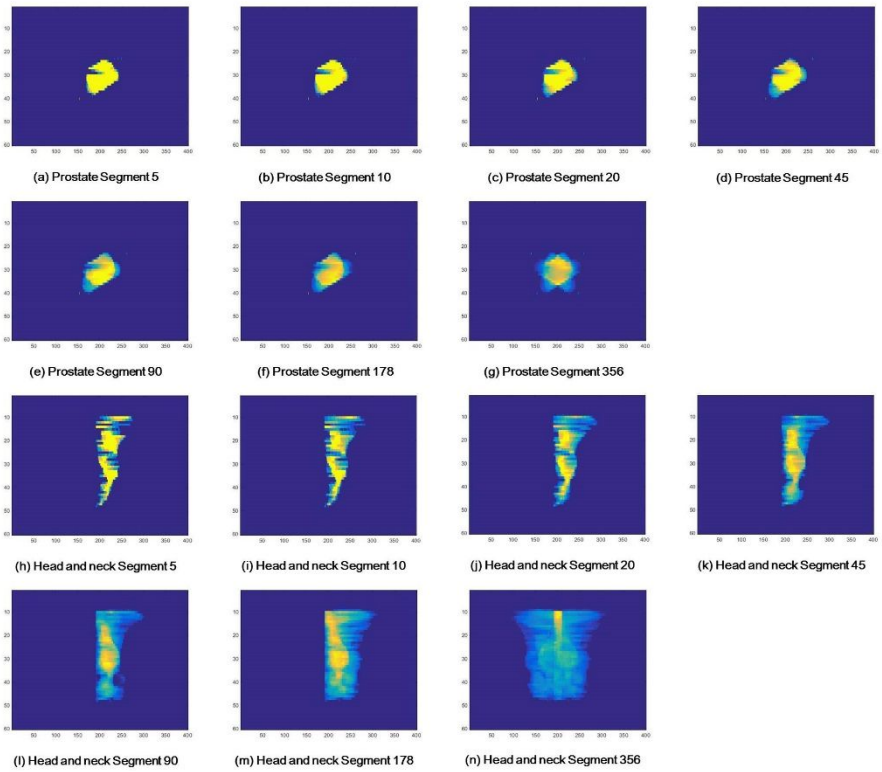

Fig. 5. The textural changes in fluence maps of prostate and head and neck volumetric modulated arc therapy (VMAT) plans according to the numbers of segments which were used to generate fluence maps are shown. The fluence maps generated with 5 (a), 10 (b), 20 (c), 45 (d), 90 (e), 178 (f) and 356 (g) segments of prostate VMAT plan are shown. Similarly, the fluence maps generated with 5 (h), 10 (i), 20 (j), 45 (k), 90 (l), 178 (m) and 356 (n) segments of head and neck VMAT plan are also shown.

According to the number of segments, textural characteristics were changed. The average values of calculated textural features from the various fluence map of both prostate and H&N VMAT plans are shown in Table 5 and 6 for Trilogy™ and TrueBeam™, respectively.

TABLE 5. Textural features calculated with prostate and head and neck volumetric modulated arc therapy plans for Trilogy™

	d = 1			*d* = 5			*d* = 10		
	Prostate	H&N	*p*	Prostate	H&N	*p*	Prostate	H&N	*p*
Segment 5									
ASM	0.22 ± 0.04	0.19 ± 0.04	0.196	0.16 ± 0.02	0.13 ± 0.03	0.012	0.19 ± 0.03	0.12 ± 0.02	< 0.001
IDM	0.50 ± 0.04	0.51 ± 0.05	0.544	0.27 ± 0.03	0.31 ± 0.05	0.011	0.19 ± 0.04	0.23 ± 0.04	0.034
Contrast	3260.85 ± 256.75	2671.69 ± 297.88	< 0.001	6763.58 ± 298.25	5114.41 ± 317.91	< 0.001	8171.76 ± 553.41	6464.27 ± 230.10	< 0.001
Variance	64.92 ± 1.40	64.91 ± 1.30	0.979	73.39 ± 0.88	71.42 ± 0.75	< 0.001	73.02 ± 2.21	73.85 ± 1.10	0.113
Correlation	0.31 ± 0.04	0.43 ± 0.04	< 0.001	-0.14 ± 0.04	0.07 ± 0.05	< 0.001	-0.25 ± 0.06	-0.11 ± 0.03	< 0.001
Entropy	1.11 ± 0.08	1.20 ± 0.10	0.014	1.14 ± 0.06	1.28 ± 0.09	< 0.001	1.04 ± 0.06	1.27 ± 0.08	< 0.001
Segment10									
ASM	0.11 ± 0.03	0.08 ± 0.03	0.052	0.08 ± 0.02	0.05 ± 0.02	0.002	0.10 ± 0.02	0.05 ± 0.01	< 0.001
IDM	0.41 ± 0.04	0.42 ± 0.04	0.585	0.19 ± 0.03	0.22 ± 0.04	0.046	0.13 ± 0.03	0.15 ± 0.03	0.160
Contrast	2334.60 ± 210.68	1725.57 ± 223.34	< 0.001	5471.57 ± 288.19	3690.83 ± 286.44	< 0.001	6814.08 ± 510.33	4842.60 ± 255.42	< 0.001
Variance	63.87 ± 1.07	63.48 ± 1.10	0.164	70.05 ± 1.06	67.49 ± 1.62	< 0.001	69.94 ± 2.32	69.00 ± 1.96	0.150
Correlation	0.47 ± 0.04	0.60 ± 0.05	< 0.001	-0.02 ± 0.04	0.24 ± 0.05	< 0.001	-0.15 ± 0.07	0.05 ± 0.04	< 0.001
Entropy	1.61 ± 0.10	1.79 ± 0.12	< 0.001	1.61 ± 0.08	1.87 ± 0.12	< 0.001	1.46 ± 0.09	1.84 ± 0.11	< 0.001
Segment 20									
ASM	0.040 ± 0.02	0.02 ± 0.01	0.003	0.03 ± 0.01	0.01 ± 0.01	< 0.001	0.04 ± 0.01	0.01 ± 0.00	< 0.001
IDM	0.32 ± 0.03	0.33 ± 0.03	0.357	0.13 ± 0.02	0.15 ± 0.02	0.047	0.09 ± 0.02	0.10 ± 0.02	0.156
Contrast	1533.18 ± 168.26	929.04 ± 148.52	< 0.001	4211.07 ± 296.33	2309.44 ± 260.86	< 0.001	5451.68 ± 522.45	3189.47 ± 258.18	< 0.001
Variance	60.34 ± 0.95	58.12 ± 2.45	0.001	64.94 ± 1.41	60.44 ± 2.81	< 0.001	65.31 ± 2.67	61.32 ± 2.94	< 0.001
Correlation	0.60 ± 0.040	0.73 ± 0.04	< 0.001	0.08 ± 0.05	0.40 ± 0.06	< 0.001	-0.060 ± 0.08	0.21 ± 0.05	< 0.001
Entropy	2.11 ± 0.09	2.40 ± 0.13	< 0.001	2.09 ± 0.08	2.49 ± 0.12	< 0.001	1.90 ± 0.10	2.45 ± 0.13	< 0.001
Segment 45									
ASM ($\times 10^{-3}$)	6.99 ± 4.92	1.20 ± 0.62	< 0.001	6.66 ± 3.21	1.74 ± 0.42	< 0.001	10.29 ± 3.58	2.11 ± 0.60	< 0.001
IDM	0.25 ± 0.03	0.25 ± 0.02	0.733	0.13 ± 0.02	0.14 ± 0.01	0.144	0.10 ± 0.01	0.11 ± 0.01	0.026
Contrast	395.80 ± 122.89	288.66 ± 91.68	0.020	1074.46 ± 355.84	716.87 ± 193.79	0.006	1510.76 ± 536.30	1012.02 ± 202.10	0.005
Variance	32.40 ± 6.08	37.00 ± 3.48	0.029	34.35 ± 6.32	38.08 ± 3.75	0.087	35.07 ± 6.46	38.61 ± 3.76	0.104
Correlation	0.64 ± 0.06	0.79 ± 0.04	< 0.001	0.19 ± 0.07	0.53 ± 0.07	< 0.001	0.03 ± 0.09	0.34 ± 0.04	< 0.001
Entropy	2.65 ± 0.06	3.04 ± 0.08	< 0.001	2.55 ± 0.07	3.06 ± 0.09	< 0.001	2.34 ± 0.09	3.01 ± 0.12	< 0.001
Segment 90									

ASM ($\times 10^{-3}$)	2.45 ± 0.54	1.03 ± 0.29	< 0.001	3.47 ± 0.80	1.01 ± 0.38	< 0.001	6.10 ± 1.67	1.25 ± 0.55	< 0.001
IDM	0.24 ± 0.03	0.24 ± 0.02	0.967	0.13 ± 0.02	0.15 ± 0.02	0.028	0.09 ± 0.02	0.11 ± 0.01	0.005
Contrast	352.13 ± 132.75	193.46 ± 62.78	0.001	1043.60 ± 399.09	557.82 ± 147.37	< 0.001	1553.68 ± 618.46	862.66 ± 174.48	0.001
Variance	34.12 ± 7.11	38.17 ± 4.31	0.084	35.74 ± 7.34	39.06 ± 4.53	0.171	36.46 ± 7.44	39.47 ± 4.45	0.208
Correlation	0.71 ± 0.06	0.86 ± 0.03	< 0.001	0.27 ± 0.08	0.65 ± 0.04	< 0.001	0.08 ± 0.10	0.49 ± 0.03	< 0.001
Entropy	2.78 ± 0.07	3.21 ± 0.09	< 0.001	2.67 ± 0.08	3.24 ± 0.11	< 0.001	2.45 ± 0.10	3.19 ± 0.14	< 0.001
Segment 178									
ASM ($\times 10^{-3}$)	1.72 ± 0.41	0.73 ± 0.18	< 0.001	2.69 ± 0.76	0.68 ± 0.28	< 0.001	4.52 ± 1.22	0.81 ± 0.50	< 0.001
IDM	0.24 ± 0.04	0.24 ± 0.018	0.522	0.12 ± 0.02	0.14 ± 0.02	0.001	0.08 ± 0.02	0.11 ± 0.01	< 0.001
Contrast	296.33 ± 137.45	152.76 ± 50.34	0.001	961.30 ± 444.53	493.21 ± 134.36	0.001	1507.88 ± 703.18	818.03 ± 181.44	0.001
Variance	34.46 ± 8.23	40.18 ± 4.39	0.022	36.75 ± 8.84	41.00 ± 46.65	0.107	37.32 ± 9.16	41.64 ± 4.67	0.110
Correlation	0.76 ± 0.03	0.91 ± 0.02	< 0.001	0.37 ± 0.06	0.73 ± 0.05	< 0.001	0.13 ± 0.11	0.57 ± 0.04	< 0.001
Entropy	2.87 ± 0.08	3.28 ± 0.09	< 0.001	2.76 ± 0.09	3.34 ± 0.12	< 0.001	2.55 ± 0.10	3.31 ± 0.16	< 0.001
Segment 356									
ASM ($\times 10^{-3}$)	1.71 ± 0.27	1.08 ± 0.25	< 0.001	2.20 ± 0.48	0.84 ± 0.25	< 0.001	3.03 ± 0.64	0.99 ± 0.45	< 0.001
IDM	0.27 ± 0.02	0.32 ± 0.02	< 0.001	0.11 ± 0.01	0.16 ± 0.02	< 0.001	0.08 ± 0.01	0.12 ± 0.01	< 0.001
Contrast	252.86 ± 63.90	108.62 ± 49.02	< 0.001	1149.75 ± 245.04	380.63 ± 153.17	< 0.001	2096.51 ± 451.88	607.10 ± 249.72	< 0.001
Variance	50.31 ± 3.75	39.72 ± 6.65	< 0.001	51.23 ± 3.98	40.90 ± 7.07	< 0.001	50.96 ± 4.83	41.35 ± 7.13	< 0.001
Correlation	0.90 ± 0.02	0.93 ± 0.01	< 0.001	0.59 ± 0.05	0.79 ± 0.04	< 0.001	0.30 ± 0.14	0.69 ± 0.06	< 0.001
Entropy	2.92 ± 0.06	3.18 ± 0.09	< 0.001	2.86 ± 0.08	3.30 ± 0.11	< 0.001	2.71 ± 0.10	3.28 ± 0.14	< 0.001

Abbreviations: *d* = particular displacement distance, prostate = volumetric modulated arc therapy plans for prostate cancer, H&N = volumetric modulated arc therapy plans for head and neck cancer, ASM = angular second moment, IDM = inverse difference moment

TABLE 6. Textural features calculated with prostate and head and neck volumetric modulated arc therapy plans for TrueBeam™

	d = 1			*d* = 5			*d* = 10		
	Prostate	H&N	*p*	Prostate	H&N	*p*	Prostate	H&N	*p*
Segment 5									
ASM	0.28 ± 0.03	0.14 ± 0.05	< 0.001	0.18 ± 0.02	0.10 ± 0.03	< 0.001	0.16 ± 0.01	0.09 ± 0.03	< 0.001
IDM	0.59 ± 0.02	0.46 ± 0.07	< 0.001	0.35 ± 0.03	0.26 ± 0.07	< 0.001	0.26 ± 0.03	0.18 ± 0.06	< 0.001
Contrast	2267.89 ± 148.46	2506.68 ± 258.51	< 0.001	5739.79 ± 261.95	4599.46 ± 382.17	< 0.001	7286.26 ± 353.11	5826.43 ± 486.05	< 0.001
Variance	60.70 ± 1.31	64.11 ± 1.83	< 0.001	72.09 ± 0.94	69.07 ± 2.74	< 0.001	75.44 ± 0.95	71.11 ± 3.36	< 0.001
Correlation	0.44 ± 0.03	0.44 ± 0.05	0.754	-0.04 ± 0.03	0.08 ± 0.06	< 0.001	-0.20 ± 0.03	-0.11 ± 0.06	< 0.001
Entropy	0.99 ± 0.06	1.33 ± 0.15	< 0.001	1.10 ± 0.06	1.39 ± 0.13	< 0.001	1.09 ± 0.04	1.38 ± 0.11	< 0.001
Segment10									
ASM	0.15 ± 0.03	0.06 ± 0.03	< 0.001	0.09 ± 0.02	0.04 ± 0.02	< 0.001	0.08 ± 0.01	0.03 ± 0.01	< 0.001
IDM	0.50 ± 0.03	0.38 ± 0.06	< 0.001	0.26 ± 0.02	0.19 ± 0.05	< 0.001	0.18 ± 0.03	0.13 ± 0.04	< 0.001
Contrast	1545.97 ± 124.78	1480.39 ± 193.68	0.211	4628.02 ± 271.38	3054.93 ± 415.94	< 0.001	6059.59 ± 331.00	4039.98 ± 581.75	< 0.001
Variance	61.18 ± 1.18	59.99 ± 3.64	0.172	69.95 ± 0.89	62.81 ± 4.78	< 0.001	72.25 ± 1.03	64.00 ± 5.26	< 0.001
Correlation	0.61 ± 0.03	0.60 ± 0.05	0.574	0.10 ± 0.04	0.26 ± 0.06	< 0.001	-0.10 ± 0.04	0.06 ± 0.06	< 0.001
Entropy	1.48 ± 0.09	1.92 ± 0.17	< 0.001	1.59 ± 0.08	2.00 ± 0.15	< 0.001	1.55 ± 0.07	1.97 ± 0.13	< 0.001
Segment 20									
ASM	0.06 ± 0.02	0.01 ± 0.01	< 0.001	0.03 ± 0.01	0.01 ± 0.01	< 0.001	0.03 ± 0.01	0.011± 0.00	< 0.001
IDM	0.40 ± 0.02	0.32 ± 0.04	< 0.001	0.18 ± 0.02	0.14 ± 0.02	< 0.001	0.012 ± 0.02	0.10 ± 0.01	< 0.001
Contrast	971.92 ± 90.74	723.36 ± 143.78	< 0.001	3485.93 ± 300.48	1748.89 ± 370.36	< 0.001	4771.81 ± 347.16	2462.01 ± 545.51	< 0.001
Variance	58.68 ± 1.20	52.21 ± 5.49	< 0.001	65.08 ± 1.10	53.82 ± 6.34	< 0.001	67.21 ± 1.33	54.56 ± 6.67	< 0.001
Correlation	0.74 ± 0.02	0.73 ± 0.05	0.367	0.21 ± 0.05	0.41 ± 0.07	< 0.001	0.00 ± 0.05	0.21 ± 0.07	< 0.001
Entropy	2.02 ± 0.09	2.50 ± 0.16	< 0.001	2.14 ± 0.08	2.60 ± 0.14	< 0.001	2.07 ± 0.08	2.56 ± 0.14	< 0.001
Segment 45									
ASM ($\times 10^{-3}$)	11.70 ± 6.60	3.20 ± 1.33	< 0.001	6.46 ± 3.39	2.09 ± 0.81	< 0.001	6.85 ± 2.72	2.27 ± 0.77	< 0.001
IDM	0.31 ± 0.02	0.29 ± 0.01	< 0.001	0.12 ± 0.01	0.14 ± 0.01	< 0.001	0.08 ± 0.01	0.10 ± 0.01	< 0.001
Contrast	479.48 ± 77.76	306.03 ± 65.88	< 0.001	2207.52 ± 328.95	831.69 ± 187.00	< 0.001	3282.67 ± 403.50	1233.13 ± 313.75	< 0.001
Variance	54.81 ± 1.27	41.97 ± 4.77	< 0.001	59.26 ± 1.33	42.91 ± 5.36	< 0.001	60.72 ± 1.75	43.42 ± 5.65	< 0.001
Correlation	0.84 ± 0.03	0.81 ± 0.04	0.020	0.39 ± 0.07	0.54 ± 0.07	< 0.001	0.016 ± 0.07	0.36 ± 0.07	< 0.001
Entropy	2.60 ± 0.08	2.96 ± 0.11	< 0.001	2.68 ± 0.07	3.07 ± 0.11	< 0.001	2.58 ± 0.08	3.03 ± 0.11	< 0.001
Segment 90									

ASM ($\times 10^{-3}$)	2.21 ± 0.55	1.42 ± 0.31	< 0.001	1.80 ± 0.26	0.98 ± 0.26	< 0.001	2.40 ± 0.44	1.11 ± 0.31	< 0.001
IDM	0.29 ± 0.02	0.29 ± 0.01	0.680	0.11 ± 0.01	0.15 ± 0.01	< 0.001	0.074 ± 0.01	0.11 ± 0.01	< 0.001
Contrast	342.20 ± 68.97	177.63 ± 38.95	< 0.001	1808.08 ± 325.41	561.24 ± 108.98	< 0.001	2794.86 ± 435.97	884.00 ± 190.66	< 0.001
Variance	54.47 ± 1.20	40.16 ± 4.66	< 0.001	57.93 ± 1.44	40.93 ± 4.98	< 0.001	58.97 ± 1.79	41.33 ± 5.20	< 0.001
Correlation	0.88 ± 0.02	0.88 ± 0.03	0.904	0.47 ± 0.08	0.666 ± 0.06	< 0.001	0.23 ± 0.09	0.50 ± 0.06	< 0.001
Entropy	2.93 ± 0.05	3.18 ± 0.07	< 0.001	2.97 ± 0.05	3.29 ± 0.08	< 0.001	2.86 ± 0.07	3.27 ± 0.09	< 0.001
				Segment 178					
ASM ($\times 10^{-3}$)	1.24 ± 0.16	0.87 ± 0.15	< 0.001	1.20 ± 0.16	0.58 ± 0.12	< 0.001	1.73 ± 0.34	0.64 ± 0.17	< 0.001
IDM	0.28 ± 0.01	0.28 ± 0.02	0.960	0.11 ± 0.01	0.15 ± 0.01	< 0.001	0.07 ± 0.00	0.11 ± 0.01	< 0.001
Contrast	217.49 ± 47.95	125.18 ± 33.26	< 0.001	1279.90 ± 268.73	454.78 ± 93.07	< 0.001	2095.43 ± 385.61	780.04 ± 171.20	< 0.001
Variance	48.18 ± 3.17	40.48 ± 5.00	< 0.001	52.08 ± 3.32	41.31 ± 5.22	< 0.001	53.46 ± 3.18	41.97 ± 5.40	< 0.001
Correlation	0.791 ± 0.02	0.92 ± 0.02	0.036	0.55 ± 0.05	0.74 ± 0.07	< 0.001	0.30 ± 0.07	0.58 ± 0.07	< 0.001
Entropy	3.06 ± 0.04	3.27 ± 0.06	< 0.001	3.08 ± 0.06	3.41 ± 0.07	< 0.001	2.97 ± 0.07	3.40 ± 0.08	< 0.001
				Segment 356					
ASM ($\times 10^{-3}$)	1.37 ± 0.20	1.07 ± 0.22	< 0.001	1.34 ± 0.26	0.74 ± 0.16	< 0.001	1.79 ± 0.56	0.83 ± 0.19	< 0.001
IDM	0.33 ± 0.02	0.32 ± 0.03	< 0.001	0.13 ± 0.01	0.18 ± 0.02	< 0.001	0.09 ± 0.01	0.13 ± 0.01	< 0.001
Contrast	118.38 ± 30.27	80.90 ± 34.74	< 0.001	831.70 ± 189.12	288.54 ± 106.53	< 0.001	1429.11 ± 273.60	475.47 ± 185.21	< 0.001
Variance	50.93 ± 3.46	35.60 ± 6.34	< 0.001	52.73 ± 3.64	36.61 ± 6.71	< 0.001	52.99 ± 3.72	37.33 ± 6.80	< 0.001
Correlation	0.95 ± 0.01	0.94 ± 0.02	< 0.001	0.71 ± 0.04	0.80 ± 0.06	< 0.001	0.51 ± 0.06	0.68 ± 0.07	< 0.001
Entropy	3.06 ± 0.04	3.20 ± 0.09	< 0.001	3.11 ± 0.06	3.35 ± 0.09	< 0.001	3.03 ± 0.08	3.36 ± 0.09	< 0.001

Abbreviations: *d* = particular displacement distance, prostate = volumetric modulated arc therapy plans for prostate cancer, H&N = volumetric modulated arc therapy plans for head and neck cancer, ASM = angular second moment, IDM = inverse difference moment

The values with 356 segments were the same as shown in our feasibility study.[32] Likewise the study for texture analysis on the edge-enhanced fluence map, the values of textural features according to *d* values of 2 and 3 for TrueBeam™ are not shown since the differences between the those according to *d* values of 1, 2 and 3 are insignificant in this study. A total of 126 textural features were calculated and 104 textural features for Trilogy™ and 118 textural features for TrueBeam™ showed statistically significant differences between prostate and H&N VMAT plans. Since it has been shown that the modulation degree of prostate VMAT plans are generally lower than those of H&N VMAT plans in feasibility study,[9] approximately 83% and 94% of the calculated textural features can identify the differences in modulation degree between lowly- and highly-modulated VMAT plans.

III.B. Plan deliverability of VMAT

Both global and local gamma passing rates of pretreatment QA according to the different gamma criteria for prostate and H&N VMAT plans with MapCHECK2 are shown in Table 7.

TABLE 7. The means and standard deviations of both global and local gamma passing rates of pretreatment QA according the different gamma criteria of 2%/2 mm, 1%/2 mm and 2%/1 mm for prostate and head and neck (H&N) volumetric modulated arc therapy (VMAT) plans

		TRG		TBX	
		prostate	H&N	prostate	H&N
local	2%/2 mm	90.4 ± 2.2	87.4 ± 2.8	91.0 ± 2.0	87.4 ± 3.6
	1%/2 mm	86.8 ± 2.9	82.2 ± 3.8	87.4 ± 2.6	82.6 ± 3.9
	2%/1 mm	77.5 ± 4.3	73.9 ± 4.6	79.7 ± 3.1	70.9 ± 6.5
global	2%/2 mm	98.6 ± 0.9	97.0 ± 1.9	99.1 ± 0.5	96.5 ± 2.5
	1%/2 mm	94.4 ± 2.0	89.2 ± 3.2	95.6 ± 1.5	89.7 ± 4.0
	2%/1 mm	95.5 ± 1.9	93.7 ± 3.0	96.4 ± 1.8	90.4 ± 5.1

Abbreviations: TRG = Trilogy™, TBX = TrueBeam™, prostate = volumetric modulated arc therapy plans for prostate cancer, H&N = volumetric modulated arc therapy plans for head and neck cancer, local = local gamma passing rates, global = global gamma passing rates

A global gamma passing rate of 2%/2 mm has been recently recommended for pretreatment VMAT QA,[32] with this criteria both prostate and H&N VMAT plans in this study were higher than 90%, and thus acceptable for patient treatment. The average differences in MLC positions, gantry angles, and MUs between the VMAT plans and 2 kinds of machine log files are shown in Fig. 6.

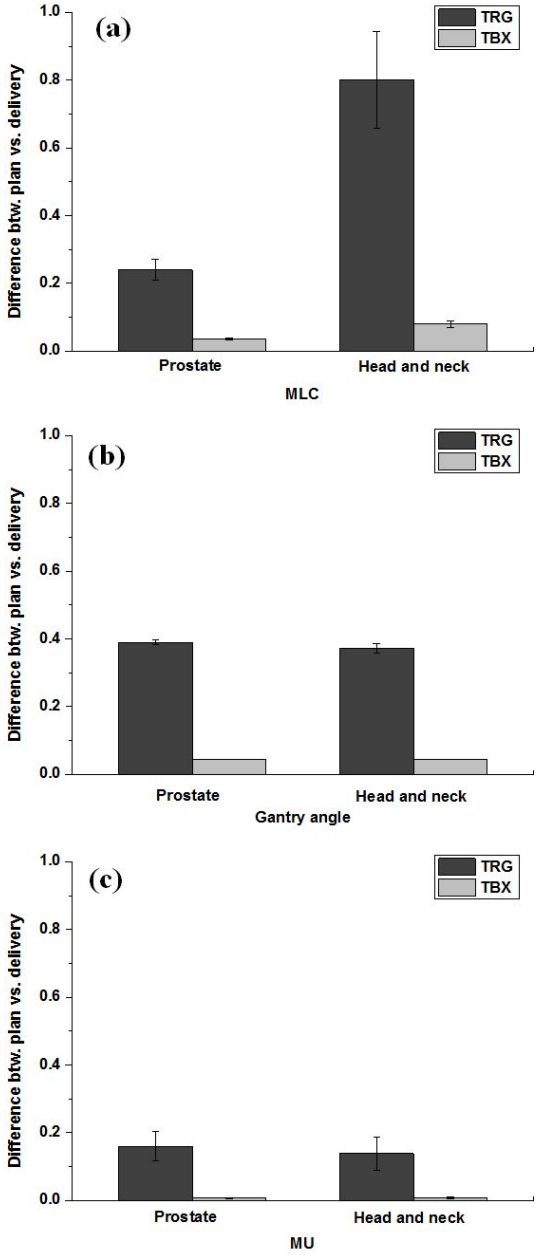

FIG. 6. The means and standard deviations of differences in multi-leaf collimator (MLC) positions (a), gantry angles (b) and MUs (c) between the volumetric modulated arc therapy (VMAT) plans and the 2 kinds of machine files for Trilogy™ and TrueBeam™ are shown. The unit of MLC positional differences and gantry angle differences are mm and degree (°), respectively.

Even though the magnitudes of the differences were minimal, the average difference in MLC positions of the H&N plans was higher than that of the prostate plans. The average differences in MLC positions, gantry angles, and MUs for Trilogy™ were higher than those for TrueBeam™. To analyze the correlation between gamma passing rates and differences in MLC positions, the results for 5 patients with prostate cancer and 5 patients with H&N cancer verified with film measurement are shown in Fig. 7. For comparison, the results for that patients verified with MacCHECK2 are also shown in Fig. 7. As the differences in MLC positions increased, global gamma passing rates with criteria of 2%/1 mm obtained using Gafchromic® EBT3 film and 1%/2 mm obtained using Gafchromic® EBT3 film and MapCHECK2 decreased while those with criteria of 2%/2 mm obtained using Gafchromic® EBT3 film and MapCHECK2, 1%/1 mm obtained using Gafchromic® EBT3 film and MapCHECK2 and 2%/1 mm obtained using MapCHECK2didn't show noticeable tendencies.

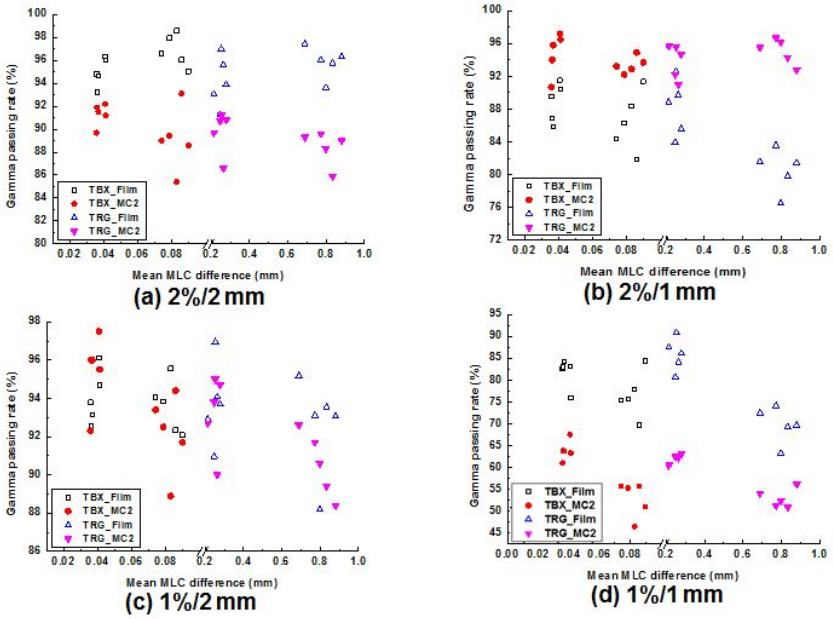

FIG. 7. Global gamma passing rates with criteria of 2%/2 mm (a), 2%/1 mm (b), 1%/2 mm (c) and 1%/1 mm (d) obtained by film and MapCHECK2 according to the values of differences in MLC positions. The Gafchromic® EBT3 film and MapCHECK2 was abbreviated to Film and MC2, respectively. The Trilogy™ and TrueBeam™ were abbreviated to TRG and TBX, respectively.

The differences in dose-volumetric parameters between the VMAT plans and the reconstructed plans with dynamic log files are shown in Fig. 8. The maximum dose to target showed the highest difference in prostate plans, while the minimum dose to target showed the highest difference in H&N plans.

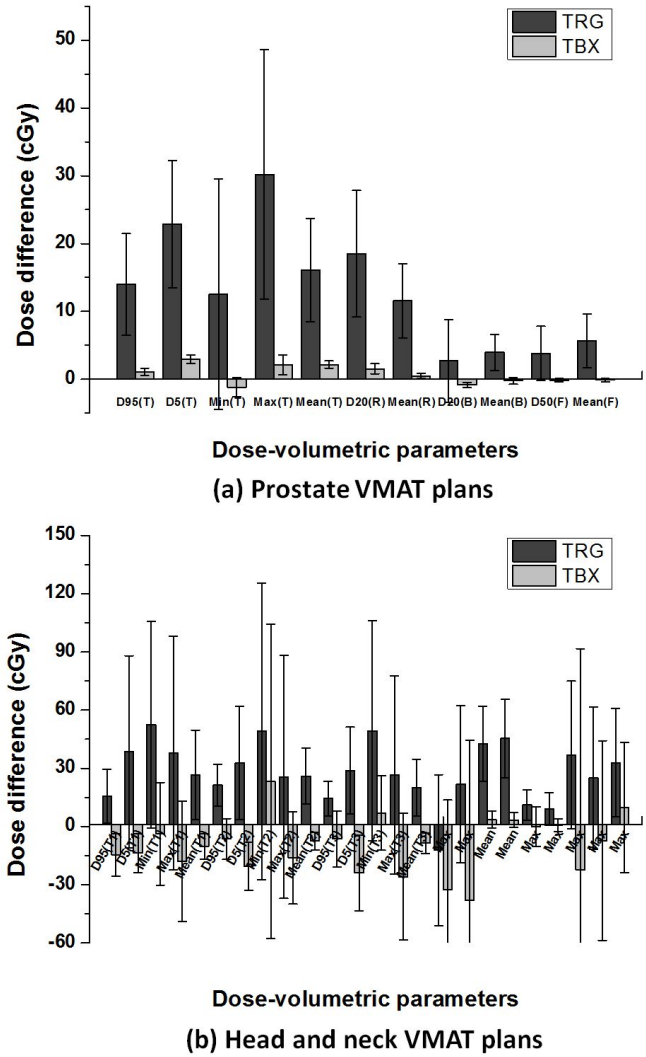

FIG. 8. The differences in dose-volumetric parameters between the prostate volumetric modulated arc therapy (VMAT) plans and the reconstructed plans with dynamic log files are shown (a). Those between head and neck (H&N) VMAT plans and the reconstructed plans are also shown (b). The D_n(structure) means dose received n% volume of certain structure. The minimum dose, maximum dose and mean dose were abbreviated to Min, Max and Mean, respectively. The target volume, target 1, target 2, target 3, rectal wall, bladder, femoral head, spinal cord, brain stem, right parotid gland, left parotid gland, right lens, left lens, optic chiasm, right optic nerve and left optic nerve were abbreviated to T, T1, T2, T3, R, B, F, SC, BS, P(R), P(L), L(R), L(L), OC, ON(R) and ON(L), respectively.

III.C. Correlations

III.C.1. Textural features vs. gamma passing rates of pretreatment QA

III.C.1.1. A single fluence map

The values of r_s with p values of textural features for a single fluence map from Trilogy™ and TrueBeam™ and the conventional modulation indices with the global gamma passing rates are shown in Table 8 and 9, respectively.

TABLE 8. Correlations of textural features calculated from a single fluence map and conventional modulation indices with global gamma passing rates for Trilogy™

		2%/2 mm		2%/1 mm		1%/2 mm	
	d	r_s	*p*	r_s	*p*	r_s	*p*
ASM	1	*0.350*	*0.027*	*0.329*	*0.038*	*0.542*	*< 0.001*
	5	*0.539*	*< 0.001*	*0.333*	*0.036*	*0.773*	*< 0.001*
	10	*0.468*	*0.002*	0.309	0.052	*0.712*	*< 0.001*
IDM	1	*-0.620*	*< 0.001*	*-0.467*	*0.002*	*-0.698*	*< 0.001*
	5	*-0.599*	*< 0.001*	*-0.386*	*0.014*	*-0.687*	*< 0.001*
	10	*-0.499*	*0.001*	-0.285	0.075	*-0.632*	*< 0.001*
Contrast	1	*0.536*	*< 0.001*	*0.473*	*0.002*	*0.718*	*< 0.001*
	5	*0.568*	*< 0.001*	*0.391*	*0.013*	*0.692*	*< 0.001*
	10	*0.525*	*0.001*	*0.321*	*0.043*	*0.695*	*< 0.001*
Variance	1	*0.551*	*< 0.001*	*0.481*	*0.002*	*0.688*	*< 0.001*
	5	*0.546*	*< 0.001*	*0.437*	*0.005*	*0.664*	*< 0.001*
	10	*0.543*	*< 0.001*	*0.478*	*0.002*	*0.635*	*< 0.001*
Correlation	1	*-0.368*	*0.019*	-0.287	0.073	*-0.619*	*< 0.001*
	5	*-0.502*	*0.001*	-0.262	0.102	*-0.694*	*< 0.001*
	10	*-0.379*	*0.016*	-0.100	0.538	*-0.634*	*< 0.001*
Entropy	1	*-0.343*	*0.030*	-0.236	0.143	*-0.634*	*< 0.001*
	5	*-0.367*	*0.020*	-0.232	0.149	*-0.619*	*< 0.001*
	10	*-0.350*	*0.027*	-0.266	0.097	*-0.622*	*< 0.001*
MCS_v		0.076	0.640	0.144	0.377	0.238	0.139
LTMCS		0.262	0.103	0.147	0.367	*0.470*	*0.002*
MI_{SPORT}		*-0.420*	*0.007*	*-0.330*	*0.037*	*-0.632*	*< 0.001*

Abbreviations: d = particular displacement distance, r_s = Spearman's rank correlation coefficients, ASM = angular second moment, IDM = inverse difference moment, MCS_v = modulation complexity score for VMAT, LTMCS = leaf travel modulation complexity score, MI_{SPORT} = modulation index supporting station parameter optimized radiation therapy

TABLE 9. Correlations of textural features calculated from a single fluence map and conventional modulation indices with global gamma passing rates for TrueBeam™

		2%/2 mm		2%/1 mm		1%/2 mm	
	d	r_s	*p*	r_s	*p*	r_s	*p*
ASM	1	*0.499*	*0.001*	*0.387*	*0.014*	*0.461*	*0.003*
	2	*0.521*	*0.001*	*0.452*	*0.003*	*0.511*	*0.001*
	3	*0.571*	*< 0.001*	*0.524*	*0.001*	*0.604*	*< 0.001*
	5	*0.595*	*< 0.001*	*0.543*	*< 0.001*	*0.639*	*< 0.001*
	10	*0.641*	*< 0.001*	*0.563*	*< 0.001*	*0.669*	*< 0.001*
IDM	1	*0.329*	*0.038*	*0.253*	*0.115*	*0.274*	*0.087*
	2	*-0.368*	*0.019*	*-0.416*	*0.008*	*-0.468*	*0.002*
	3	*-0.528*	*< 0.001*	*-0.569*	*< 0.001*	*-0.616*	*< 0.001*
	5	*-0.640*	*< 0.001*	*-0.647*	*< 0.001*	*-0.714*	*< 0.001*
	10	*-0.653*	*< 0.001*	*-0.634*	*< 0.001*	*-0.722*	*< 0.001*
Contrast	1	*0.396*	*0.011*	*0.471*	*0.002*	*0.370*	*0.019*
	2	*0.545*	*< 0.001*	*0.599*	*< 0.001*	*0.540*	*< 0.001*
	3	*0.586*	*< 0.001*	*0.648*	*< 0.001*	*0.604*	*< 0.001*
	5	*0.626*	*< 0.001*	*0.676*	*< 0.001*	*0.661*	*< 0.001*
	10	*0.606*	*< 0.001*	*0.670*	*< 0.001*	*0.670*	*< 0.001*
Variance	1	*0.662*	*< 0.001*	*0.740*	*< 0.001*	*0.660*	*< 0.001*
	2	*0.653*	*< 0.001*	*0.729*	*< 0.001*	*0.652*	*< 0.001*
	3	*0.651*	*< 0.001*	*0.730*	*< 0.001*	*0.648*	*< 0.001*
	5	*0.663*	*< 0.001*	*0.731*	*< 0.001*	*0.666*	*< 0.001*
	10	*0.643*	*< 0.001*	*0.717*	*< 0.001*	*0.652*	*< 0.001*
Correlation	1	*0.579*	*< 0.001*	*0.568*	*< 0.001*	*0.673*	*< 0.001*
	2	*0.069*	*0.671*	*0.075*	*0.645*	*0.107*	*0.511*
	3	*-0.176*	*0.276*	*-0.170*	*0.293*	*-0.177*	*0.274*
	5	*-0.375*	*0.017*	*-0.358*	*0.023*	*-0.398*	*0.011*
	10	*-0.440*	*0.004*	*-0.398*	*0.011*	*-0.514*	*0.001*
Entropy	1	*-0.562*	*< 0.001*	*-0.487*	*0.001*	*-0.550*	*< 0.001*
	2	*-0.577*	*< 0.001*	*-0.500*	*0.001*	*-0.568*	*< 0.001*
	3	*-0.587*	*< 0.001*	*-0.527*	*< 0.001*	*-0.591*	*< 0.001*
	5	*-0.608*	*< 0.001*	*-0.560*	*< 0.001*	*-0.636*	*< 0.001*
	10	*-0.617*	*< 0.001*	*-0.582*	*< 0.001*	*-0.647*	*< 0.001*
MCS_v		*0.121*	*0.332*	*0.431*	*0.012*	*0.125*	*0.221*
LTMCS		*0.425*	*0.015*	*0.218*	*0.010*	*0.354*	*0.012*
MI_{SPORT}		*-0.357*	*0.002*	*-0.456*	*0.005*	*-0.551*	*0.001*

Abbreviations: d = particular displacement distance, r_s = Spearman's rank correlation coefficients, ASM = angular second moment, IDM = inverse difference moment, MCS_v = modulation complexity score for VMAT, LTMCS

= leaf travel modulation complexity score, MI_{SPORT} = modulation index supporting station parameter optimized radiation therapy

In the cases of 2%/2 mm gamma criteria, every value of r_s of textural features for Trilogy™ and textural features except for *correlation* (d = 2 and 3) for TrueBeam™ was statistically significant with p values less than 0.05. In the cases 1%/2 mm gamma criteria, every value of r_s of textural features for Trilogy™ and textural features except for *correlation* (d = 2 and 3) and *IDM* (d = 1) for TrueBeam™ was statistically significant with p values less than 0.05. In the case of 2%/1 mm, only the values of r_s of *ASM* (d = 1 and 5), *IDM* (d = 1 and 5), *contrast* (d = 1, 5 and 10) and *variance* (d = 1, 5 and 10) for Trilogy™ and textural features except for *correlation* (d = 2 and 3) for TrueBeam™ were statistically significant. In the case of conventional modulation indices, the value of r_s of MI_{SPORT} with the passing rates of 2%/2 mm, 2%/1 mm and 1%/2 mm for both Trilogy™ and TrueBeam™ were statistically significant.

In the results for Trilogy™, the values of r_s for *ASM* (d = 5), *IDM* (d = 1 and 5), every *contrast*, every *variance* and *correlation* (d = 5) to the global gamma passing rates with gamma criterion of 2%/2 mm were higher than 0.5. In the case of 2%/1 mm, the values of r_s for *IDM* (d = 1), *contrast* (d = 1) and every *variance* to the gamma passing rates were higher than 0.4. In the case of 1%/2 mm, except for *ASM* (d = 1), every value of r_s between textural features and global gamma passing rates was higher than 0.6. In this case, the values of r_s of *ASM* (d = 5 and 10), *contrast* (d = 1) were higher than 0.7.

The values of r_s between *ASM* (d = 5), *IDM* (d = 1 and 5), *contrast* (d = 1 and 5) and *variance* (d = 1, 5 and 10) were always higher with statistical significance than those of conventional modulation indices to the passing rates

with every gamma criterion for Trilogy™.

In the results for TrueBeam™, the values of r_s for *ASM* (d = 10), *IDM* (d = 5 and 10), *contrast* (d = 5 and 10), every *variance* and *entropy* (d = 5 and 10) to the global gamma passing rates with gamma criterion of 2%/2 mm were higher than 0.6. In the case of 2%/1 mm, the values of r_s for every *variance* to the gamma passing rates were higher than 0.7. In the case of 1%/2 mm, the values of r_s for *ASM* (d = 3, 5 and 10), *IDM* (d = 5 and 10), *contrast* (d = 3, 5 and 10), every *variance, correlation* (d = 1) and *entropy* (d = 5 and 10) to global gamma passing rates was higher than 0.6. In this case, the values of r_s of *ASM* (d = 5 and 10), *contrast* (d = 1) were higher than 0.6.

The values of r_s between *ASM* (d = 3, 5 and 10), *IDM* (d = 3, 5 and 10), *contrast* (d = 3, 5 and 10), every *variance, correlation* (d = 1, 5 and 10) and *entropy* (d = 2, 3, 5 and 10) were always higher with statistical significance than those of conventional modulation indices to the passing rates with every gamma criterion for TrueBeam™.

The values of r_s with p values of textural features from Trilogy™ and TrueBeam™, and the conventional modulation indices with the local gamma passing rates of pretreatment QA are shown in Table 10 and 11, respectively.

TABLE 10. Correlations of textural features calculated from a single fluence map and conventional modulation indices with local gamma passing rates for Trilogy™

		2%/2 mm		2%/1 mm		1%/2 mm	
	d	r_s	*p*	r_s	*p*	r_s	*p*
ASM	1	*0.462*	*0.003*	*0.595*	*< 0.001*	*0.509*	*0.001*
	5	*0.587*	*< 0.001*	*0.539*	*< 0.001*	*0.655*	*< 0.001*
	10	*0.523*	*0.001*	*0.512*	*0.001*	*0.607*	*< 0.001*
IDM	1	*-0.506*	*0.001*	*-0.426*	*0.006*	*-0.616*	*< 0.001*
	5	*-0.494*	*0.001*	*-0.402*	*0.010*	*-0.560*	*< 0.001*
	10	*-0.438*	*0.005*	-0.303	0.057	*-0.501*	*0.001*
Contrast	1	*0.547*	*< 0.001*	*0.578*	*< 0.001*	*0.620*	*< 0.001*
	5	*0.557*	*< 0.001*	*0.515*	*0.001*	*0.605*	*< 0.001*
	10	*0.586*	*< 0.001*	*0.511*	*0.001*	*0.619*	*< 0.001*
Variance	1	*0.519*	*0.001*	*0.527*	*< 0.001*	*0.569*	*< 0.001*
	5	*0.523*	*0.001*	*0.499*	*0.001*	*0.559*	*< 0.001*
	10	*0.463*	*0.003*	*0.451*	*0.003*	*0.516*	*0.001*
Correlation	1	*-0.465*	*0.002*	*-0.469*	*0.002*	*-0.566*	*< 0.001*
	5	*-0.582*	*< 0.001*	*-0.505*	*0.001*	*-0.648*	*< 0.001*
	10	*-0.567*	*< 0.001*	*-0.431*	*0.005*	*-0.609*	*< 0.001*
Entropy	1	*-0.501*	*0.001*	*-0.513*	*0.001*	*-0.551*	*< 0.001*
	5	*-0.475*	*0.002*	*-0.485*	*0.002*	*-0.551*	*< 0.001*
	10	*-0.473*	*0.002*	*-0.489*	*0.001*	*-0.552*	*< 0.001*
MCS_v		0.186	0.251	*0.365*	*0.021*	0.157	0.334
LTMCS		*0.312*	*0.050*	*0.371*	*0.018*	*0.343*	*0.030*
MI_{SPORT}		*-0.455*	*0.003*	*-0.490*	*0.001*	*-0.502*	*0.001*

Abbreviations: d = particular displacement distance, r_s = Spearman's rank correlation coefficients, ASM = angular second moment, IDM = inverse difference moment, MCS_v = modulation complexity score for VMAT, LTMCS = leaf travel modulation complexity score, MI_{SPORT} = modulation index supporting station parameter optimized radiation therapy

TABLE 11. Correlations of textural features calculated from a single fluence map and conventional modulation indices with local gamma passing rates for TrueBeam™

		2%/2 mm		2%/1 mm		1%/2 mm	
	d	r_s	*p*	r_s	*p*	r_s	*p*
ASM	1	*0.299*	*0.061*	*0.426*	*0.006*	*0.381*	*0.015*
	2	*0.308*	*0.053*	*0.472*	*0.002*	*0.387*	*0.014*
	3	*0.386*	*0.014*	*0.533*	*< 0.001*	*0.463*	*0.003*
	5	*0.406*	*0.009*	*0.522*	*0.001*	*0.479*	*0.002*
	10	*0.409*	*0.009*	*0.537*	*< 0.001*	*0.488*	*0.001*
IDM	1	*0.359*	*0.023*	*0.341*	*0.031*	*0.341*	*0.031*
	2	*-0.212*	*0.190*	*-0.291*	*0.069*	*-0.245*	*0.128*
	3	*-0.337*	*0.034*	*-0.469*	*0.002*	*-0.390*	*0.013*
	5	*-0.485*	*0.002*	*-0.587*	*< 0.001*	*-0.526*	*0.001*
	10	*-0.550*	*< 0.001*	*-0.604*	*< 0.001*	*-0.578*	*< 0.001*
Contrast	1	*0.174*	*0.283*	*0.361*	*0.022*	*0.205*	*0.204*
	2	*0.296*	*0.064*	*0.505*	*0.001*	*0.333*	*0.036*
	3	*0.348*	*0.028*	*0.557*	*< 0.001*	*0.383*	*0.015*
	5	*0.406*	*0.009*	*0.596*	*< 0.001*	*0.439*	*0.005*
	10	*0.483*	*0.002*	*0.610*	*< 0.001*	*0.514*	*0.001*
Variance	1	*0.403*	*0.010*	*0.616*	*< 0.001*	*0.443*	*0.004*
	2	*0.397*	*0.011*	*0.606*	*< 0.001*	*0.435*	*0.005*
	3	*0.395*	*0.012*	*0.603*	*< 0.001*	*0.434*	*0.005*
	5	*0.415*	*0.008*	*0.615*	*< 0.001*	*0.457*	*0.003*
	10	*0.410*	*0.009*	*0.597*	*< 0.001*	*0.449*	*0.004*
Correlation	1	*0.552*	*0.000*	*0.596*	*< 0.001*	*0.579*	*0.000*
	2	*0.167*	*0.303*	*0.070*	*0.668*	*0.170*	*0.296*
	3	*-0.036*	*0.824*	*-0.179*	*0.270*	*-0.048*	*0.768*
	5	*-0.201*	*0.215*	*-0.348*	*0.028*	*-0.220*	*0.173*
	10	*-0.355*	*0.023*	*-0.420*	*0.007*	*-0.387*	*0.014*
Entropy	1	*-0.309*	*0.053*	*-0.472*	*0.002*	*-0.396*	*0.011*
	2	*-0.337*	*0.034*	*-0.498*	*0.001*	*-0.416*	*0.008*
	3	*-0.348*	*0.028*	*-0.510*	*0.001*	*-0.419*	*0.007*
	5	*-0.384*	*0.015*	*-0.537*	*< 0.001*	*-0.451*	*0.004*
	10	*-0.377*	*0.016*	*-0.533*	*< 0.001*	*-0.446*	*0.004*
MCS_v		*0.168*	*0.542*	*0.374*	*0.052*	*0.352*	*0.452*
LTMCS		*0.388*	*0.005*	*0.405*	*0.010*	*0.052*	*0.08*
MI_{SPORT}		*-0.357*	*0.485*	*-0.355*	*0.008*	*-0.25*	*0.005*

Abbreviations: d = particular displacement distance, r_s = Spearman's rank correlation coefficients, ASM = angular second moment, IDM = inverse

difference moment, MCS_v = modulation complexity score for VMAT, LTMCS = leaf travel modulation complexity score, MI_{SPORT} = modulation index supporting station parameter optimized radiation therapy

In the results of Triogy™, every value of r_s of the textural features, as well as the conventional modulation indices to the local gamma passing rates with gamma criteria of 2%/2 mm, 2%/1 mm and 1%/2 mm were statistically significant with p values less than 0.05, except for the MCS_v to the passing rates with criteria of 2%/2 mm and 1%/2 mm.

In the case of 2%/2 mm, the values of r_s of *ASM* (d = 5 and 10), *IDM* (d = 1), every *contrast*, *variance* (d = 1 and 5), *correlation* (d = 5 and 10) and *entropy* (d = 1) were higher than 0.5. In the case of 2%/1 mm, the values of r_s of every *ASM*, every *contrast*, *variance* (d = 1), *correlation* (d = 5) and *entropy* (d = 1) were higher than 0.5. In the case of 1%/2 mm, the values of r_s for *ASM* (d = 5 and 10), *IDM* (d = 1), every *contrast*, and *correlation* (d = 5 and 10) were higher than 0.6.

The values of r_s for *ASM* (d = 1, 5 and 10), *contrast* (d = 1, 5 and 10), *variance* (d = 1 and 5), *correlation* (d = 5) and *entropy* (d = 1) were always higher than the conventional modulation indices with statistical significances.

In the results of TrueBeam™, the values of r_s of *ASM* (d = 3, 5 and 10), *IDM* (d = 1, 3, 5 and 10), *contrast* (d = 3, 5 and 10), every *variance*, *correlation* (d = 1 and 10) and *entropy* (d = 2, 3, 5 and10) as well as LTMCS in the conventional modulation indices to the local gamma passing rates with gamma criteria of 2%/2 mm, 2%/1 mm and 1%/2 mm were statistically significant with p values less than 0.05.

In the case of 2%/2 mm, the values of r_s of *ASM* (d = 5 and 10), *IDM* (d = 5 and 10), *contrast* (d = 5 and 10), *variance* (d = 1, 5 and 10) and *correlation* (d = 1) were higher than 0.4. In the case of 2%/1 mm, the values of r_s of *IDM* (d

= 10), *contrast* (d = 10) and every *variance* were higher than 0.6. In the case of 1%/2 mm, the values of r_s for *IDM* (d = 5 and 10), *contrast* (d = 10) and *correlation* (d = 10) were higher than 0.5.

The values of r_s for *ASM* (d = 5 and 10), *IDM* (d = 5 and 10), *contrast* (d = 5 and 10), every *variance* and *correlation* (d = 1) were always higher than the conventional modulation indices with statistical significances.

III.C.1.2. Edge-enhanced fluence map

The values of r_s and corresponding p values of each textural feature calculated from edge-enhanced fluence map for Trilogy™ and TrueBeam™ to global gamma passing rates are shown in Table 12 and 13, respectively.

TABLE 12. The values of r_s between textural features calculated from edge-enhanced fluence map and global gamma passing rates for Trilogy™

		2%/2 mm		1%/2 mm		2%/1 mm	
	d	r_s	*p*	r_s	*p*	r_s	*p*
ASM	1	0.373	0.018	0.623	< 0.001	0.174	0.282
	5	0.400	0.011	0.569	< 0.001	0.133	0.415
	10	0.381	0.015	0.571	< 0.001	0.187	0.249
IDM	1	-0.610	< 0.001	-0.690	< 0.001	-0.503	0.001
	5	-0.582	< 0.001	-0.713	< 0.001	-0.417	0.007
	10	-0.540	< 0.001	-0.668	< 0.001	-0.362	0.022
Contrast	1	0.546	< 0.001	0.744	< 0.001	0.487	0.001
	5	0.570	< 0.001	0.725	< 0.001	0.450	0.004
	10	0.554	< 0.001	0.740	< 0.001	0.402	0.010
Variance	1	0.486	0.001	0.623	< 0.001	0.485	0.002
	5	0.507	0.001	0.630	< 0.001	0.490	0.001
	10	0.486	0.001	0.587	< 0.001	0.530	< 0.001
Correlation	1	-0.390	0.013	-0.648	< 0.001	-0.279	0.082
	5	-0.486	0.001	-0.678	< 0.001	-0.247	0.125
	10	-0.374	0.017	-0.633	< 0.001	-0.093	0.569
Entropy	1	-0.303	0.057	-0.581	< 0.001	-0.210	0.194
	5	-0.363	0.021	-0.594	< 0.001	-0.201	0.213
	10	-0.312	0.050	-0.597	< 0.001	-0.200	0.216

Abbreviations: d = particular displacement distance, r_s = Spearman's rank correlation coefficient, ASM = angular second moment, IDM = inverse difference moment

TABLE 13. The values of r_s between textural features calculated from edge-enhanced fluence map and global gamma passing rates for TrueBeam™

		2%/2 mm		1%/2 mm		2%/1 mm	
	d	r_s	*p*	r_s	*p*	r_s	*p*
ASM	1	0.296	0.063	0.353	0.026	0.251	0.118
	5	0.459	0.003	0.532	< 0.001	0.405	0.010
	10	0.515	0.001	0.575	< 0.001	0.460	0.003
IDM	1	0.108	0.507	0.140	0.390	0.071	0.661
	5	-0.617	< 0.001	-0.635	< 0.001	-0.617	< 0.001
	10	-0.736	< 0.001	-0.744	< 0.001	-0.695	< 0.001
Contrast	1	0.494	0.001	0.436	0.005	0.495	0.001
	5	0.693	< 0.001	0.678	< 0.001	0.694	< 0.001
	10	0.705	< 0.001	0.701	< 0.001	0.703	< 0.001
Variance	1	0.707	< 0.001	0.665	< 0.001	0.725	< 0.001
	5	0.716	< 0.001	0.671	< 0.001	0.730	< 0.001
	10	0.709	< 0.001	0.668	< 0.001	0.724	< 0.001
Correlation	1	0.430	0.006	0.410	0.009	0.440	0.005
	5	-0.363	0.021	-0.396	0.011	-0.345	0.029
	10	-0.418	0.007	-0.495	0.001	-0.382	0.015
Entropy	1	-0.313	0.049	-0.356	0.024	-0.246	0.126
	5	-0.443	0.004	-0.491	0.001	-0.373	0.018
	10	-0.536	0< 0.001	-0.581	< 0.001	-0.459	0.003

Abbreviations: d = particular displacement distance, r_s = Spearman's rank correlation coefficient, ASM = angular second moment, IDM = inverse difference moment

In the results for Trilogy™, with the exceptions of r_s values between global 2%/2 mm and *entropy* (d = 1), global 2%/1 mm and *ASM* (d = 1, 5 and 10), and *correlation* (d = 1, 5 and 10) and *entropy* (d = 1, 5 and 10), every value of r_s was statistically significant, showing p values less than 0.05. In the results for TrueBeam™, every value of r_s of the textural features was statistically significant with corresponding p values less than 0.05, except for *ASM* (d = 1) and *IDM* (d = 1). The highest correlation was observed in *contrast* (d = 1) and global 1%/2 mm (r_s = 0.744 with $p < 0.001$) for Trilogy™, and *variance* (d = 5) and global 2%/1 mm (r_s = 0.730 with $p < 0.001$) for TrueBeam™. The values of r_s of *contrast* (d = 1) for Trilogy™ and *variance* (d = 5) for TrueBeam™ calculated with edge-enhanced fluence maps to global gamma passing rates were generally higher than those of *contrast* (d = 1) and *variance* (d = 1) with non-edge-enhanced fluence maps, which showed the best performance in our feasibility study.[28]

The values of r_s and corresponding p values of each textural feature calculated from edge-enhanced fluence map for Trilogy™ and TrueBeam™ to local gamma passing rates are shown in Table 14 and 15, respectively.

TABLE 14. The values of r_s between textural features calculated from edge-enhanced fluence map and local gamma passing rates for Trilogy™

		2%/2 mm		1%/2 mm		2%/1 mm	
	d	r_s	*p*	r_s	*p*	r_s	*p*
ASM	1	0.522	0.001	0.603	< 0.001	0.469	0.002
	5	0.421	0.007	0.496	0.001	0.356	0.024
	10	0.389	0.013	0.489	0.001	0.334	0.035
IDM	1	-0.504	0.001	-0.605	< 0.001	-0.451	0.003
	5	-0.528	< 0.001	-0.571	< 0.001	-0.494	0.001
	10	-0.462	0.003	-0.528	< 0.001	-0.402	0.010
Contrast	1	0.588	< 0.001	0.640	< 0.001	0.644	< 0.001
	5	0.593	< 0.001	0.629	< 0.001	0.613	< 0.001
	10	0.603	< 0.001	0.642	< 0.001	0.584	< 0.001
Variance	1	0.519	0.001	0.525	0.001	0.594	< 0.001
	5	0.538	< 0.001	0.538	< 0.001	0.599	< 0.001
	10	0.464	0.003	0.477	0.002	0.549	< 0.001
Correlation	1	-0.473	0.002	-0.585	< 0.001	-0.458	0.003
	5	-0.565	< 0.001	-0.633	< 0.001	-0.492	0.001
	10	-0.561	< 0.001	-0.605	< 0.001	-0.430	0.006
Entropy	1	-0.467	0.002	-0.527	< 0.001	-0.470	0.002
	5	-0.447	0.004	-0.529	< 0.001	-0.437	0.005
	10	-0.443	0.004	-0.534	< 0.001	-0.418	0.007

Abbreviations: *d* = particular displacement distance, r_s = Spearman's rank correlation coefficient, ASM = angular second moment, IDM = inverse difference moment

TABLE 15. The values of r_s between textural features calculated from edge-enhanced fluence map and local gamma passing rates for TrueBeam™

		2%/2 mm		1%/2 mm		2%/1 mm	
	d	r_s	*p*	r_s	*p*	r_s	*p*
ASM	1	0.264	0.100	0.286	0.073	0.218	0.176
	5	0.335	0.034	0.389	0.013	0.342	0.031
	10	0.364	0.021	0.430	0.006	0.397	0.011
IDM	1	0.219	0.175	0.175	0.280	0.064	0.697
	5	-0.357	0.024	-0.453	0.003	-0.621	< 0.001
	10	-0.502	0.001	-0.568	< 0.001	-0.710	< 0.001
Contrast	1	0.175	0.279	0.234	0.147	0.445	0.004
	5	0.416	0.008	0.476	0.002	0.682	< 0.001
	10	0.459	0.003	0.522	0.001	0.700	< 0.001
Variance	1	0.417	0.007	0.489	0.001	0.719	< 0.001
	5	0.432	0.005	0.500	0.001	0.729	< 0.001
	10	0.421	0.007	0.496	0.001	0.725	< 0.001
Correlation	1	0.403	0.010	0.435	0.005	0.520	0.001
	5	-0.192	0.234	-0.213	0.188	-0.322	0.043
	10	-0.328	0.039	-0.361	0.022	-0.385	0.014
Entropy	1	-0.248	0.123	-0.264	0.099	-0.189	0.244
	5	-0.304	0.056	-0.347	0.028	-0.306	0.055
	10	-0.360	0.022	-0.407	0.009	-0.390	0.013

Abbreviations: d = particular displacement distance, r_s = Spearman's rank correlation coefficient, ASM = angular second moment, IDM = inverse difference moment

All values of r_s to local gamma passing rates were statistically significant, showing p values less than 0.05 in the results of Trilogy™ while those for *ASM* (d = 5 and 10), *IDM* (d = 5 and 10), *contrast* (d = 5 and 10), every *variance*, *correlation* (d = 1 and 10) and *entropy* (d = 10) were statistically significant with p values less than 0.05 in the results of TrueBeam™. The highest value of r_s was observed between *contrast* (d = 1) and gamma passing rates with 2%/1 mm (r_s = 0.644 with $p < 0.001$) for Trilogy™, and *variation* (d = 5) and gamma passing rates with 2%/1 mm (r_s = 0.729 with $p < 0.001$) for TrueBeam™. *contrast* (d = 1) for Trilogy™ and *variance* (d = 5) for TrueBeam™ always showed higher values of r_s with statistical significances than the other textural features to local gamma passing rates with every gamma criterion tested in this study. The values of r_s of *contrast* (d = 1) for Trilogy™ and *variance* (d = 5) for TrueBeam™ with edge-enhanced fluence map were always higher than those of *contrast* (d = 1) and *variance* (d = 1) with non-edge-enhanced fluence map.[28] In addition, *contrast* (d = 1) for Trilogy™ and *variance* (d = 5) for TrueBeam™ with edge-enhanced fluence map always showed higher correlations than did MCS_v, LTMCS and MI_{SPORT}.

III.C.1.3. Segmental fluence maps

The statistically significant correlations ($p < 0.05$) between textural features calculated with 5, 10, 20, 45, 90, 178 and 356 segments for Trilogy™ and the gamma passing rates are shown in Tables 16, 17, 18, 19, 20, 21 and 22, respectively.

TABLE 16. Statistically significant correlation coefficients between textural features calculated from fluence maps generated with 5 segments and the gamma passing rates for Trilogy™

		2%/2 mm				1%/2 mm				2%/1 mm			
		Global		Local		Global		Local		Global		Local	
	d	r_s	*p*	r_s	*p*	r_s	*p*	r_s	*p*	r_s	*p*	r_s	*p*
ASM	5	-	-	-	-	-	-	0.314	0.048	-	-	-	-
	10	0.501	0.001	-	-	0.512	0.001	0.591	< 0.001	0.522	0.001	-	-
IDM	5	-	-	-0.420	0.007	-	-	-0.452	0.003	-	-	-	-
	10	-	-	-0.352	0.026	-	-	-0.416	0.008	-	-	-	-
Contrast	1	0.660	< 0.001	0.585	< 0.001	0.743	< 0.001	0.778	< 0.001	0.570	< 0.001	0.465	0.002
	5	0.640	< 0.001	0.611	< 0.001	0.674	< 0.001	0.758	< 0.001	0.505	0.001	0.333	0.036
	10	0.683	< 0.001	0.613	< 0.001	0.715	< 0.001	0.801	< 0.001	0.589	< 0.001	0.394	0.012
Variance	5	0.545	< 0.001	0.640	< 0.001	0.543	< 0.001	0.658	< 0.001	0.395	0.012	0.391	0.013
Correlation	1	-0.663	< 0.001	-0.600	< 0.001	-0.741	< 0.001	-0.804	< 0.001	-0.609	< 0.001	-0.473	0.002
	5	-0.567	< 0.001	-0.634	< 0.001	-0.633	< 0.001	-0.735	< 0.001	-0.449	0.004	-0.340	0.032
	10	-0.563	< 0.001	-0.563	< 0.001	-0.633	< 0.001	-0.733	< 0.001	-0.432	0.005	-	-
Entropy	5	-0.374	0.018	-	-	-0.337	0.033	-0.450	0.004	-0.380	0.016	-	-
	10	-0.529	< 0.001	-0.360	0.023	-0.542	< 0.001	-0.650	< 0.001	-0.515	0.001	-	-

Abbreviations: global, global gamma evaluation; local, local gamma evaluation; *d* = particular displacement distance; r_s = Spearman's rank correlation coefficient; ASM, angular second moment; IDM, inverse difference moment.

TABLE 17. Statistically significant correlation coefficients between textural features calculated from fluence maps generated with 10 segments and the gamma passing rates for Trilogy™

		2%/2 mm				1%/2 mm				2%/1 mm			
		Global		Local		Global		Local		Global		Local	
	d	r_s	*p*	r_s	*p*	r_s	*p*	r_s	*p*	r_s	*p*	r_s	*p*
ASM	5	0.373	0.018	-	-	0.319	0.045	0.385	0.014	0.461	0.003	-	-
	10	0.480	0.002	0.315	0.048	0.495	0.001	0.591	< 0.001	0.504	0.001	-	-
IDM	5	-	-	-0.361	0.022	-	-	-0.391	0.013	-	-	-	-
	10	-	-	-0.341	0.031	-	-	-0.388	0.013	-	-	-	-
Contrast	1	0.686	< 0.001	0.582	< 0.001	0.748	< 0.001	0.792	< 0.001	0.629	< 0.001	0.469	0.002
	5	0.656	< 0.001	0.632	< 0.001	0.662	< 0.001	0.759	< 0.001	0.570	< 0.001	0.406	0.009
	10	0.666	< 0.001	0.573	< 0.001	0.692	< 0.001	0.798	< 0.001	0.626	< 0.001	0.422	0.007
Variance	5	0.472	0.002	0.427	0.006	0.430	0.006	0.531	< 0.001	0.383	0.015	-	-
	10	-	-	-	-	-	-	-	-	-	-	-	-
Correlation	1	-0.642	< 0.001	-0.564	< 0.001	-0.725	< 0.001	-0.791	< 0.001	-0.602	< 0.001	-0.457	0.003
	5	-0.581	< 0.001	-0.638	< 0.001	-0.640	< 0.001	-0.733	< 0.001	-0.476	0.002	-0.354	0.025
	10	-0.604	< 0.001	-0.576	< 0.001	-0.675	< 0.001	-0.759	< 0.001	-0.495	0.001	-0.327	0.039
Entropy	1	-	-	-	-	-	-	-0.403	0.010	-	-	-	-
	5	-0.442	0.004	-0.332	0.036	-0.445	0.004	-0.581	< 0.001	-0.434	0.005	-	-
	10	-0.505	0.001	-0.376	0.017	-0.533	< 0.001	-0.655	< 0.001	-0.498	0.001	-	-

Abbreviations: global, global gamma evaluation; local, local gamma evaluation; *d* = particular displacement distance; r_s = Spearman's rank correlation coefficient; ASM, angular second moment; IDM, inverse difference moment.

TABLE 18. Statistically significant correlation coefficients between textural features calculated from fluence maps generated with 20 segments and the gamma passing rates for Trilogy™

		2%/2 mm				1%/2 mm				2%/1 mm			
		Global		Local		Global		Local		Global		Local	
	d	r_s	*p*	r_s	*p*	r_s	*p*	r_s	*p*	r_s	*p*	r_s	*p*
ASM	1	-	-	-	-	-	-	0.326	0.040	-	-	-	-
	5	0.372	0.018	-	-	0.378	0.016	0.469	0.002	0.436	0.005	-	-
	10	0.478	0.002	0.398	0.011	0.518	0.001	0.621	< 0.001	0.511	0.001	-	-
IDM	5	-	-	-0.355	0.024	-	-	-0.404	0.010	-	-	-	-
	10	-	-	-0.389	0.013	-	-	-0.430	0.006	-	-	-	-
Contrast	1	0.652	< 0.001	0.585	< 0.001	0.703	< 0.001	0.779	< 0.001	0.629	< 0.001	0.469	0.002
	5	0.621	< 0.001	0.563	< 0.001	0.625	< 0.001	0.722	< 0.001	0.564	< 0.001	0.350	0.027
	10	0.622	< 0.001	0.510	0.001	0.649	< 0.001	0.744	< 0.001	0.600	< 0.001	0.368	0.019
Variance	5	0.446	0.004	0.342	0.031	0.395	0.012	0.503	0.001	0.435	0.005	-	-
	10	-	-	0.322	0.043	-	-	0.362	0.022	-	-	-	-
Correlation	1	-0.622	< 0.001	-0.549	< 0.001	-0.700	< 0.001	-0.774	< 0.001	-0.586	< 0.001	-0.413	0.008
	5	-0.611	< 0.001	-0.636	< 0.001	-0.670	< 0.001	-0.748	< 0.001	-0.504	0.001	-0.355	0.025
	10	-0.644	< 0.001	-0.592	< 0.001	-0.709	< 0.001	-0.782	< 0.001	-0.538	< 0.001	-0.362	0.022
Entropy	1	-0.385	0.014	-	-	-0.393	0.012	-0.519	0.001	-0.406	0.009	-	-
	5	-0.454	0.003	-0.351	0.026	-0.478	0.002	-0.606	< 0.001	-0.448	0.004	-	-
	10	-0.514	0.001	-0.389	0.013	-0.550	< 0.001	-0.658	< 0.001	-0.507	0.001	-	-

Abbreviations: global, global gamma evaluation; local, local gamma evaluation; *d* = particular displacement distance; r_s = Spearman's rank correlation coefficient; ASM, angular second moment; IDM, inverse difference moment.

TABLE 19. Statistically significant correlation coefficients between textural features calculated from fluence maps generated with 45 segments and the gamma passing rates for Trilogy™

		2%/2 mm				1%/2 mm				2%/1 mm			
		Global		Local		Global		Local		Global		Local	
	d	r_s	*p*	r_s	*p*	r_s	*p*	r_s	*p*	r_s	*p*	r_s	*p*
ASM	1	0.355	0.025	0.381	0.015	0.554	< 0.001	0.415	0.008	-	-	0.389	0.013
	5	0.357	0.024	0.424	0.006	0.600	< 0.001	0.471	0.002	-	-	0.406	0.009
	10	0.349	0.027	0.461	0.003	0.624	< 0.001	0.517	0.001	-	-	0.428	0.006
Contrast	1	0.314	0.049	-	-	0.447	0.004	0.344	0.030	0.318	0.045	0.323	0.042
Variance	1	-0.324	0.042	-	-	-0.332	0.037	-0.340	0.032	-	-	-	-
Correlation	1	-0.561	< 0.001	-0.595	< 0.001	-0.760	< 0.001	-0.672	< 0.001	-0.470	0.002	-0.596	< 0.001
	5	-0.604	< 0.001	-0.603	< 0.001	-0.742	< 0.001	-0.655	< 0.001	-0.365	0.020	-0.540	< 0.001
	10	-0.532	< 0.001	-0.625	< 0.001	-0.752	< 0.001	-0.673	< 0.001	-0.312	0.050	-0.527	< 0.001
Entropy	1	-0.386	0.014	-0.476	0.002	-0.632	< 0.001	-0.529	< 0.001	-	-	-0.477	0.002
	5	-0.416	0.008	-0.512	0.001	-0.671	< 0.001	-0.582	< 0.001	-	-	-0.488	0.001
	10	-0.395	0.012	-0.544	< 0.001	-0.680	< 0.001	-0.614	< 0.001	-	-	-0.507	0.001

Abbreviations: global, global gamma evaluation; local, local gamma evaluation; *d* = particular displacement distance; r_s = Spearman's rank correlation coefficient; ASM, angular second moment.

TABLE 20. Statistically significant correlation coefficients between textural features calculated from fluence maps generated with 90 segments and the gamma passing rates for Trilogy™

		2%/2 mm				1%/2 mm				2%/1 mm			
		Global		Local		Global		Local		Global		Local	
	d	r_s	*p*	r_s	*p*	r_s	*p*	r_s	*p*	r_s	*p*	r_s	*p*
ASM	1	0.372	0.018	0.503	0.001	0.598	< 0.001	0.536	< 0.001	-	-	0.391	0.013
	5	0.418	0.007	0.550	< 0.001	0.649	< 0.001	0.594	< 0.001	-	-	0.462	0.003
	10	0.445	0.004	0.564	< 0.001	0.691	< 0.001	0.621	< 0.001	-	-	0.471	0.002
Contrast	1	0.355	0.025	0.380	0.016	0.518	0.001	0.419	0.007	-	-	0.416	0.008
Variance	1	-	-	-	-	-	-	-0.334	0.035	-	-	-	-
Correlation	1	-0.544	< 0.001	-0.571	< 0.001	-0.751	< 0.001	-0.648	< 0.001	-0.428	0.006	-0.558	< 0.001
	5	-0.574	< 0.001	-0.588	< 0.001	-0.717	< 0.001	-0.634	< 0.001	-0.356	0.024	-0.521	0.001
	10	-0.561	< 0.001	-0.626	< 0.001	-0.744	< 0.001	-0.662	< 0.001	-0.352	0.026	-0.531	< 0.001
Entropy	1	-0.454	0.003	-0.567	< 0.001	-0.665	< 0.001	-0.619	< 0.001	-	-	-0.497	0.001
	5	-0.446	0.004	-0.579	< 0.001	-0.675	< 0.001	-0.636	< 0.001	-	-	-0.517	0.001
	10	-0.423	0.007	-0.590	< 0.001	-0.691	< 0.001	-0.650	< 0.001	-	-	-0.532	< 0.001

Abbreviations: global, global gamma evaluation; local, local gamma evaluation; *d* = particular displacement distance; r_s = Spearman's rank correlation coefficient; ASM, angular second moment.

TABLE 21. Statistically significant correlation coefficients between textural features calculated from fluence maps generated with 178 segments and the gamma passing rates for Trilogy™

		2%/2 mm				1%/2 mm				2%/1 mm			
		Global		Local		Global		Local		Global		Local	
	d	r_s	*p*	r_s	*p*	r_s	*p*	r_s	*p*	r_s	*p*	r_s	*p*
ASM	1	0.445	0.004	0.513	0.001	0.672	< 0.001	0.601	< 0.001	-	-	0.436	0.005
	5	0.426	0.006	0.481	0.002	0.646	< 0.001	0.572	< 0.001	-	-	0.410	0.009
	10	0.419	0.007	0.530	< 0.001	0.671	< 0.001	0.609	< 0.001	-	-	0.475	0.002
IDM	10	-	-	-0.405	0.010	-	-	-0.398	0.011	-	-	-0.375	0.017
Contrast	1	0.353	0.026	0.320	0.044	0.520	0.001	0.386	0.014	0.457	0.003	0.410	0.009
	5	-	-	0.312	0.050	0.449	0.004	0.339	0.032	0.334	0.035	0.350	0.027
Correlation	1	-0.542	< 0.001	-0.570	< 0.001	-0.764	< 0.001	-0.639	< 0.001	-0.403	0.010	-0.547	< 0.001
	5	-0.602	< 0.001	-0.582	< 0.001	-0.738	< 0.001	-0.641	< 0.001	-0.406	0.009	-0.540	< 0.001
	10	-0.533	< 0.001	-0.592	< 0.001	-0.695	< 0.001	-0.620	< 0.001	-	-	-0.452	0.003
Entropy	1	-0.424	0.006	-0.500	0.001	-0.658	< 0.001	-0.586	< 0.001	-	-	-0.447	0.004
	5	-0.423	0.006	-0.513	0.001	-0.663	< 0.001	-0.602	< 0.001	-	-	-0.472	0.002
	10	-0.427	0.006	-0.538	< 0.001	-0.684	< 0.001	-0.629	< 0.001	-	-	-0.497	0.001

Abbreviations: global, global gamma evaluation; local, local gamma evaluation; *d* = particular displacement distance; r_s = Spearman's rank correlation coefficient; ASM, angular second moment; IDM, inverse difference moment.

TABLE 22. Statistically significant correlation coefficients between textural features calculated from fluence maps generated with 356 segments (a single fluence map) and the gamma passing rates for Trilogy™

		2%/2 mm				1%/2 mm				2%/1 mm			
		Global		Local		Global		Local		Global		Local	
	d	r_s	*p*	r_s	*p*	r_s	*p*	r_s	*p*	r_s	*p*	r_s	*p*
ASM	1	0.350	0.027	0.462	0.003	0.542	< 0.001	0.509	0.001	0.329	0.038	0.595	< 0.001
	5	0.539	< 0.001	0.587	0.000	0.773	< 0.001	0.655	< 0.001	0.333	0.036	0.539	< 0.001
	10	0.468	0.002	0.523	0.001	0.712	< 0.001	0.607	< 0.001	-	-	0.512	0.001
IDM	1	-0.620	< 0.001	-0.506	0.001	-0.698	< 0.001	-0.616	< 0.001	-0.467	0.002	-0.426	0.006
	5	-0.599	< 0.001	-0.494	0.001	-0.687	< 0.001	-0.560	< 0.001	-0.386	0.014	-0.402	0.010
	10	-0.499	0.001	-0.438	0.005	-0.632	< 0.001	-0.501	0.001	-	-	-0.303	0.057
Contrast	1	0.536	< 0.001	0.547	< 0.001	0.718	< 0.001	0.620	< 0.001	0.473	0.002	0.578	< 0.001
	5	0.568	< 0.001	0.557	< 0.001	0.692	< 0.001	0.605	< 0.001	0.391	0.013	0.515	0.001
	10	0.525	0.001	0.586	< 0.001	0.695	< 0.001	0.619	< 0.001	0.321	0.043	0.511	0.001
Variance	1	0.551	< 0.001	0.519	0.001	0.688	< 0.001	0.569	< 0.001	0.481	0.002	0.527	< 0.001
	5	0.546	< 0.001	0.523	0.001	0.664	< 0.001	0.559	< 0.001	0.437	0.005	0.499	0.001
	10	0.543	< 0.001	0.463	0.003	0.635	< 0.001	0.516	0.001	0.478	0.002	0.451	0.003
Correlation	1	-0.368	0.019	-0.465	0.002	-0.619	< 0.001	-0.566	< 0.001	-	-	-0.469	0.002
	5	-0.502	0.001	-0.582	< 0.001	-0.694	< 0.001	-0.648	< 0.001	-	-	-0.505	0.001
	10	-0.379	0.016	-0.567	< 0.001	-0.634	< 0.001	-0.609	< 0.001	-	-	-0.431	0.005
Entropy	1	-0.343	0.030	-0.501	0.001	-0.634	< 0.001	-0.551	< 0.001	-	-	-0.513	0.001
	5	-0.367	0.020	-0.475	0.002	-0.619	< 0.001	-0.551	< 0.001	-	-	-0.485	0.002
	10	-0.350	0.027	-0.473	0.002	-0.622	< 0.001	-0.552	< 0.001	-	-	-0.489	0.001

Abbreviations: global, global gamma evaluation; local, local gamma evaluation; *d* = particular displacement distance; r_s = Spearman's rank correlation coefficient; ASM, angular second moment; IDM, inverse difference moment.

In the case of 5 segments, the highest correlation with statistical significance was observed between *correlation* (d = 1) and local gamma passing rate with gamma criterion of 1%/2 mm (r_s = -0.804 and $p < 0.001$). *Correlation* (d = 1) and *contrast* (d = 10) showed generally superior performance than the others, showing r_s values higher than 0.6 (all with $p < 0.001$) to all gamma passing rates except to the gamma passing rate with 2%/1 mm. For 10 segments, the highest correlation with statistical significance was observed between *contrast* (d = 10) and local gamma passing rate with 1%/2 mm (r_s = 0.798 and $p < 0.001$). *Contrast* (d = 1, 5 and 10) and *correlation* (d = 1) generally showed superior performance to the others showing r_s values higher than 0.6 most frequently. For 20 segments, the highest correlation was observed between *correlation* (d = 10) and local gamma passing rate with gamma criterion of 1%/2 mm (r_s = -0.782 and $p < 0.001$). *Contrast* (d = 1 and 10) and *correlation* (d = 10) generally showed superior performance to the others showing r_s values higher than 0.6 most frequently. For 45 segments, *correlation* (d = 1) showed the highest correlations to the global gamma passing rate with 1%/2 mm (r_s = -0.760 and $p < 0.001$). *Correlation* (d = 1 and 5) generally showed superior performance to the others showing r_s values higher than 0.6 most frequently. For 90 segments, the highest correlation was observed between *correlation* (d = 1) and global gamma passing rate with 1%/2 mm (r_s = -0.751 and $p < 0.001$). *Correlation* (d = 1 and 10) generally showed superior performance to the others showing r_s values higher than 0.6 most frequently. For 178 segments, the highest correlation with statistical significance was observed between *correlation* (d = 1) and global gamma

passing rate with gamma criterion of 1%/2 mm (r_s = -0.764 and $p < 0.001$). *Correlation* (d = 1 and 5) generally showed superior performance to the others showing r_s values higher than 0.6 most frequently. For 356 segments which was identical to the data shown in our feasibility study (Tables 8, 10), the highest correlation with statistical significance was observed between *ASM* (d = 5) and global gamma passing rate with gamma criterion of 1%/2 mm (r_s = 0.773 and $p < 0.001$). *Contrast* (d = 1), *variance* (d = 1), *ASM* (d = 5) and *IDM* (d = 1) generally showed superior performance to the others.

Several textural features showed r_s values higher than 0.75 to the global gamma passing rates, these were *ASM* (d = 5) with 356 segments, *correlation* (d = 1) with 45, 90 and 178 segments and *correlation* (d = 10) with 45 segments. In the case of local gamma passing rates, textural features showing r_s values higher than 0.79 were *correlation* (d = 1) with 5 and 10 segments, *contrast* (d = 1) with 10 segments and *contrast* (d = 10) with 5 and 10 segments. The highest correlation was observed between *correlation* (d = 1) with 5 segments and local gamma passing rates with gamma criterion of 1%/2 mm (r_s = -0.804 and $p < 0.001$). The statistically significant correlations ($p < 0.05$) between textural features calculated with 5, 10, 20, 45, 90, 178 and 356 segments for TrueBeam™ and the gamma passing rates are shown in Tables 23, 24, 25, 26, 27, 28 and 29, respectively.

TABLE 23. Statistically significant correlation coefficients between textural features calculated from fluence maps generated with 5 segments and the gamma passing rates for TrueBeam™

		2%/2 mm				1%/2 mm				2%/1 mm			
		Global		Local		Global		Local		Global		Local	
	d	r_s	*p*	r_s	*p*	r_s	*p*	r_s	*p*	r_s	*p*	r_s	*p*
ASM	1	0.667	< 0.001	0.513	0.001	0.674	< 0.001	0.526	< 0.001	0.683	< 0.001	0.650	< 0.001
	5	0.664	< 0.001	0.497	0.001	0.653	< 0.001	0.511	0.001	0.678	< 0.001	0.645	< 0.001
	10	0.686	< 0.001	0.512	0.001	0.677	< 0.001	0.531	0.000	0.705	< 0.001	0.662	< 0.001
IDM	1	0.662	< 0.001	0.491	0.001	0.653	< 0.001	0.506	0.001	0.671	< 0.001	0.656	< 0.001
	5	0.587	< 0.001	0.422	0.007	0.540	< 0.001	0.409	0.009	0.624	< 0.001	0.596	< 0.001
	10	0.579	< 0.001	0.422	0.007	0.532	< 0.001	0.396	0.011	0.607	< 0.001	0.587	< 0.001
Contrast	5	0.701	< 0.001	0.597	< 0.001	0.781	< 0.001	0.650	< 0.001	0.624	< 0.001	0.628	< 0.001
	10	0.758	< 0.001	0.646	< 0.001	0.827	< 0.001	0.700	< 0.001	0.703	< 0.001	0.693	< 0.001
Variance	5	0.756	< 0.001	0.742	< 0.001	0.840	< 0.001	0.758	< 0.001	0.684	< 0.001	0.710	< 0.001
	10	0.743	< 0.001	0.683	< 0.001	0.808	< 0.001	0.702	< 0.001	0.683	< 0.001	0.700	< 0.001
Correlation	5	-0.439	0.005	-	-	-0.532	< 0.001	-	-	-	-	-	-
	10	-0.429	0.006	-	-	-0.533	< 0.001	-	-	-	-	-	-
Entropy	1	-0.664	< 0.001	-0.502	0.001	-0.663	< 0.001	-0.514	0.001	-0.692	< 0.001	-0.648	< 0.001
	5	-0.673	< 0.001	-0.491	0.001	-0.665	< 0.001	-0.505	0.001	-0.695	< 0.001	-0.640	< 0.001
	10	-0.682	< 0.001	-0.509	0.001	-0.686	< 0.001	-0.526	< 0.001	-0.709	< 0.001	-0.650	< 0.001

Abbreviations: global, global gamma evaluation; local, local gamma evaluation; *d* = particular displacement distance; r_s = Spearman's rank correlation coefficient; ASM, angular second moment; IDM, inverse difference moment.

TABLE 24. Statistically significant correlation coefficients between textural features calculated from fluence maps generated with 10 segments and the gamma passing rates for TrueBeam™

		2%/2 mm				1%/2 mm				2%/1 mm			
		Global		Local		Global		Local		Global		Local	
	d	r_s	*p*	r_s	*p*	r_s	*p*	r_s	*p*	r_s	*p*	r_s	*p*
ASM	1	0.681	< 0.001	0.505	0.001	0.682	< 0.001	0.517	0.001	0.692	< 0.001	0.636	< 0.001
	5	0.679	< 0.001	0.479	0.002	0.664	< 0.001	0.495	0.001	0.688	< 0.001	0.628	< 0.001
	10	0.704	< 0.001	0.529	< 0.001	0.706	< 0.001	0.545	< 0.001	0.707	< 0.001	0.659	< 0.001
IDM	1	0.672	< 0.001	0.490	0.001	0.658	< 0.001	0.505	0.001	0.673	< 0.001	0.651	< 0.001
	5	0.603	< 0.001	0.428	0.006	0.558	< 0.001	0.426	0.006	0.642	< 0.001	0.596	< 0.001
	10	0.589	< 0.001	0.432	0.005	0.545	< 0.001	0.409	0.009	0.602	< 0.001	0.578	< 0.001
Contrast	5	0.733	< 0.001	0.628	< 0.001	0.801	< 0.001	0.670	< 0.001	0.665	< 0.001	0.668	< 0.001
	10	0.761	< 0.001	0.680	< 0.001	0.831	< 0.001	0.724	< 0.001	0.697	< 0.001	0.708	< 0.001
Variance	5	0.784	< 0.001	0.718	< 0.001	0.836	< 0.001	0.720	< 0.001	0.701	< 0.001	0.727	< 0.001
	10	0.757	< 0.001	0.667	< 0.001	0.812	< 0.001	0.672	< 0.001	0.684	< 0.001	0.688	< 0.001
Correlation	5	-0.505	0.001	-	-	-0.578	< 0.001	-	-	-0.447	0.004	-0.408	0.009
	10	-0.559	< 0.001	-	-	-0.640	< 0.001	-0.464	0.003	-0.483	0.002	-0.453	0.003
Entropy	1	-0.638	< 0.001	-0.450	0.004	-0.636	< 0.001	-0.466	0.002	-0.686	< 0.001	-0.613	< 0.001
	5	-0.642	< 0.001	-0.443	0.004	-0.640	< 0.001	-0.464	0.003	-0.692	< 0.001	-0.608	< 0.001
	10	-0.650	< 0.001	-0.478	0.002	-0.661	< 0.001	-0.498	0.001	-0.697	< 0.001	-0.622	< 0.001

Abbreviations: global, global gamma evaluation; local, local gamma evaluation; *d* = particular displacement distance; r_s = Spearman's rank correlation coefficient; ASM, angular second moment; IDM, inverse difference moment.

TABLE 25. Statistically significant correlation coefficients between textural features calculated from fluence maps generated with 20 segments and the gamma passing rates for TrueBeam™

		2%/2 mm				1%/2 mm				2%/1 mm			
		Global		Local		Global		Local		Global		Local	
	d	r_s	*p*	r_s	*p*	r_s	*p*	r_s	*p*	r_s	*p*	r_s	*p*
ASM	1	0.678	< 0.001	0.486	0.001	0.670	< 0.001	0.488	0.001	0.700	< 0.001	0.629	< 0.001
	5	0.637	< 0.001	0.438	0.005	0.626	< 0.001	0.435	0.005	0.659	< 0.001	0.593	< 0.001
	10	0.638	< 0.001	0.434	0.005	0.647	< 0.001	0.442	0.004	0.662	< 0.001	0.578	< 0.001
IDM	1	0.639	< 0.001	0.457	0.003	0.614	< 0.001	0.465	0.002	0.676	< 0.001	0.619	< 0.001
	5	0.567	< 0.001	-	-	0.506	0.001	0.335	0.034	0.635	< 0.001	0.546	< 0.001
	10	0.442	0.004	-	-	-	-	-	-	0.510	0.001	0.451	0.004
Contrast	1	0.599	< 0.001	0.479	0.002	0.604	< 0.001	0.511	0.001	0.576	< 0.001	0.552	< 0.001
	5	0.748	< 0.001	0.645	< 0.001	0.794	< 0.001	0.683	< 0.001	0.677	< 0.001	0.691	< 0.001
	10	0.784	< 0.001	0.702	< 0.001	0.839	< 0.001	0.738	< 0.001	0.712	< 0.001	0.722	< 0.001
Variance	1	0.724	< 0.001	0.687	< 0.001	0.733	< 0.001	0.660	< 0.001	0.639	< 0.001	0.724	< 0.001
	5	0.787	< 0.001	0.661	< 0.001	0.803	< 0.001	0.659	< 0.001	0.678	< 0.001	0.692	< 0.001
	10	0.765	< 0.001	0.649	< 0.001	0.780	< 0.001	0.649	< 0.001	0.658	< 0.001	0.665	< 0.001
Correlation	5	-0.535	< 0.001	-	-	-0.588	< 0.001	-0.411	0.008	-0.485	0.002	-0.453	0.003
	10	-0.580	< 0.001	-	-	-0.652	< 0.001	-0.476	0.002	-0.505	0.001	-0.478	0.002
Entropy	1	-0.613	< 0.001	-	-	-0.619	< 0.001	-0.423	0.007	-0.674	< 0.001	-0.578	< 0.001
	5	-0.587	< 0.001	-	-	-0.604	< 0.001	-0.399	0.011	-0.658	< 0.001	-0.555	< 0.001
	10	-0.586	< 0.001	-	-	-0.621	< 0.001	-0.404	0.010	-0.660	< 0.001	-0.558	< 0.001

Abbreviations: global, global gamma evaluation; local, local gamma evaluation; *d* = particular displacement distance; r_s = Spearman's rank correlation coefficient; ASM, angular second moment; IDM, inverse difference moment.

TABLE 26. Statistically significant correlation coefficients between textural features calculated from fluence maps generated with 45 segments and the gamma passing rates for TrueBeam™

		2%/2 mm				1%/2 mm				2%/1 mm			
		Global		Local		Global		Local		Global		Local	
	d	r_s	*p*	r_s	*p*	r_s	*p*	r_s	*p*	r_s	*p*	r_s	*p*
ASM	1	0.547	< 0.001	-	-	0.540	< 0.001	-	-	0.552	< 0.001	0.504	0.001
	5	0.499	0.001	-	-	0.497	0.001	-	-	0.510	0.001	0.451	0.003
	10	0.566	< 0.001	-	-	0.586	< 0.001	-	-	0.560	< 0.001	0.502	0.001
Contrast	1	0.622	< 0.001	0.406	0.009	0.609	< 0.001	0.453	0.003	0.613	< 0.001	0.551	< 0.001
	5	0.746	< 0.001	0.548	< 0.001	0.773	< 0.001	0.600	< 0.001	0.721	< 0.001	0.686	< 0.001
	10	0.757	< 0.001	0.601	< 0.001	0.799	< 0.001	0.643	< 0.001	0.736	< 0.001	0.693	< 0.001
Variance	1	0.790	< 0.001	0.744	< 0.001	0.816	< 0.001	0.744	< 0.001	0.690	< 0.001	0.771	< 0.001
	5	0.790	< 0.001	0.682	< 0.001	0.793	< 0.001	0.700	< 0.001	0.696	< 0.001	0.727	< 0.001
	10	0.766	< 0.001	0.630	< 0.001	0.764	< 0.001	0.642	< 0.001	0.681	< 0.001	0.690	< 0.001
Correlation	10	-0.547	< 0.001	-	-	-0.617	< 0.001	-	-	-0.530	< 0.001	-0.439	0.005
Entropy	1	-0.553	< 0.001	-	-	-0.571	< 0.001	-	-	-0.605	< 0.001	-0.545	< 0.001
	5	-0.548	< 0.001	-	-	-0.572	< 0.001	-	-	-0.592	< 0.001	-0.544	< 0.001
	10	-0.578	< 0.001	-	-	-0.620	< 0.001	-0.435	0.005	-0.620	< 0.001	-0.576	< 0.001

Abbreviations: global, global gamma evaluation; local, local gamma evaluation; *d* = particular displacement distance; r_s = Spearman's rank correlation coefficient; ASM, angular second moment.

TABLE 27. Statistically significant correlation coefficients between textural features calculated from fluence maps generated with 90 segments and the gamma passing rates for TrueBeam™

		2%/2 mm				1%/2 mm				2%/1 mm			
		Global		Local		Global		Local		Global		Local	
	d	r_s	*p*	r_s	*p*	r_s	*p*	r_s	*p*	r_s	*p*	r_s	*p*
ASM	1	0.407	0.009	-	-	0.406	0.009	-	-	0.460	0.003	-	-
	5	0.480	0.002	-	-	0.529	< 0.001	-	-	0.504	0.001	0.441	0.004
	10	0.587	< 0.001	0.404	0.010	0.626	< 0.001	0.481	0.002	0.541	< 0.001	0.539	< 0.001
IDM	5	-0.719	< 0.001	-0.584	< 0.001	-0.750	< 0.001	-0.593	< 0.001	-0.636	< 0.001	-0.668	< 0.001
	10	-0.814	< 0.001	-0.615	< 0.001	-0.815	< 0.001	-0.638	< 0.001	-0.715	< 0.001	-0.728	< 0.001
Contrast	1	0.560	< 0.001	-	-	0.566	< 0.001	0.432	0.005	0.537	< 0.001	0.520	0.001
	5	0.675	< 0.001	0.505	0.001	0.709	< 0.001	0.559	< 0.001	0.655	< 0.001	0.665	< 0.001
	10	0.705	< 0.001	0.571	< 0.001	0.746	< 0.001	0.616	< 0.001	0.662	< 0.001	0.686	< 0.001
Variance	1	0.790	< 0.001	0.705	< 0.001	0.808	< 0.001	0.719	< 0.001	0.712	< 0.001	0.782	< 0.001
	5	0.755	< 0.001	0.624	< 0.001	0.758	< 0.001	0.642	< 0.001	0.688	< 0.001	0.709	< 0.001
	10	0.742	< 0.001	0.595	< 0.001	0.745	< 0.001	0.615	< 0.001	0.675	< 0.001	0.681	< 0.001
Correlation	10	-0.550	< 0.001	-	-	-0.626	< 0.001	-0.429	0.006	-0.525	0.001	-0.485	0.002
Entropy	1	-0.557	< 0.001	-	-	-0.594	< 0.001	-	-	-0.582	< 0.001	-0.531	< 0.001
	10	-0.566	< 0.001	-	-	-0.609	< 0.001	-0.436	0.005	-0.532	< 0.001	-0.516	0.001

Abbreviations: global, global gamma evaluation; local, local gamma evaluation; d = particular displacement distance; r_s = Spearman's rank correlation coefficient; ASM, angular second moment.

TABLE 28. Statistically significant correlation coefficients between textural features calculated from fluence maps generated with 178 segments and the gamma passing rates for TrueBeam™

		2%/2 mm				1%/2 mm				2%/1 mm			
		Global		Local		Global		Local		Global		Local	
	d	r_s	*p*	r_s	*p*	r_s	*p*	r_s	*p*	r_s	*p*	r_s	*p*
ASM	1	0.540	< 0.001	-	-	0.560	< 0.001	-	-	0.558	< 0.001	0.489	0.001
	5	0.599	< 0.001	-	-	0.647	< 0.001	0.430	0.006	0.576	< 0.001	0.522	0.001
	10	0.640	< 0.001	0.419	0.007	0.670	< 0.001	0.470	0.002	0.589	< 0.001	0.554	< 0.001
IDM	10	-0.806	< 0.001	-0.649	< 0.001	-0.831	< 0.001	-0.679	< 0.001	-0.728	< 0.001	-0.718	< 0.001
Contrast	5	0.634	< 0.001	0.433	0.005	0.670	< 0.001	0.513	0.001	0.644	< 0.001	0.599	< 0.001
	10	0.676	< 0.001	0.512	0.001	0.703	< 0.001	0.569	< 0.001	0.657	< 0.001	0.629	< 0.001
Variance	5	0.680	< 0.001	0.415	0.008	0.636	< 0.001	0.441	0.004	0.646	< 0.001	0.562	< 0.001
Correlation	5	-0.581	< 0.001	-0.406	0.009	-0.625	< 0.001	-0.480	0.002	-0.549	< 0.001	-0.535	< 0.001
	10	-0.631	< 0.001	-0.487	0.001	-0.704	< 0.001	-0.562	< 0.001	-0.590	< 0.001	-0.605	< 0.001
Entropy	1	-0.605	< 0.001	-	-	-0.631	< 0.001	-0.412	0.008	-0.589	< 0.001	-0.541	< 0.001
	5	-0.609	< 0.001	-	-	-0.644	< 0.001	-0.419	0.007	-0.576	< 0.001	-0.519	0.001
	10	-0.642	< 0.001	-0.414	0.008	-0.671	< 0.001	-0.476	0.002	-0.599	< 0.001	-0.571	< 0.001

Abbreviations: global, global gamma evaluation; local, local gamma evaluation; *d* = particular displacement distance; r_s = Spearman's rank correlation coefficient; ASM, angular second moment; IDM, inverse difference moment.

TABLE 29. Statistically significant correlation coefficients between textural features calculated from fluence maps generated with 356 segments (a single fluence map) and the gamma passing rates for TrueBeam™

		2%/2 mm				1%/2 mm				2%/1 mm			
		Global		Local		Global		Local		Global		Local	
	d	r_s	*p*	r_s	*p*	r_s	*p*	r_s	*p*	r_s	*p*	r_s	*p*
ASM	1	0.499	0.001	-	-	0.461	0.003	-	-	-	-	0.426	0.006
	5	0.595	< 0.001	0.406	0.009	0.639	< 0.001	0.479	0.002	0.543	< 0.001	0.522	0.001
	10	0.641	< 0.001	0.409	0.009	0.669	< 0.001	0.488	0.001	0.563	< 0.001	0.537	< 0.001
IDM	1	0.329	0.038	-	-	-	-	0.341	0.031	-	-	-	-
	5	-0.640	< 0.001	-0.485	0.002	-0.714	< 0.001	-0.526	0.001	-0.647	< 0.001	-0.587	< 0.001
	10	-0.653	< 0.001	-0.550	< 0.001	-0.722	< 0.001	-0.578	< 0.001	-0.634	< 0.001	-0.604	< 0.001
Contrast	1	-	-	-	-	-	-	-	-	0.471	0.002	-	-
	5	0.626	< 0.001	0.406	0.009	0.661	< 0.001	0.439	0.005	0.676	< 0.001	0.596	< 0.001
	10	0.606	< 0.001	0.483	0.002	0.670	< 0.001	0.514	0.001	0.670	< 0.001	0.610	< 0.001
Variance	1	0.662	< 0.001	0.403	0.010	0.660	< 0.001	0.443	0.004	0.740	< 0.001	0.616	< 0.001
	5	0.663	< 0.001	0.415	0.008	0.666	< 0.001	0.457	0.003	0.731	< 0.001	0.615	< 0.001
	10	0.643	< 0.001	0.410	0.009	0.652	< 0.001	0.449	0.004	0.717	< 0.001	0.597	< 0.001
Correlation	1	0.579	< 0.001	0.552	0.000	0.673	< 0.001	0.579	0.000	0.568	< 0.001	0.596	< 0.001
	5	-	-	-	-	-	-	-	-	-	-	-	-
	10	-0.440	0.004	-	-	-0.514	0.001	-	-	-	-	-0.420	0.007
Entropy	1	-0.562	< 0.001	-	-	-0.550	< 0.001	-	-	-0.487	0.001	-0.472	0.002
	5	-0.608	< 0.001	-	-	-0.636	< 0.001	-0.451	0.004	-0.560	< 0.001	-0.537	< 0.001
	10	-0.617	< 0.001	-	-	-0.647	< 0.001	-0.446	0.004	-0.582	< 0.001	-0.533	< 0.001

Abbreviations: global, global gamma evaluation; local, local gamma evaluation; *d* = particular displacement distance; r_s = Spearman's rank correlation coefficient; ASM, angular second moment; IDM, inverse difference moment.

In the case of 5 segments, the highest correlation with statistical significance was observed between *variance* (d = 5) and global gamma passing rate with gamma criterion of 1%/2 mm (r_s = -0.840 and $p < 0.001$). *Contrast* (d = 10) and *variance* (d = 5) showed generally superior performance than the others, showing r_s values higher than 0.7 (all with $p < 0.001$) to all gamma passing rates except to the gamma passing rate with 2%/1 mm. For 10 segments, the highest correlation with statistical significance was observed between *variance* (d = 5) and global gamma passing rate with 1%/2 mm (r_s = 0.836 and $p < 0.001$). *Contrast* (d = 5 and 10) and *variance* (d = 5 and 10) generally showed superior performance to the others showing r_s values higher than 0.7 most frequently. For 20 segments, the highest correlation was observed between *contrast* (d = 10) and global gamma passing rate with gamma criterion of 1%/2 mm (r_s = 0.839 and $p < 0.001$). *Contrast* (d = 5 and 10) and *variance* (d = 5 and 10) generally showed superior performance to the others showing r_s values higher than 0.7 most frequently. For 45 segments, *variance* (d = 1) showed the highest correlations to the global gamma passing rate with 1%/2 mm (r_s = 0.816 and $p < 0.001$). *Contrast* (d = 1 and 5) and *variance* (d = 1, 5 and 10) generally showed superior performance to the others showing r_s values higher than 0.6 most frequently. For 90 segments, the highest correlation was observed between *IDM* (d = 10) and global gamma passing rate with 1%/2 mm (r_s = -0.815 and $p < 0.001$). *IDM* (d = 10) and *variance* (d = 1) generally showed superior performance to the others showing r_s values higher than 0.7 most frequently. For 178 segments, the highest correlation with statistical significance was

observed between *IDM* (d = 10) and global gamma passing rate with gamma criterion of 1%/2 mm (r_s = -0.831 and p < 0.001). *Correlation* (d = 10) generally showed superior performance to the others showing r_s values higher than 0.6 most frequently. For 356 segments which was identical to the data shown in our feasibility study (Tables 9, 11), the highest correlation with statistical significance was observed between *variance* (d = 1) and global gamma passing rate with gamma criterion of 2%/1 mm (r_s = 0.740 and p < 0.001). *Variance* (d = 1, 5 and 10) and *IDM* (d = 10) generally showed superior performance to the others.

Several textural features showed r_s values higher than 0.74 to the global gamma passing rates, these were *IDM* (d = 10) with 90 and 178 segments, *contrast* (d = 10) with 20 segments, *variance* (d = 1) with 45 and 356 segments and *variance* (d = 5) with 5 and 10 segments. In the case of local gamma passing rates, textural features showing r_s values higher than 0.62 were *IDM* (d = 10) with 178 segments, *contrast* (d = 10) with 20 segments, *variance* (d = 1) with 45, 90 and 356 segments and *variance* (d = 5) with 5 and 10 segments. The highest correlation was observed between *variance* (d = 5) with 5 segments and local gamma passing rates with gamma criterion of 1%/2 mm (r_s = 0.840 and p < 0.001).

III.C.2. Textural features vs. differences in modulating parameters between VMAT plans and machine log files

III.C.2.1. A single fluence map

The values of r_s with p values of textural features, and the conventional

modulation indices with the differences in modulating parameters between the VMAT plans and the machine log files are shown in Table 30 and 31 for Trilogy™ and TrueBeam™, respectively.

TABLE 30. Correlations of textural features for a single fluence map and conventional modulation indices with differences in modulating parameters between VMAT plans and dynamic log files for Trilogy™

		MLC		Gantry angle		MU	
	d	r_s	*p*	r_s	*p*	r_s	*p*
ASM	1	*-0.749*	*< 0.001*	*0.514*	*0.001*	0.088	0.587
	5	*-0.864*	*< 0.001*	*0.632*	*< 0.001*	0.270	0.092
	10	*-0.875*	*< 0.001*	*0.643*	*< 0.001*	0.156	0.337
IDM	1	*0.704*	*< 0.001*	*-0.529*	*< 0.001*	-0.108	0.508
	5	*0.805*	*< 0.001*	*-0.683*	*< 0.001*	-0.141	0.385
	10	*0.755*	*< 0.001*	*-0.704*	*< 0.001*	-0.087	0.596
Contrast	1	*-0.863*	*< 0.001*	*0.639*	*< 0.001*	-0.018	0.914
	5	*-0.823*	*< 0.001*	*0.622*	*< 0.001*	0.050	0.759
	10	*-0.827*	*< 0.001*	*0.645*	*< 0.001*	0.062	0.703
Variance	1	*-0.828*	*< 0.001*	*0.628*	*< 0.001*	0.022	0.894
	5	*-0.801*	*< 0.001*	*0.605*	*< 0.001*	-0.025	0.877
	10	*-0.748*	*< 0.001*	*0.589*	*< 0.001*	-0.033	0.838
Correlation	1	*0.749*	*< 0.001*	*-0.495*	*0.001*	-0.025	0.876
	5	*0.764*	*< 0.001*	*-0.543*	*< 0.001*	-0.124	0.446
	10	*0.728*	*< 0.001*	*-0.531*	*< 0.001*	-0.151	0.352
Entropy	1	*0.848*	*< 0.001*	*-0.559*	*< 0.001*	-0.214	0.185
	5	*0.843*	*< 0.001*	*-0.546*	*< 0.001*	-0.237	0.142
	10	*0.870*	*< 0.001*	*-0.622*	*< 0.001*	-0.167	0.303
MCS_v		*-0.635*	*< 0.001*	*-0.620*	*< 0.001*	0.136	0.403
LTMCS		*-0.857*	*< 0.001*	*-0.714*	*< 0.001*	-0.083	0.609
MI_{SPORT}		*0.795*	*< 0.001*	*0.721*	*< 0.001*	0.065	0.691

Abbreviations: MLC = multi-leaf collimator, MU = monitoring unit, *d* = particular displacement distance, r_s = Spearman's rank correlation coefficients, ASM = angular second moment, IDM = inverse difference moment, MCS_v = modulation complexity score for VMAT, LTMCS = leaf travel modulation complexity score, MI_{SPORT} = modulation index supporting station parameter optimized radiation therapy

TABLE 31. Correlations of textural features for a single fluence map and conventional modulation indices with differences in modulating parameters between VMAT plans and dynamic log files for TrueBeam™

		MLC		Gantry angle		MU	
	d	r_s	*p*	r_s	*p*	r_s	*p*
ASM	1	-0.643	0.000	0.253	0.115	0.100	0.539
	2	-0.702	0.000	0.261	0.104	0.018	0.910
	3	-0.767	0.000	0.335	0.034	-0.013	0.937
	5	-0.826	0.000	0.389	0.013	-0.001	0.996
	10	-0.862	0.000	0.443	0.004	-0.051	0.754
IDM	1	-0.249	0.121	0.336	0.034	-0.002	0.991
	2	0.517	0.001	-0.170	0.295	0.165	0.310
	3	0.658	0.000	-0.315	0.048	0.258	0.108
	5	0.774	0.000	-0.435	0.005	0.291	0.068
	10	0.735	0.000	-0.500	0.001	0.252	0.117
Contrast	1	-0.609	0.000	0.233	0.149	-0.286	0.073
	2	-0.758	0.000	0.328	0.039	-0.289	0.070
	3	-0.804	0.000	0.389	0.013	-0.313	0.050
	5	-0.829	0.000	0.418	0.007	-0.324	0.041
	10	-0.802	0.000	0.468	0.002	-0.320	0.044
Variance	1	-0.822	0.000	0.444	0.004	-0.456	0.003
	2	-0.821	0.000	0.436	0.005	-0.452	0.003
	3	-0.822	0.000	0.436	0.005	-0.458	0.003
	5	-0.829	0.000	0.436	0.005	-0.448	0.004
	10	-0.817	0.000	0.452	0.003	-0.456	0.003
Correlation	1	-0.443	0.005	0.485	0.001	-0.276	0.085
	2	0.248	0.123	0.145	0.372	-0.140	0.389
	3	0.485	0.002	-0.030	0.852	-0.053	0.744
	5	0.622	0.000	-0.118	0.470	-0.020	0.901
	10	0.656	0.000	-0.227	0.158	-0.051	0.754
Entropy	1	0.731	0.000	-0.326	0.040	-0.017	0.917
	2	0.755	0.000	-0.324	0.042	0.015	0.926
	3	0.787	0.000	-0.328	0.039	0.035	0.830
	5	0.822	0.000	-0.371	0.018	0.035	0.832
	10	0.852	0.000	-0.416	0.008	0.048	0.768
MCS_v		*-0.646*	*< 0.001*	*-0.345*	*< 0.001*	0.234	0.403
LTMCS		*-0.756*	*< 0.001*	*-0.700*	*< 0.001*	-0.215	0.609
MI_{SPORT}		*0.705*	*< 0.001*	*0.436*	*< 0.001*	0.124	0.691

Abbreviations: MLC = multi-leaf collimator, MU = monitoring unit, *d* = particular displacement distance, r_s = Spearman's rank correlation coefficients,

ASM = angular second moment, IDM = inverse difference moment, MCS_v = modulation complexity score for VMAT, LTMCS = leaf travel modulation complexity score, MI_{SPORT} = modulation index supporting station parameter optimized radiation therapy

In the results of Trilogy™, the values of r_s for every textural feature, as well as the conventional modulation indices to the differences in MLC positions and the gantry angles were statistically significant, showing p values less than or equal to 0.001. However the values for differences in MU were not statistically significant, with p values larger than 0.05. In the results of TrueBeam™, the values of r_s for every textural feature, as well as the conventional modulation indices to the differences in MLC positions and the gantry angles were statistically significant, showing p values less than or equal to 0.001 except for *ASM* (d = 1 and 2), *IDM* (d = 1 and 2), *contrast* (d = 1) and *correlation* (d = 2, 3, 5 and 10). However the values for differences in MU were not statistically significant, with p values larger than 0.05 except to *contrast* (d = 3, 5 and 10) and every *variance*.

For Trilogy™, in the case of differences in MLC positions, the values of r_s for *ASM* (d = 5 and 10), *IDM* (d = 5), every *contrast*, *variance* (d = 1 and 5) and every *entropy* were larger than 0.8, showing strong correlations. In the case of differences in gantry angle, the values of r_s for *ASM* (d = 5 and 10), *IDM* (d = 5 and 10), every *contrast*, *variance* (d = 1 and 5) and *entropy* (d = 10) were higher than 0.6. In the case of differences in MLC positions, the *ASM* (d = 5 and 10), *contrast* (d = 1) and *entropy* (d = 10) showed higher values of r_s than the conventional modulation indices. In the case of gantry angle, MI_{SPORT} showed the highest value of r_s (0.721) among all the indicators.

For TrueBeam™, in the case of differences in MLC positions, the values of r_s for *ASM* (d = 5 and 10), *contrast* (d = 3, 5 and 10), every *variance* and *entropy* (d = 5 and 10) were larger than 0.8, showing strong correlations. In

the case of differences in gantry angle, the values of r_s for *ASM* (d = 10), *IDM* (d = 5 and 10), *contrast* (d = 5 and 10), every *variance*, *correlation* (d = 1) and *entropy* (d = 10) were higher than 0.4. In the case of differences in MLC positions, the *ASM* (d = 3, 5 and 10), *contrast* (d = 2, 3, 5 and 10), every *variance* and *entropy* (d = 2, 3, 5 and 10) showed higher values of r_s than the conventional modulation indices. In the case of gantry angle, LTMCS showed the highest value of r_s (0.700) among all the indicators.

III.C.2.2. Edge-enhanced fluence map

The r_s values and corresponding p values of textural features calculated from edge-enhanced fluence map to the differences in mechanical parameters are shown in Table 32 and 33 for Trilogy™ and TrueBeam™, respectively.

TABLE 32. The values of r_s between textural features calculated from edge-enhanced fluence map and mechanical parameter differences for Trilogy™

		MLC		Gantry angle		MU	
	d	r_s	*p*	r_s	*p*	r_s	*p*
ASM	1	-0.747	< 0.001	0.445	0.004	0.108	0.506
	5	-0.749	< 0.001	0.499	0.001	0.165	0.309
	10	-0.785	< 0.001	0.600	< 0.001	0.106	0.513
IDM	1	0.604	< 0.001	-0.444	0.004	-0.243	0.131
	5	0.821	< 0.001	-0.705	< 0.001	-0.217	0.179
	10	0.787	< 0.001	-0.716	< 0.001	-0.206	0.203
Contrast	1	-0.853	< 0.001	0.655	< 0.001	0.145	0.372
	5	-0.843	< 0.001	0.643	< 0.001	0.160	0.323
	10	-0.825	< 0.001	0.636	< 0.001	0.217	0.179
Variance	1	-0.699	< 0.001	0.526	< 0.001	0.110	0.501
	5	-0.690	< 0.001	0.510	0.001	0.090	0.579
	10	-0.648	< 0.001	0.507	0.001	0.040	0.808
Correlation	1	0.766	< 0.001	-0.510	0.001	-0.050	0.761
	5	0.758	< 0.001	-0.540	< 0.001	-0.132	0.416
	10	0.728	< 0.001	-0.533	< 0.001	-0.157	0.332
Entropy	1	0.820	< 0.001	-0.516	0.001	-0.095	0.559
	5	0.823	< 0.001	-0.538	< 0.001	-0.169	0.297
	10	0.841	< 0.001	-0.592	< 0.001	-0.117	0.474

Abbreviations: MLC = multi-leaf collimator, MU = monitor unit, *d* = particular displacement distance, r_s = Spearman's rank correlation coefficient, ASM = angular second moment, IDM = inverse difference moment

TABLE 33. The values of r_s between textural features calculated from edge-enhanced fluence map and mechanical parameter differences for TrueBeam™

		MLC		Gantry angle		MU	
	d	r_s	*p*	r_s	*p*	r_s	*p*
ASM	1	-0.625	< 0.001	0.373	0.018	0.123	0.450
	5	-0.746	< 0.001	0.476	0.002	0.077	0.636
	10	-0.801	< 0.001	0.502	0.001	0.018	0.913
IDM	1	-0.311	0.052	0.388	0.013	0.124	0.447
	5	0.543	< 0.001	-0.247	0.125	0.267	0.096
	10	0.678	< 0.001	-0.396	0.011	0.274	0.087
Contrast	1	-0.534	< 0.001	0.154	0.343	-0.240	0.135
	5	-0.719	< 0.001	0.300	0.060	-0.311	0.050
	10	-0.722	< 0.001	0.333	0.036	-0.296	0.064
Variance	1	-0.592	< 0.001	0.270	0.092	-0.442	0.004
	5	-0.598	< 0.001	0.280	0.080	-0.455	0.003
	10	-0.580	< 0.001	0.289	0.071	-0.462	0.003
Correlation	1	-0.062	0.702	0.266	0.097	-0.371	0.018
	5	0.636	< 0.001	-0.134	0.411	-0.033	0.838
	10	0.654	< 0.001	-0.241	0.133	-0.067	0.683
Entropy	1	0.635	< 0.001	-0.365	0.021	-0.099	0.545
	5	0.737	< 0.001	-0.453	0.003	-0.068	0.675
	10	0.813	< 0.001	-0.506	0.001	0.002	0.992

Abbreviations: MLC = multi-leaf collimator, MU = monitor unit, *d* = particular displacement distance, r_s = Spearman's rank correlation coefficient, ASM = angular second moment, IDM = inverse difference moment

In the results of Trilogy™, no statistically significant correlations were observed between textural features and the differences in MU.

For MLC positional errors in Trilogy™, the highest r_s value was observed between *contrast* (d = 1) and MLC errors (r_s = -0.853 with $p < 0.001$). In the case of *contrast* (d = 1) with edge-enhanced fluence maps, the r_s value to MLC errors was smaller than that of *contrast* (d = 1) with non-edge-enhanced fluence maps (r_s = -0.863 with $p < 0.001$), LTMCS (r_s = -0.857 with $p < 0.001$) and MI_t (r_s = 0.917 with $p < 0.001$) while it was larger than that of *variance* (d = 1) with non-edge-enhanced fluence maps (r_s = -0.828 with $p < 0.001$), MCS_v (r_s = -0.635 with $p < 0.001$) and MI_{SPORT} (r_s = 0.795 with $p < 0.001$).

For gantry angle errors in Trilogy™, the highest correlation was observed between *IDM* (d = 10) and gantry angles (r_s = -0.716 with $p < 0.001$). In the case of *contrast* (d = 1) with edge-enhanced fluence maps, r_s value to gantry angle error (0.655 with $p < 0.001$) was smaller than those of LTMCS (r_s = -0.714 with $p < 0.001$) and MI_{SPORT} (r_s = 0.721 with $p < 0.001$) while it was larger than those of MCS_v (r_s = -0.620 with $p < 0.001$), MI_t (r_s = 0.630 with $p < 0.001$) and *contrast* (d = 1) and *variance* (d = 1) with non-edge-enhanced fluence maps (r_s = 0.639 with $p < 0.001$ and r_s = 0.628 with $p < 0.001$, respectively).[28]

For MU errors in TrueBeam™, no statistically significant correlations were observed between most textural features and the differences in MU except to every *variance* and *correlation* (d = 1). The highest r_s value was observed between *variance* (d = 10) and MU errors (r_s = -0.462 with p = 0.003).

For MLC positional errors in TrueBeam™, the highest r_s value was

observed between *entropy* (d = 10) and MLC errors (r_s = 0.813 with p < 0.001). In the case of *entropy* (d = 10) with edge-enhanced fluence maps, the r_s value to MLC errors was smaller than that of *ASM* (d = 10) with non-edge-enhanced fluence maps (r_s = -0.862 with p < 0.001) while it was larger than that of *contrast* (d = 10) with non-edge-enhanced fluence maps (r_s = -0.802 with p < 0.001), MCS_v (r_s = -0.646 with p < 0.001), LTMCS (r_s = -0.756 with p < 0.001) and MI_{SPORT} (r_s = 0.705 with p < 0.001).

For gantry angle errors in TrueBeam™, the highest correlation was observed between *entropy* (d = 10) and gantry angles (r_s = -0.506 with p < 0.001). In the case of *entropy* (d = 10) with edge-enhanced fluence maps, r_s value to gantry angle error was smaller than those of LTMCS (r_s = -0.700 with p < 0.001) while it was larger than those of MCS_v (r_s = -0.345 with p < 0.001)) and MI_{SPORT} (r_s = 0.436 with p < 0.001).

III.C.2.3. Segmental fluence maps

The statistically significant values of r_s of textural features calculated with 5, 10, 20, 45, 90, 178 and 356 segments for Trilogy™ to the MLC positional errors between plan and delivery are shown in Table 34.

TABLE 34. Statistically significant correlation coefficients between textural features calculated with 5, 10, 20, 45, 90, 178 and 356 segments and MLC positional errors during volumetric modulated arc therapy delivery for Trilogy™

Segment		5		10		20		45		90		178		356	
	d	r_s	*p*	r_s	*p*	r_s	*p*	r_s	*p*	r_s	*p*	r_s	*p*	r_s	*p*
ASM	1	-0.452	0.003	-0.565	<0.001	-0.700	<0.001	-0.805	<0.001	-0.742	<0.001	-0.779	<0.001	-0.749	<0.001
	5	-0.683	<0.001	-0.759	<0.001	-0.820	<0.001	-0.822	<0.001	-0.774	<0.001	-0.766	<0.001	-0.864	<0.001
	10	-0.872	<0.001	-0.889	<0.001	-0.885	<0.001	-0.817	<0.001	-0.773	<0.001	-0.796	<0.001	-0.875	<0.001
IDM	1	-	-	-	-	-	-	-	-	-	-	-	-	0.704	<0.001
	5	-	-	-	-	-	-	0.376	0.017	0.528	<0.001	0.504	0.001	0.805	<0.001
	10	-	-	-	-	-	-	0.488	0.001	0.627	<0.001	0.552	<0.001	0.755	<0.001
Con	1	-0.726	<0.001	-0.839	<0.001	-0.883	<0.001	-0.581	<0.001	-0.728	<0.001	-0.622	<0.001	-0.863	<0.001
	5	-0.747	<0.001	-0.816	<0.001	-0.869	<0.001	-0.556	<0.001	-0.654	<0.001	-0.566	<0.001	-0.823	<0.001
	10	-0.807	<0.001	-0.895	<0.001	-0.910	<0.001	-0.562	<0.001	-0.657	<0.001	-0.481	0.002	-0.826	<0.001
Var	1	-	-	-	-	-0.542	<0.001	-	-	-	-	-	-	-0.828	<0.001
	5	-0.599	<0.001	-0.687	<0.001	-0.784	<0.001	-	-	-	-	-	-	-0.801	<0.001
	10	-	-	-0.356	0.024	-0.624	<0.001	-	-	-	-	-	-	-0.748	<0.001
Cor	1	0.827	<0.001	0.846	<0.001	0.844	<0.001	0.847	<0.001	0.849	<0.001	0.869	<0.001	0.749	<0.001
	5	0.718	<0.001	0.734	<0.001	0.761	<0.001	0.794	<0.001	0.808	<0.001	0.789	<0.001	0.764	<0.001
	10	0.717	<0.001	0.775	<0.001	0.797	<0.001	0.809	<0.001	0.793	<0.001	0.705	<0.001	0.728	<0.001
Ent	1	0.616	<0.001	0.727	<0.001	0.807	<0.001	0.845	<0.001	0.797	<0.001	0.822	<0.001	0.848	<0.001
	5	0.750	<0.001	0.836	<0.001	0.853	<0.001	0.849	<0.001	0.814	<0.001	0.821	<0.001	0.843	<0.001
	10	0.887	<0.001	0.887	<0.001	0.884	<0.001	0.856	<0.001	0.825	<0.001	0.849	<0.001	0.870	<0.001

Abbreviations: d = particular displacement distance; r_s = Spearman's rank correlation coefficient; ASM, angular second moment; IDM, inverse difference moment; Con, contrast; Var, variance; Cor, correlation; Ent, entropy.

TABLE 35. Statistically significant correlation coefficients between textural features calculated with 5, 10, 20, 45, 90, 178 and 356 segments and gantry angle errors during volumetric modulated arc therapy delivery for Trilogy™

Segment		5		10		20		45		90		178		356	
	d	r_s	*p*	r_s	*p*	r_s	*p*	r_s	*p*	r_s	*p*	r_s	*p*	r_s	*p*
ASM	1	0.390	0.013	0.485	0.002	0.552	<0.001	0.739	<0.001	0.587	<0.001	0.625	<0.001	0.514	0.001
	5	0.520	0.001	0.554	<0.001	0.621	<0.001	0.698	<0.001	0.584	<0.001	0.603	<0.001	0.631	<0.001
	10	0.679	<0.001	0.696	<0.001	0.697	<0.001	0.653	<0.001	0.568	<0.001	0.626	<0.001	0.643	<0.001
IDM	1	-	-	-	-	-	-	-	-	-	-	-	-	-0.529	<0.001
	5	-	-	-	-	-	-	-	-	-0.393	0.012	-0.400	0.011	-0.683	<0.001
	10	-	-	-	-	-	-	-	-	-0.499	0.001	-0.452	0.003	-0.704	<0.001
Con	1	0.449	0.004	0.568	<0.001	0.667	<0.001	0.367	0.020	0.524	0.001	0.492	0.001	0.639	<0.001
	5	0.585	<0.001	0.634	<0.001	0.682	<0.001	0.407	0.009	0.580	<0.001	0.491	0.001	0.622	<0.001
	10	0.678	<0.001	0.727	<0.001	0.702	<0.001	0.396	0.011	0.544	<0.001	0.397	0.011	0.645	<0.001
Var	1	-	-	-	-	0.529	<0.001	-	-	-	-	-	-	0.628	<0.001
	5	0.647	<0.001	0.674	<0.001	0.695	<0.001	-	-	-	-	-	-	0.605	<0.001
	10	-	-	0.372	0.018	0.567	<0.001	-	-	-	-	-	-	0.589	<0.001
Cor	1	-0.506	0.001	-0.540	<0.001	-0.571	<0.001	-0.568	<0.001	-0.591	<0.001	-0.679	<0.001	-0.495	0.001
	5	-0.524	0.001	-0.524	0.001	-0.531	<0.001	-0.538	<0.001	-0.592	<0.001	-0.685	<0.001	-0.543	<0.001
	10	-0.623	<0.001	-0.608	<0.001	-0.597	<0.001	-0.549	<0.001	-0.636	<0.001	-0.637	<0.001	-0.531	<0.001
Ent	1	-0.618	<0.001	-0.701	<0.001	-0.748	<0.001	-0.704	<0.001	-0.577	<0.001	-0.608	<0.001	-0.559	<0.001
	5	-0.712	<0.001	-0.761	<0.001	-0.764	<0.001	-0.678	<0.001	-0.576	<0.001	-0.608	<0.001	-0.546	<0.001
	10	-0.759	<0.001	-0.762	<0.001	-0.751	<0.001	-0.638	<0.001	-0.581	<0.001	-0.617	<0.001	-0.622	<0.001

Abbreviations: *d* = particular displacement distance; r_s = Spearman's rank correlation coefficient; ASM, angular second moment; IDM, inverse difference moment; Con, contrast; Var, variance; Cor, correlation; Ent, entropy.

TABLE 36. Statistically significant correlation coefficients between textural features calculated with 5, 10, 20, 45, 90, 178 and 356 segments and MLC positional errors during volumetric modulated arc therapy delivery for TrueBeam™

Segment		5		10		20		45		90		178		356	
	d	r_s	*p*	r_s	*p*	r_s	*p*	r_s	*p*	r_s	*p*	r_s	*p*	r_s	*p*
ASM	1	-0.874	<0.001	-0.875	<0.001	-0.861	<0.001	-0.803	<0.001	-0.720	<0.001	-0.805	<0.001	-0.643	<0.001
	5	-0.859	<0.001	-0.859	<0.001	-0.852	<0.001	-0.792	<0.001	-0.774	<0.001	-0.833	<0.001	-0.826	<0.001
	10	-0.862	<0.001	-0.878	<0.001	-0.874	<0.001	-0.791	<0.001	-0.792	<0.001	-0.810	<0.001	-0.862	<0.001
IDM	1	-0.832	<0.001	-0.847	<0.001	-0.813	<0.001	-0.525	0.001	-	-	-	-	-	-
	5	-0.729	<0.001	-0.762	<0.001	-0.710	<0.001	0.509	0.001	0.808	<0.001	0.829	<0.001	0.774	<0.001
	10	-0.705	<0.001	-0.738	<0.001	-0.634	<0.001	0.721	<0.001	0.814	<0.001	0.812	<0.001	0.735	<0.001
Con	1	-	-	-0.401	0.011	-0.802	<0.001	-0.863	<0.001	-0.833	<0.001	-0.754	<0.001	-0.609	<0.001
	5	-0.833	<0.001	-0.874	<0.001	-0.884	<0.001	-0.905	<0.001	-0.858	<0.001	-0.842	<0.001	-0.829	<0.001
	10	-0.834	<0.001	-0.862	<0.001	-0.881	<0.001	-0.897	<0.001	-0.847	<0.001	-0.831	<0.001	-0.802	<0.001
Var	1	0.665	<0.001	-	-	-0.740	<0.001	-0.817	<0.001	-0.814	<0.001	-0.740	<0.001	-0.822	<0.001
	5	-0.757	<0.001	-0.851	<0.001	-0.867	<0.001	-0.862	<0.001	-0.854	<0.001	-0.787	<0.001	-0.829	<0.001
	10	-0.861	<0.001	-0.877	<0.001	-0.894	<0.001	-0.881	<0.001	-0.865	<0.001	-0.795	<0.001	-0.817	<0.001
Cor	1	-	-	-	-	-	-	-	-	-	-	0.403	0.010	-0.443	0.005
	5	0.761	<0.001	0.811	<0.001	0.793	<0.001	0.743	<0.001	0.787	<0.001	0.795	<0.001	0.622	<0.001
	10	0.701	<0.001	0.803	<0.001	0.823	<0.001	0.827	<0.001	0.788	<0.001	0.817	<0.001	0.656	<0.001
Ent	1	0.868	<0.001	0.855	<0.001	0.849	<0.001	0.814	<0.001	0.827	<0.001	0.840	<0.001	0.731	<0.001
	5	0.879	<0.001	0.855	<0.001	0.867	<0.001	0.822	<0.001	0.816	<0.001	0.829	<0.001	0.822	<0.001
	10	0.876	<0.001	0.859	<0.001	0.866	<0.001	0.806	<0.001	0.792	<0.001	0.818	<0.001	0.852	<0.001

Abbreviations: d = particular displacement distance; r_s = Spearman's rank correlation coefficient; ASM, angular second moment; IDM, inverse difference moment; Con, contrast; Var, variance; Cor, correlation; Ent, entropy.

TABLE 37. Statistically significant correlation coefficients between textural features calculated with 5, 10, 20, 45, 90, 178 and 356 segments and gantry angle errors during volumetric modulated arc therapy delivery for TrueBeam™

Segment		5		10		20		45		90		178		356	
	d	r_s	*p*	r_s	*p*	r_s	*p*	r_s	*p*	r_s	*p*	r_s	*p*	r_s	*p*
ASM	1	0.569	<0.001	0.584	<0.001	0.505	0.001	0.347	0.028	-	-	0.341	0.031	-	-
	5	0.546	<0.001	0.540	<0.001	0.449	0.004	-	-	0.321	0.043	0.437	0.005	0.389	0.013
	10	0.562	<0.001	0.565	<0.001	0.443	0.004	0.338	0.033	0.367	0.020	0.434	0.005	0.443	0.004
IDM	1	0.572	<0.001	0.590	<0.001	0.570	<0.001	0.464	0.003	-	-	-	-	0.336	0.034
	5	0.545	<0.001	0.547	<0.001	0.473	0.002	-0.387	0.014	-0.477	0.002	-0.422	0.007	-0.435	0.005
	10	0.514	0.001	0.558	<0.001	0.426	0.006	-0.516	0.001	-0.539	<0.001	-0.507	0.001	-0.500	0.001
Con	1	-0.391	0.013	-	-	0.355	0.025	0.384	0.014	0.348	0.028	-	-	-	-
	5	0.408	0.009	0.482	0.002	0.499	0.001	0.515	0.001	0.408	0.009	0.389	0.013	0.418	0.007
	10	0.494	0.001	0.533	<0.001	0.569	<0.001	0.612	<0.001	0.510	0.001	0.398	0.011	0.468	0.002
Var	1	-0.337	0.034	-	-	0.547	<0.001	0.646	<0.001	0.575	<0.001	0.419	0.007	0.444	0.004
	5	0.464	0.003	0.555	<0.001	0.549	<0.001	0.605	<0.001	0.538	<0.001	0.466	0.002	0.436	0.005
	10	0.536	0.000	0.574	<0.001	0.562	<0.001	0.609	<0.001	0.561	<0.001	0.469	0.002	0.452	0.003
Cor	1	0.373	0.018	0.422	0.007	0.424	0.006	0.519	0.001	0.328	0.039	-	-	0.485	0.001
	5	-	-	-	-	-	-	-	-	-	-	-	-	-	-
	10	-	-	-	-	-0.316	0.047	-	-	-	-	-0.346	0.029	-	-
Ent	1	-0.573	<0.001	-0.553	<0.001	-0.496	0.001	-0.386	0.014	-0.381	0.015	-0.413	0.008	-0.326	0.040
	5	-0.568	<0.001	-0.524	0.001	-0.479	0.002	-0.357	0.024	-0.360	0.022	-0.430	0.006	-0.371	0.018
	10	-0.575	<0.001	-0.546	<0.001	-0.457	0.003	-0.364	0.021	-0.346	0.029	-0.437	0.005	-0.416	0.008

Abbreviations: *d* = particular displacement distance; r_s = Spearman's rank correlation coefficient; ASM, angular second moment; IDM, inverse difference moment; Con, contrast; Var, variance; Cor, correlation; Ent, entropy.

The r_s values of textural features to the MLC errors were generally larger than those to the gamma passing rates. The highest correlations was observed between *contrast* (d = 10) with 20 segments and MLC positional errors (r_s = -0.910 and $p < 0.001$). The *ASM* (d = 10) with 10 and 20 segments, *contrast* (d = 1) with 20 segments, *contrast* (d = 10) with 10 and 20 segments, *entropy* (d = 10) with 5, 10 and 20 segments also showed strong correlations to the MLC errors, showing r_s values higher than 0.88 (all with $p < 0.001$).

The statistically significant values of r_s of textural features calculated with 5, 10, 20, 45, 90, 178 and 356 segments for Trilogy™ to the gantry angle errors between plan and delivery are shown in Table 35.

The r_s values of textural features to the gantry angle errors were generally lower than those to the MLC positional errors. The highest correlations compared to the others was observed between *entropy* (d = 5) with 20 segments and gantry angle errors (r_s = -0.764 and $p < 0.001$). *Entropy* (d = 5) with 10 segments and *entropy* (d = 10) with 5, 10 and 20 segments also showed strong correlations, showing r_s values higher than 0.75 (always $p < 0.001$).

The statistically significant values of r_s of textural features calculated with 5, 10, 20, 45, 90, 178 and 356 segments for TrueBeam™ to the MLC positional errors and gantry angle errors between plan and delivery are shown in Table 36 and 37, respectively.

The r_s values of textural features to the MLC errors were generally larger than those to the gamma passing rates. The highest correlations was observed between *contrast* (d = 10) with 20 segments and MLC positional errors (r_s = -

0.910 and $p < 0.001$). The *ASM* ($d = 10$) with 10 and 20 segments, *contrast* ($d = 1$) with 20 segments, *contrast* ($d = 10$) with 10 and 20 segments, *entropy* ($d = 10$) with 5, 10 and 20 segments also showed strong correlations to the MLC errors, showing r_s values higher than 0.88 (all with $p < 0.001$).

The r_s values of textural features to the gantry angle errors were generally lower than those to the MLC positional errors. The highest correlations compared to the others was observed between *entropy* ($d = 5$) with 20 segments and gantry angle errors ($r_s = -0.764$ and $p < 0.001$). *Entropy* ($d = 5$) with 10 segments and *entropy* ($d = 10$) with 5, 10 and 20 segments also showed strong correlations, showing r_s values higher than 0.75 (always $p < 0.001$).

III.C.3. Textural features vs. differences in dose-volumetric parameters between VMAT plans and reconstructed DICOM-RT format plans using dynamic log files

III.C.3.1. A single fluence map

For Trilogy™ and TrueBeam™, the statistically significant values of r_s of textural features calculated from a single fluence map, and the conventional modulation indices with the differences in dose-volumetric parameters between the prostate VMAT plans and the reconstructed DICOM-RT format plans using dynamic log files are shown in Table 38 and 39, respectively.

TABLE 38. Correlations of textural features calculated from a single fluence map and conventional modulation indices with differences in dose-volumetric parameters between prostate VMAT plans and reconstructed plans with machine log files for Trilogy™

		Mean dose to target		Max dose to target		$D_{5\%}$ of target		Mean dose to rectal wall		Mean dose to femoral head		$D_{5\%}$ of femoral head	
	d	r_s	*p*	r_s	*p*	r_s	*p*	r_s	*p*	r_s	*p*	r_s	*p*
ASM	10	-	-	-	-	-	-	-0.575	0.008	-	-	-	-
IDM	1	-0.504	0.023	-	-	-	-	-	-	-	-	-	-
IDM	10	-	-	-	-	-	-	-	-	0.500	0.025	-	-
Contrast	1	-	-	-	-	-	-	-0.499	0.025	-	-	-	-
Variance	10	-	-	-	-	-	-	-	-	-0.524	0.018	-	-
Entropy	1	-	-	-	-	-	-	0.489	0.029	-	-	-	-
MCS_v		-	-	-0.548	0.012	-0.456	0.043	-	-	-	-	-	-
LTMCS		-	-	-0.553	0.011	-	-	-	-	-	-	-	-
MI_{SPORT}		-	-	-	-	-	-	-	-	-	-	0.461	0.041

Abbreviations: $D_{n\%}$ = dose received by n% volume of structure, *d* = particular displacement distance, r_s = Spearman's rank correlation coefficients, ASM = angular second moment, IDM = inverse difference moment, MCS_v = modulation complexity score for VMAT, LTMCS = leaf travel modulation complexity score, MI_{SPORT} = modulation index supporting station parameter optimized radiation therapy

TABLE 39. Correlations of textural features calculated from a single fluence map and conventional modulation indices with differences in dose-volumetric parameters between prostate VMAT plans and reconstructed plans with machine log files for TrueBeam™

		Mean dose to target		Max dose to target		$D_{5\%}$ of target		Mean dose to rectal wall		Mean dose to femoral head		$D_{5\%}$ of femoral head	
	d	r_s	*p*	r_s	*p*	r_s	*p*	r_s	*p*	r_s	*p*	r_s	*p*
ASM	5	-	-	-	-	-	-	-0.481	0.032	-	-	-	-
ASM	10	-	-	-	-	-	-	-0.527	0.017	-	-	-	-
IDM	1	-	-	-0.468	0.037	-	-	-	-	-	-	-	-
Entropy	1	-	-	-	-	-	-	-0.581	0.007	-	-	-	-
Entropy	2	-	-	-	-	-	-	-0.612	0.004	-	-	-	-
Entropy	3	-	-	-	-	-	-	-0.554	0.008	-	-	-	-
MCS_v		-0.251	0.001	-	-	-	-	-	-	-	-	-	-
LTMCS		-	-	-	-	-0.412	0.001	-	-	-	-	-	-
MI_{SPORT}		-	-	-	-	-	-	-	-	-0.310	0.042	-	-

Abbreviations: $D_{n\%}$ = dose received by n% volume of structure, *d* = particular displacement distance, r_s = Spearman's rank correlation coefficients, ASM = angular second moment, IDM = inverse difference moment, MCS_v = modulation complexity score for VMAT, LTMCS = leaf travel modulation complexity score, MI_{SPORT} = modulation index supporting station parameter optimized radiation therapy

In the case of Trilogy™, the dose-volumetric parameter which most frequently showed *p* values less than 0.05 was the mean dose to rectal wall. In this case, the values of r_s of *ASM* (d = 10), *contrast* (d = 1) and *entropy* (d = 1) were statistically significant. The highest value of r_s observed between the mean dose to rectal wall and *ASM* (-0.575 with d = 10).

In the case of TrueBeam™, the dose-volumetric parameter which most frequently showed *p* values less than 0.05 was also the mean dose to rectal wall. In this case, the values of r_s of *ASM* (d = 5 and 10), *IDM* (d = 1) and *entropy* (d = 1, 2 and 3) were statistically significant. The highest value of r_s observed between the mean dose to rectal wall and *entropy* (-0.612 with d = 2).

For Trilogy™ and TrueBeam™, the statistically significant values of r_s of textural features calculated from a single fluence map, and the conventional modulation indices with the differences in dose-volumetric parameters between the H&N VMAT plans and the reconstructed DICOM-RT format plans using dynamic log files are shown in Table 40 and 41, respectively.

TABLE 40. Correlations of textural features calculated from a single fluence map and conventional modulation indices with differences in dose-volumetric parameters between head and neck VMAT plans and reconstructed plans with machine log files for Trilogy™

		$D_{95\%}$		$D_{5\%}$		Maximum dose		Minimum dose		Mean dose	
	d	r_s	*p*	r_s	*p*	r_s	*p*	r_s	*p*	r_s	*p*
Target 1											
IDM	5	0.554	0.011	-	-	-	-	-	-	-	-
	10	0.463	0.040	-	-	-	-	-	-	-	-
Contrast	1	-0.452	0.046	-	-	-	-	-	-	-	-
	10	-0.464	0.039	-	-	-	-	-	-	-	-
Variance	1	-0.725	< 0.001	-0.582	0.007	-	-	-	-	-0.647	0.002
	5	-0.747	< 0.001	-0.606	0.005	-	-	-	-	-0.646	0.002
	10	-0.745	< 0.001	-0.596	0.006	-	-	-	-	-0.616	0.004
Correlation	1	-	-	-0.504	0.023	-	-	-	-	-	-
	5	-	-	-0.488	0.029	-0.457	0.043	-	-	-	-
Entropy	1	-0.457	0.043	-	-	-	-	-	-	-	-
	5	-0.524	0.018	-	-	-	-	-	-	-	-
Target 2											
Variance	1	-0.568	0.009	-0.617	0.005	-	-	-	-	-0.627	0.003
	5	-0.570	0.009	-0.639	0.003	-	-	-	-	-0.603	0.005
	10	-0.463	0.040	-0.594	0.007	-	-	-	-	-0.543	0.013
MI_{SPORT}		-	-	-	-	-	-	-	-	0.517	0.020
Target 3											
IDM	5	-	-	0.578	0.009	-	-	-	-	-	-
Contrast	1	-	-	-0.537	0.018	-	-	-	-	-	-
	10	-	-	-0.458	0.049	-	-	-	-	-	-
Variance	1	-	-	-0.772	< 0.001	-	-	-	-	-0.546	0.016
	5	-	-	-0.750	< 0.001	-	-	-	-	-0.515	0.024
	10	-	-	-0.701	0.001	-	-	-	-	-0.493	0.032
Correlation	10	-	-	-	-	-0.471	0.042	-	-	-	-
Entropy	1	-	-	-0.616	0.005	-	-	-	-	-0.466	0.045
	5	-	-	-0.640	0.003	-	-	-	-	-0.481	0.037
MCS_v		-	-	-	-	-	-	-0.479	0.033	-	-
LTMCS		-	-	-	-	-	-	-	-	-0.467	0.038
MI_{SPORT}		-	-	0.506	0.023	-	-	-	-	0.590	0.006
Mean dose to right parotid											
Variance	1	-0.520	0.019	-	-	-	-	-	-	-	-
Maximum dose to right optic nerve											
Contrast	1	-0.532	0.016	-	-	-	-	-	-	-	-

Abbreviations: $D_{n\%}$ = dose received by n% volume of structure, *d* = particular displacement distance, r_s = Spearman's rank correlation coefficients, IDM = inverse difference moment, MCS_v = modulation complexity score for VMAT, LTMCS = leaf travel modulation complexity score, MI_{SPORT} = modulation index supporting station parameter optimized radiation therapy

TABLE 41. Correlations of textural features calculated from a single fluence map and conventional modulation indices with differences in dose-volumetric parameters between head and neck VMAT plans and reconstructed plans with machine log files for TrueBeam™

		$D_{95\%}$		$D_{5\%}$		Maximum dose		Minimum dose		Mean dose	
	d	r_s	*p*	r_s	*p*	r_s	*p*	r_s	*p*	r_s	*p*
Target 1											
ASM	1	-	-	-	-	0.611	0.005	-	-	-	-
	5	-	-	-	-	0.540	0.015	-	-	-	-
		-	-	-	-	-	-	-	-	-	-
IDM	1	-	-	-	-	0.752	< 0.001	-	-	-	-
	2	-	-	-	-	0.672	0.002	-	-	-	-
		-	-	-	-	-	-	-	-	-	-
Variance	1	-	-	0.525	0.019	-	-	-	-	-	-
	2	-	-	0.508	0.024	-	-	-	-	-	-
	10	-	-	0.495	0.028	-	-	-	-	-	-
		-	-	-	-	-	-	-	-	-	-
Correlation	1	-	-	0.698	< 0.001	0.456	0.045	-	-	0.716	< 0.001
	5	-	-	0.480	0.034	-	-	-	-	0.544	0.014
		-	-	-	-	-	-	-	-	-	-
Entropy	1	-	-	-	-	-0.550	0.13	-	-	-	-
	5	-	-	-	-	-0.472	0.037	-	-	-	-
Target 2											
Correlation	1	-	-	0.651	0.002	0.645	0.003	-0.581	0.007	0.768	< 0.001
	2	-	-	0.567	0.010	-	-	-0.448	0.048	0.647	0.002
	5	-	-	0.52	0.026	-	-	-0.471	0.036	0.572	0.008
		-	-	-	-	-	-	-	-	-	-
MI_{SPORT}		0.154	0.002	-	-	0.351	0.021	-	-	-	-
Target 3											
ASM	5	0.488	0.036	-	-	-	-	-	-	-	-
		-	-	-	-	-	-	-	-	-	-
Variance	1	-0.470	0.044	0.565	0.013	-	-	-	-	-	-
	2	-0.463	0.048	0.510	0.019	-	-	-	-	-	-
	10	-0.474	0.042	0.518	0.025	-	-	-	-	-	-
		-	-	-	-	-	-	-	-	-	-
Correlation	5	-	-	0.535	0.020	0.586	< 0.001	-	-	-	-
		-	-	-	-	-	-	-	-	-	-
Entropy	1	-0.488	0.034	-	-	-	-	-	-	-	-
	10	-0.463	0.047	-0.470	0.044	-	-	-	-	-	-
		-	-	-	-	-	-	-	-	-	-
MCS_v		-	-	0.421	0.002	-	-	0.115	0.015	-	-
LTMCS		-	-	-	-	0.542	0.002	-	-	-	-
MI_{SPORT}		-	-	-	-	0.442	0.048	-	-	-	-

Abbreviations: $D_{n\%}$ = dose received by n% volume of structure, *d* = particular displacement distance, r_s = Spearman's rank correlation coefficients, IDM = inverse difference moment, MCS_v = modulation complexity score for VMAT, LTMCS = leaf travel modulation complexity score, MI_{SPORT} = modulation index supporting station parameter optimized radiation therapy

In the case of Trilogy™, the dose-volumetric parameter which most frequently showed p values less than 0.05 was $D_{5\%}$ of target (17 cases). The second most frequent dose-volumetric parameter was mean dose to target (14 cases). The value of r_s for *variance* (d = 1) most frequently showed statistical significances with the dose-volumetric parameters among all (9 cases). The *variance* (d = 1) showed noticeable correlations to $D_{95\%}$ of target 1 (-0.725 with $p < 0.001$) and target 2 (-0.568 with $p = 0.009$), $D_{5\%}$ of target 1 (-0.582 with p =0.007), target 2 (-0.617 with $p = 0.005$) and target 3 (-0.772 with $p < 0.001$), mean dose to target 1 (-0.647 with $p = 0.002$), target 2 (-0.627 with $p = 0.003$) and target 3 (-0.546 with $p = 0.016$) and the mean dose to right parotid gland (-0.520 with $p = 0.019$).

In the case of TrueBeam™, the dose-volumetric parameter which most frequently showed p values less than 0.05 was $D_{5\%}$ of target (14 cases). The second most frequent dose-volumetric parameter was maximum dose to target (12 cases). The value of r_s for *correlation* (d = 1) most frequently showed statistical significances with the dose-volumetric parameters among all (7 cases). The *correlation* (d = 1) showed noticeable correlations to $D_{5\%}$ of target 1 (0.698 with $p < 0.001$) and target 2 (0.651 with $p = 0.002$), maximum dose to target 1 (0.456 with p =0.045) and target 2 (0.645 with $p = 0.00$), minimum dose dose to target 2 (-0.581 with $p = 0.007$) and mean dose to target 1 0.716 with $p < 0.002$) and target 2 (0.768 with $p < 0.001$).

III.C.3.2. Edge-enhanced fluence map

The statistically significant r_s values of textural features calculated with

edge-enhanced fluence maps generated from prostate and H&N VMAT plans for Trilogy™ to differences in the clinically relevant dose-volumetric parameters between plan and delivery are shown in Table 42 and 43, respectively.

TABLE 42. The values of statistically significant r_s of textural features calculated from edge-enhanced fluence map to dose-volumetric parameter differences of prostate VMAT plans for Trilogy™

	Contrast				Correlation			
	$d = 1$		$d = 10$		$d = 1$		$d = 10$	
Dose-volumetric parameter	r_s	p	r_s	p	r_s	p	r_s	p
D20% of rectal wall	-	-	-	-	0.485	0.030	-	-
Mean dose to rectal wall	-0.493	0.027	-0.473	0.035	0.446	0.048	-	-
Mean dose to bladder	-0.456	0.043	-	-	-	-	-	-
D50% of femoral heads	-	-	-	-	-	-	0.448	0.047

Abbreviations: d = particular displacement distance, r_s = Spearman's rank correlation coefficient, Dn% = dose received by n% volume of structure

TABLE 43. The values of statistically significant r_s of textural features calculated from edge-enhanced fluence map to dose-volumetric parameter differences of head and neck VMAT plans for Trilogy™

	$d = 1$		$d = 5$		$d = 10$	
	r_s	p	r_s	p	r_s	p
			ASM			
$D_{5\%}$ of target 2	-	-	0.501	0.026	-	-
Mean dose to target 2	0.532	0.016	0.565	0.009	-	-
$D_{95\%}$ of target 3	-	-	0.641	0.003	-	-
$D_{5\%}$ of target 3	0.558	0.013	0.635	0.003	-	-
Mean dose to target 3	0.489	0.034	0.635	0.003	-	-
			IDM			
$D_{5\%}$ of target 1	-	-	0.511	0.021	0.478	0.033
Mean dose to target 1	-	-	0.562	0.010	0.520	0.019
$D_{95\%}$ of target 2	-	-	0.490	0.028	-	-
Minimum dose to target 2	0.447	0.048	-	-	-	-
Mean dose to target 2	0.501	0.024	0.593	0.006	0.548	0.012
$D_{5\%}$ of target 3	-	-	0.512	0.025	-	-
Mean dose to right parotid gland	0.540	0.014	0.619	0.004	-	-
Mean dose to left parotid gland	-	-	0.506	0.023	-	-
Maximum dose to right optic nerve	0.498	0.025	0.517	0.020	-	-
			Contrast			
$D_{5\%}$ of target 1	-	-	-0.454	0.044	-0.502	0.024
Mean dose to target 1	-0.486	0.030	-0.539	0.014	-0.488	0.029
$D_{95\%}$ of target 2	-0.494	0.027	-0.651	0.002	-	-
$D_{5\%}$ of target 2	-0.534	0.017	-0.618	0.004	-0.477	0.035
Minimum dose to target 2	-0.478	0.033	-	-	-	-
Mean dose to target 2	-0.626	0.003	-0.704	0.001	-0.521	0.018
$D_{95\%}$ of target 3	-	-	-0.508	0.026	-	-
$D_{5\%}$ of target 3	-0.576	0.010	-0.635	0.003	-	-
Mean dose to target 3	-0.484	0.036	-0.493	0.032	-	-
Mean dose to right parotid gland	-0.595	0.006	-0.516	0.020	-	-
Maximum dose to right optic nerve	-0.631	0.003	-0.477	0.033	-	-
			Variance			
$D_{95\%}$ of target 1	-0.553	0.012	-0.558	0.011	-0.589	0.006
$D_{5\%}$ of target 1	-0.693	0.001	-0.689	0.001	-0.688	0.001
Mean dose to target 1	-0.705	0.001	-0.708	< 0.001	-0.727	< 0.001
$D_{95\%}$ of target 2	-0.630	0.003	-0.617	0.004	-0.626	0.003
$D_{5\%}$ of target 2	-0.668	0.002	-0.672	0.002	-0.645	0.003
Mean dose to target 2	-0.734	< 0.001	-0.733	< 0.001	-0.734	< 0.001
$D_{95\%}$ of target 3	-0.553	0.014	-0.548	0.015	-0.519	0.023
$D_{5\%}$ of target 3	-0.665	0.002	-0.670	0.002	-0.691	0.001
Maximum dose to target 3	-0.511	0.025	-0.490	0.033	-0.497	0.030
Mean dose to target 3	-0.487	0.035	-0.502	0.029	-0.519	0.023
Mean dose to right	-0.705	0.001	-0.675	0.001	-0.709	< 0.001

parotid gland						
Mean dose to left parotid gland	-0.479	0.033	-0.444	0.050	-0.458	0.042
Maximum dose to right optic nerve	-0.568	0.009	-0.560	0.010	-0.560	0.010
			Correlation			
$D_{5\%}$ of target 1	-0.589	0.006	-0.546	0.013	-	-
Maximum dose to target 1	-	-	-0.490	0.028	-	-
			Entropy			
$D_{5\%}$ of target 1	-	-	-0.487	0.029	-	-
Mean dose to target 1	-	-	-0.466	0.038	-	-
$D_{5\%}$ of target 2	-	-	-0.519	0.021	-0.451	0.047
Mean dose to target 2	-0.465	0.039	-0.537	0.015	-	-
$D_{95\%}$ of target 3	-0.522	0.022	-0.584	0.009	-0.497	0.030
$D_{5\%}$ of target 3	-0.598	0.007	-0.656	0.002	-0.543	0.016
Mean dose to target 3	-0.487	0.035	-0.552	0.014	-	-

Abbreviations: d = particular displacement distance, r_s = Spearman's rank correlation coefficient, Dn% = dose received by n% volume of structure, ASM = angular second moment, IDM = inverse difference moment

Statistically significant values of r_s were found more frequently between *variance* (d = 1, 5 and 10) and the differences in dose-volumetric parameters (13 cases from a total of 35 cases), than between other textural features and the dose-volumetric differences. *Contrast* (d = 1) showed statistically significant r_s values in 11 cases to the dose-volumetric parameter differences. The numbers of statistically significant r_s values to the dose-volumetric parameter differences of MCS_v, LTMCS, MI_{SPORT}, MI_t and *contrast* (d = 1) and *variance* (d = 1) with non-edge-enhanced fluence maps were 3, 2, 4, 15, 4 and 10, respectively.[28] Therefore, the performance of *contrast* (d = 1) with edge-enhanced fluence maps was better than those of MCS_v, LTMCS, MI_{SPORT}, *contrast* (d = 1) and *variance* (d = 1) with non-edge-enhanced fluence maps while it was inferior to that of MI_t.

The statistically significant r_s values of textural features calculated with edge-enhanced fluence maps generated from prostate and H&N VMAT plans for TrueBeam™ to differences in the clinically relevant dose-volumetric parameters between plan and delivery are shown in Table 44 and 45, respectively.

TABLE 44. The values of statistically significant r_s of textural features calculated from edge-enhanced fluence map to dose-volumetric parameter differences of prostate VMAT plans for TrueBeam™

	IDM				Contrast			
	$d = 5$		$d = 10$		$d = 5$		$d = 10$	
Dose-volumetric parameter	r_s	p	r_s	p	r_s	p	r_s	p
D95% of target	-0.512	0.021	-0.520	0.019	-	-	-	-
D20% of bladder	-	-	-0.484	0.032	-	-	0.562	0.011
Mean dose to bladder	-	-	-	-	-	-	0.554	0.011
Mean dose to femoral heads	-	-	-	-	-	-	0.476	0.034

Abbreviations: d = particular displacement distance, r_s = Spearman's rank correlation coefficient, Dn% = dose received by n% volume of structure

TABLE 45. The values of statistically significant r_s of textural features calculated from edge-enhanced fluence map to dose-volumetric parameter differences of head and neck VMAT plans for TrueBeam™

	$d = 1$		$d = 5$		$d = 10$	
	r_s	p	r_s	p	r_s	p
ASM						
Max dose to target 1	0.532	0.017	0.493	0.029	0.471	0.038
IDM						
Max dose to target 1	0.555	0.012	-	-	-	-
Variance						
Mean dose to right parotid gland	-0.469	0.037	-0.454	0.044	-	-
Correlation						
$D_{5\%}$ of target 1	0.720	< 0.001	0.469	0.038	0.583	0.008
Max dose to target 1	0.484	0.032	-	-	-	-
Mean dose to target 1	0.602	0.006	0.535	0.016	0.486	0.031
$D_{5\%}$ of target 2	0.538	0.016	0.492	0.029	0.406	0.077
Max dose to target 2	0.650	0.002	-	-	0.453	0.047
Min dose to target 2	-0.649	0.002	-0.490	0.028	-0.666	0.001
Mean dose to target 2	0.705	0.001	0.568	0.009	0.551	0.012
Max dose to target 3	-	-	0.702	0.001	0.565	0.013
Max dose to right optic nerve	0.478	0.035	0.553	0.013	-	-
Entropy						
Max dose to target 1	-0.511	0.023	-	-	-	-
$D_{5\%}$ of target 3	-	-	-	-	0.465	0.047

Abbreviations: d = particular displacement distance, r_s = Spearman's rank correlation coefficient, Dn% = dose received by n% volume of structure, ASM = angular second moment, IDM = inverse difference moment

Statistically significant values of r_s were found more frequently between *correlation* (d = 1, 5 and 10) and the differences in dose-volumetric parameters (22 cases from a total of 35 cases), than between other textural features and the dose-volumetric differences. *Contrast* (d = 10) showed statistically significant r_s values in 3 cases to the dose-volumetric parameter differences.

III.C.3.3. Segmental fluence maps

The numbers of statistically significant r_s values of textural features calculated with 5, 10, 20, 45, 90, 178 and 356 segments to the clinically relevant dose-volumetric parameters for both prostate and H&N VMAT plans are plotted in Fig. 9 and 10 for Trilogy™ and TrueBeam™, respectively.

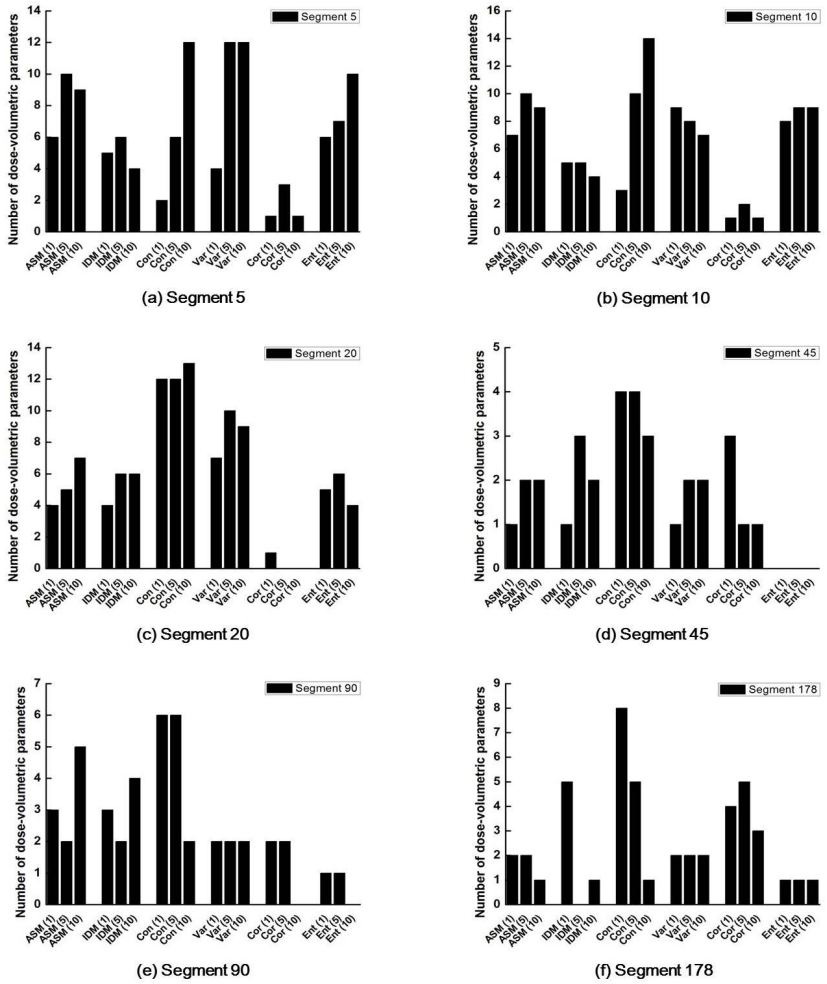

Fig. 9. For Trilogy™, the numbers of statistically significant r_s values ($p < 0.05$) of textural features calculated with 5, 10, 20, 45, 90, 178 and 356 segments to the clinically relevant dose-volumetric parameters for prostate and head and neck volumetric modulated arc therapy (VMAT) plans are shown for each number of segments used to generate fluence maps. The numbers of segment numbers were 5 (a), 10 (b), 20 (c), 45 (d), 90 (e) and 178 (f). Textural features tested in this study were angular second moment (ASM), inverse difference moment (IDM), contrast (Con), variance (Var), correlation (Cor) and entropy (Ent) with 1, 5 and 10 values of particular displacement distance (d).

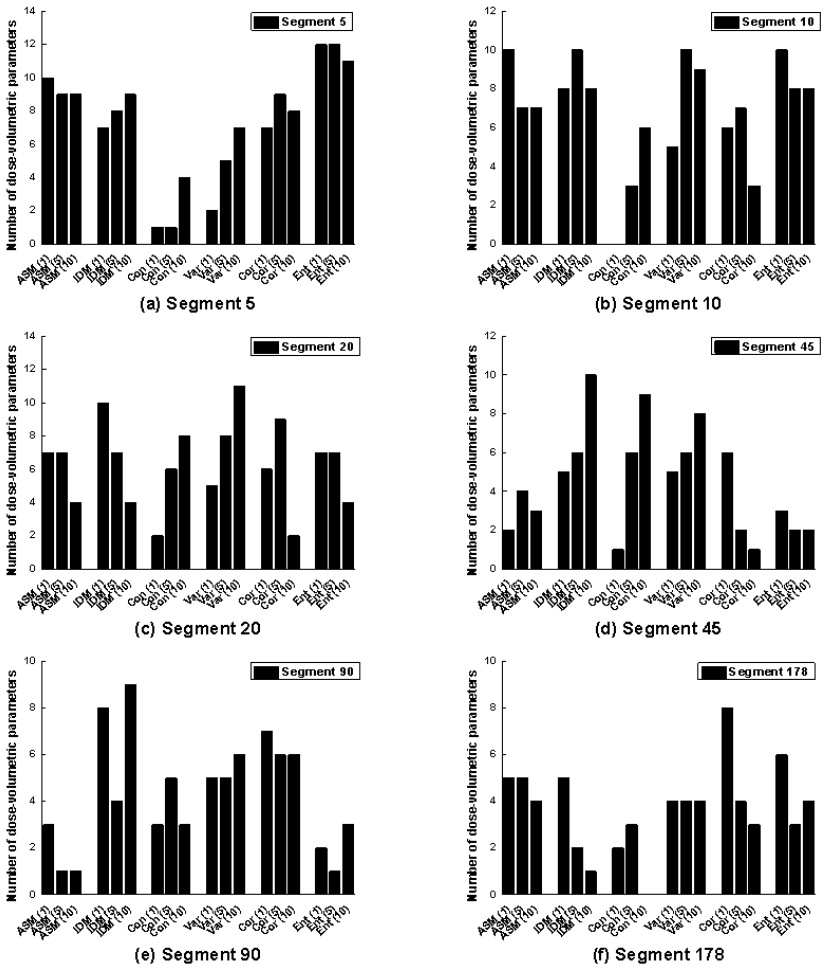

Fig. 10. For TrueBeam™, the numbers of statistically significant r_s values ($p < 0.05$) of textural features calculated with 5, 10, 20, 45, 90, 178 and 356 segments to the clinically relevant dose-volumetric parameters for prostate and head and neck volumetric modulated arc therapy (VMAT) plans are shown for each number of segments used to generate fluence maps. The numbers of segment numbers were 5 (a), 10 (b), 20 (c), 45 (d), 90 (e) and 178 (f). Textural features tested in this study were angular second moment (ASM), inverse difference moment (IDM), contrast (Con), variance (Var), correlation (Cor) and entropy (Ent) with 1, 5 and 10 values of particular displacement distance (d).

The statistically significant r_s values were most frequently observed at *contrast* (d = 10) with 10 segments for Trilogy™ (14 cases) and *entropy* (d = 5 and 10) with 5 segments for TrueBeam™ (12 cases).

In the case of Trilogy™, *ASM* (d = 5) with 5 and 10 segments, *contrast* (d = 1) with 20 segments, *contrast* (d = 5) with 10 and 20 segments, *contrast* (d = 10) with 5, 10 and 20 segments, *variance* (d = 5) with 5 and 20 segments, *variance* (d = 10) with 5 segments and *entropy* (d = 10) with 5 segments showed r_s values with statistical significances in larger than 10 cases. The number of statistically significant r_s values of textural features was the largest at the fluence maps with 10 segments (a total of 121 cases) and smallest at the fluence maps with 45 segments (a total of 32 cases).

In the case of TrueBeam™, *ASM* (d = 1) with 5 and 10 segments, *IDM* (d = 1) with 20 segments, *IDM* (d = 5) with 10 segments, *IDM* (d = 10) with 45 segments, *variance* (d = 5) with 10 segments, *variance* (d = 10) with 20 segments, *entropy* (d = 1) with 5 and 10 segments, *entropy* (d = 5) with 5 segments and *entropy* (d = 10) with 5 segments showed r_s values with statistical significances in larger than 10 cases. The number of statistically significant r_s values of textural features was the largest at the fluence maps with 5 segments (a total of 131 cases) and smallest at the fluence maps with 178 segments (a total of 67 cases).

III.D. Sensitivity and specificity

The sensitivity and specificity of the textural features were analyzed with ROC curves and corresponding AUC values. All of the VMAT plans in this

study were clinically acceptable in terms of previously recommended pretreatment QA results for VMAT QA.[32] Thus in order to apply ROC analysis to the textural features for study purposes, we set a 90% passing rate as a tolerance level, and analyzed only the local gamma passing rates of 2%/2 mm, and global gamma passing rate of 1%/2 mm, which were uniformly distributed around 90%. The ROC curves of the textural features calculated from a single fluence map and the conventional modulation indices to the local gamma passing rates with 2%/2 mm criterion and the global gamma passing rates with 1%/2 mm criterion for Trilogy™ are shown in Fig. 11 and Fig. 12, respectively. The corresponding AUC values are shown in Table 46.

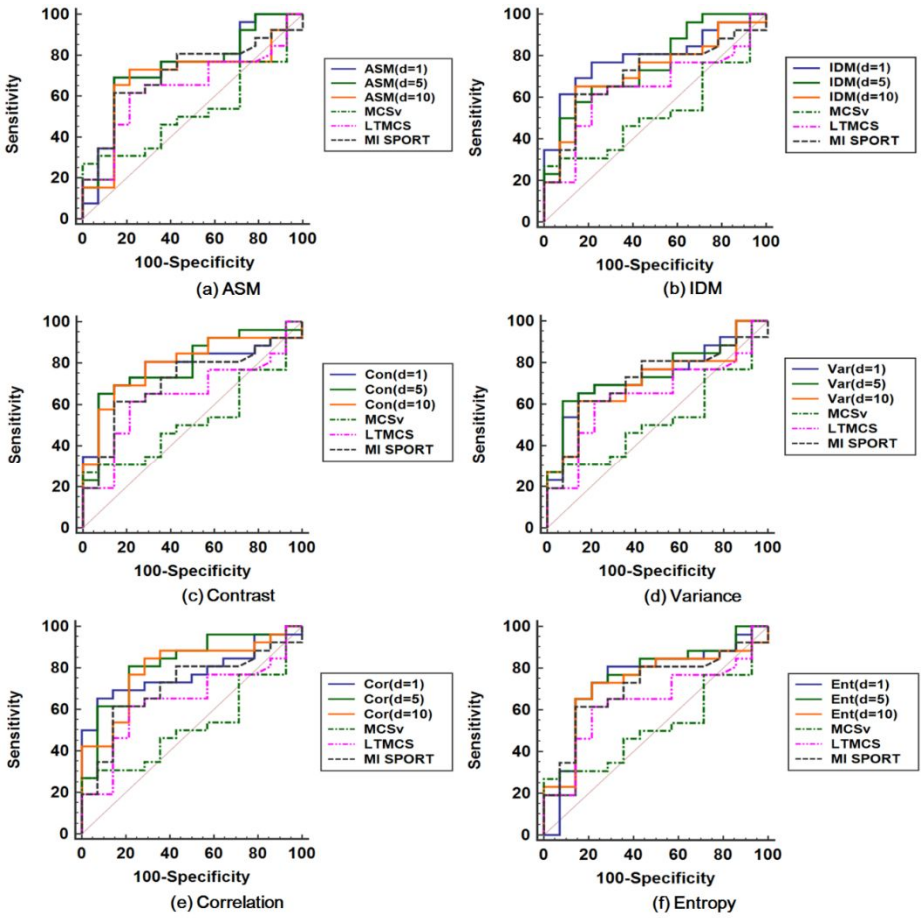

FIG. 11. The receiver operating characteristic (ROC) curves of textural features which were angular second moment (ASM) (a), inverse difference moment (IDM) (b), contrast (c), variance (d), correlation (e) and entropy (f), as well as the conventional modulation indices to the local gamma passing rates with 2%/2 mm criterion for Trilogy™ are shown.

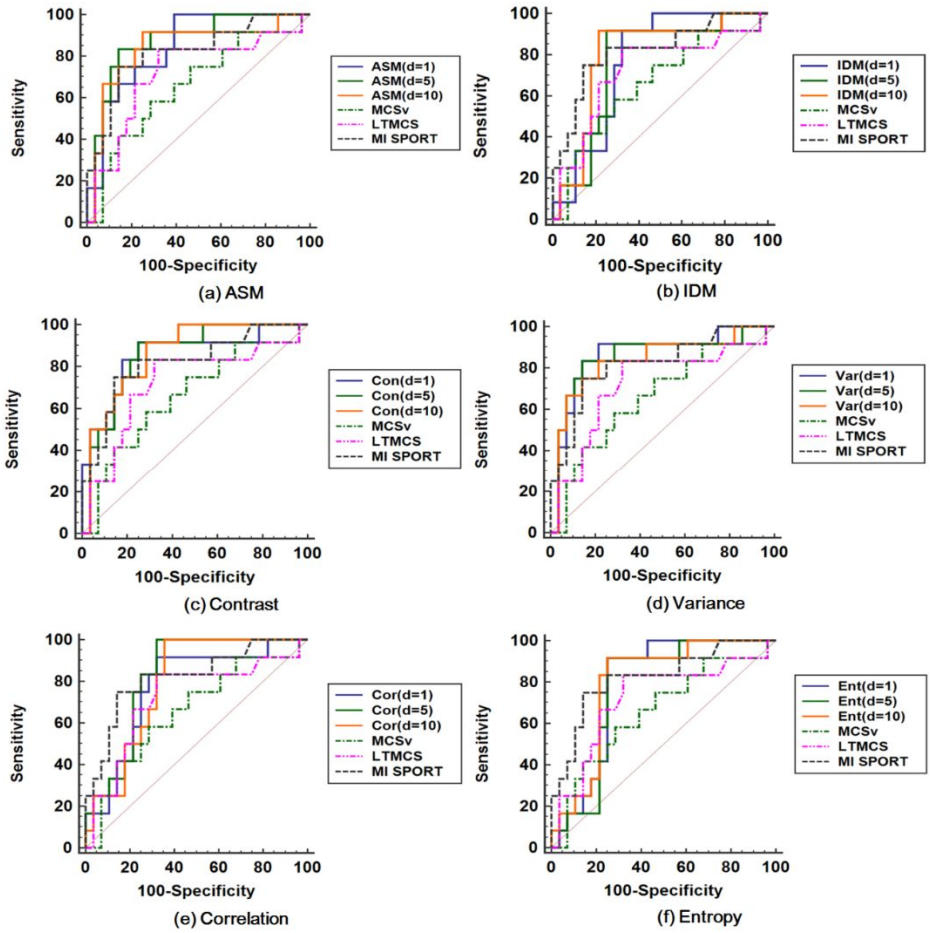

FIG. 12. The receiver operating characteristic (ROC) curves of the textural features which were angular second moment (ASM) (a), inverse difference moment (IDM) (b), contrast (c), variance (d), correlation (e) and entropy (f), as well as the conventional modulation indices to the global gamma passing rates with 1%/2 mm criterion for Trilogy™ are shown.

TABLE 46. The values of area under the curve (AUC) for each textural feature calculated from a single fluence map and conventional modulation index for Trilogy™

	$d = 1$	$d = 5$	$d = 10$
Local gamma evaluation with 2%2 mm criterion			
ASM	0.736	0.731	0.692
IDM	0.794	0.755	0.723
Contrast	0.783	0.791	0.794
Variance	0.745	0.750	0.709
Correlation	0.777	*0.824*	0.799
Entropy	0.742	0.750	0.731
MCS_v		0.527	
LTMCS		0.644	
MI_{SPORT}		0.710	
Global gamma evaluation with 1%2 mm criterion			
ASM	0.768	0.762	0.798
IDM	0.845	*0.872*	0.842
Contrast	0.854	0.857	0.863
Variance	0.863	0.854	0.836
Correlation	0.771	0.827	0.792
Entropy	0.786	0.771	0.795
MCS_v		0.658	
LTMCS		0.720	
MI_{SPORT}		0.820	

Abbreviations: d = particular displacement distance, ASM = angular second moment, IDM = inverse difference moment, MCS_v = modulation complexity score for VMAT, LTMCS = leaf travel modulation complexity score, MI_{SPORT} = modulation index supporting station parameter optimized radiation therapy

In the case of local gamma evaluation with 2%/2 mm criterion, the AUC value of *correlation* (d = 5) showed the highest value of 0.824, while the MCS_v showed the lowest value of 0.527. In the case of global gamma evaluation with 1%/2 mm criterion, *IDM* (d = 5) showed the highest AUC value of 0.872, while MCS_v showed the lowest value of 0.658.

The AUC values of the textural features calculated from a single fluence map and the conventional modulation indices to the local gamma passing rates with 2%/2 mm criterion and the global gamma passing rates with 1%/2 mm criterion for TrueBeam™ are shown in Fig. 47.

TABLE 47. The values of area under the curve (AUC) for each textural feature calculated from a single fluence map and conventional modulation index for TrueBeam™

	$d = 1$	$d = 2$	$d = 3$	$d = 5$	$d = 10$
Local gamma evaluation with 2%2 mm criterion					
ASM	0.721	0.725	0.702	0.711	0.752
IDM	0.702	0.715	0.689	0.699	0.765
Contrast	0.787	0.791	0.795	0.802	0.732
Variance	0.785	0.725	0.751	0.744	0.781
Correlation	0.764	0.744	0.732	0.756	0.750
Entropy	0.732	0.712	0.687	0.701	0.723
MCS_v			0.485		
LTMCS			0.687		
MI_{SPORT}			0.600		
Global gamma evaluation with 1%2 mm criterion					
ASM	0.798	0.785	0.801	0.820	0.791
IDM	0.811	0.800	0.784	0.832	0.812
Contrast	0.834	0.845	0.812	0.871	0.824
Variance	0.875	0.815	0.885	0.862	0.842
Correlation	0.780	0.777	0.798	0.803	0.821
Entropy	0.782	0.743	0.792	0.795	0.806
MCS_v			0.640		
LTMCS			0.741		
MI_{SPORT}			0.708		

Abbreviations: d = particular displacement distance, ASM = angular second moment, IDM = inverse difference moment, MCS_v = modulation complexity score for VMAT, LTMCS = leaf travel modulation complexity score, MI_{SPORT} = modulation index supporting station parameter optimized radiation therapy

In the case of local gamma evaluation with 2%/2 mm criterion, the AUC value of *correlation* (d = 5) showed the highest value of 0.802, while the MCS_v showed the lowest value of 0.485. In the case of global gamma evaluation with 1%/2 mm criterion, *variance* (d = 3) showed the highest AUC value of 0.85, while MCS_v showed the lowest value of 0.640.

DISCUSSION

Although modulation is a key feature of both IMRT and VMAT, the dose distribution of excessively modulated IMRT or VMAT plans is not always delivered as intended, because of increased uncertainties in the mechanical components of the linac, and inaccurate dose calculations by TPS for small or irregular fields.[18] Therefore, quantification of the degree of modulation for both IMRT and VMAT plans is useful for eliminating excessively modulated plans at the planning stage.[7-19] Various attempts have been made to quantify the degree of modulation of both IMRT and VMAT in association with the plan deliverability.[7-19] Most feasibility studies have focused on IMRT;[7, 10-13, 15-19] studies of VMAT[8, 9, 14] have been limited, as mentioned above.

In our feasibility study, we performed texture analysis on a single fluence map generated from VMAT plans. This study was the first attempt to evaluate the degree of modulation by performing texture analysis on the fluence map. The textural features analyzed in this study were *ASM*, *IDM*, *contrast*, *variance*, *correlation*, and *entropy*; each feature was calculated according to *d* values of 1, 5, and 10 for Trilogy™, and 1, 2, 3, 5, and 10 for TrueBeam™. The performance of each feature was tested using Spearman's rank correlation analysis for plan deliverability. For comparison, conventional modulation indices for VMAT such as MCS_v, LTMCS, and MI_{SPORT} were calculated and their correlations analyzed in the same way. In addition, to evaluate the sensitivity and specificity of the textural features, ROC curves and their corresponding AUC values were acquired using local and global gamma

passing rates (2%/2 mm and 1%/2 mm, respectively) with 90% as the tolerance level. Most of the textural features showed higher values of r_s (with statistical significance) than the conventional modulation indices for plan deliverability, thus exhibiting better performance. In the case of ROC analysis, most of the textural features performed better, exhibiting higher values of AUC than the conventional modulation indices.

The fluence maps of prostate VMAT plans had relatively larger proportions of beamlets with high intensity than did the H&N plans, as shown in Fig. 13.

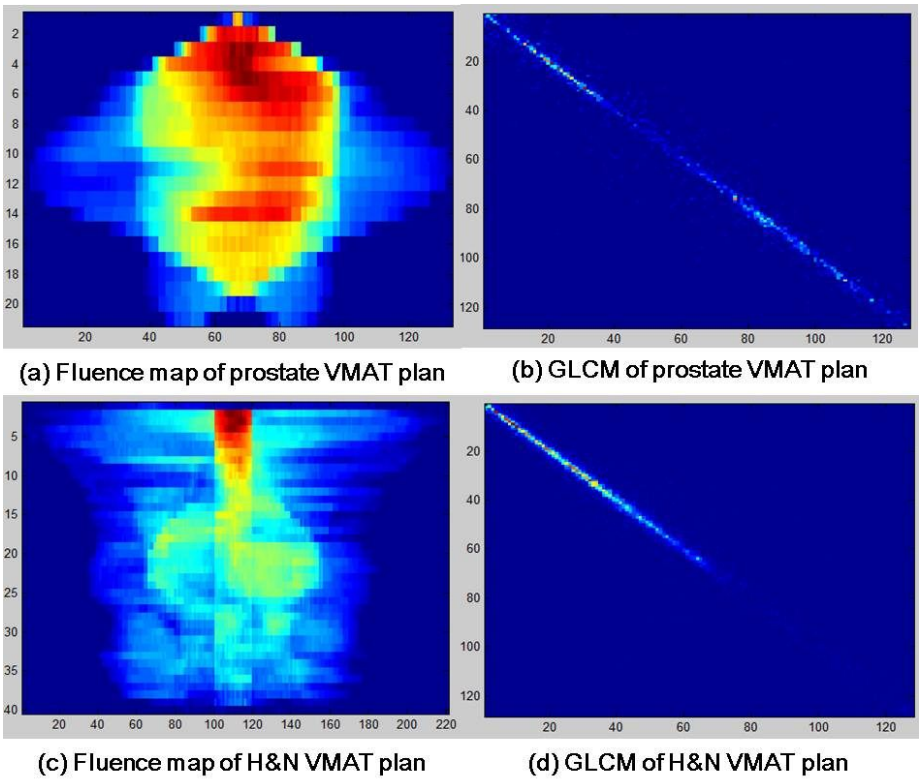

FIG. 13. Fluence maps of prostate (a) and head-and-neck (H&N) (c) volumetric modulated arc therapy (VMAT) plans are shown. The gray level co-occurrence matrix (GLCM) of prostate (b) and H&N (d) plans are also shown.

Therefore, the values of *variance* of the prostate plans were higher than those of the H&N plans. In addition, because the fluence maps of the prostate plans contained fewer gray levels than those of H&N plans, the values of *ASM* of prostate plans were higher, indicating more texturally uniform fluence maps than the H&N plans. The values of *IDM* of prostate plans were lower than those of H&N plans, whereas the values of *contrast* of prostate plans were higher than those of H&N plans. Because the $(i - j)$ term is located in the denominator for *IDM*, but in the numerator for *contrast*, the opposite tendency is expected. The values of both *IDM* and *contrast* indicated that the local variations in fluence maps of prostate plans were more drastic than those of H&N plans. Because the fluence maps of H&N plans were generated from the summation of a greater number of various irregular fields and smaller fields than were the prostate plans, the variations of each neighboring beamlet of the fluence maps summed over each irregular and small field were smaller than those of prostate plans. Therefore, the tendencies of *IDM* and *contrast* in this study were reasonable. When $d = 10$ was used in this study, the variations of each neighboring beamlet of the fluence map for prostate plans were higher than those of prostate plans with $d = 1$ or 5. The values of *correlation* and *entropy* showed that the fluence maps of H&N plans were more linearly dependent on gray levels and more random than those of prostate plans.

Metrics for comparing plan deliverability were pretreatment QA results, differences in modulating parameters, and differences in dose-volumetric parameters. There was no particular textural feature that consistently showed the best correlations with every measure of plan deliverability. Taken together,

the results for *contrast* (d = 1) and *variance* (d = 1) for Trilogy™ and *variance* (d = 1) for TrueBeam™ performed well as indicators of modulation degree for VMAT plans. Both *contrast* (d = 1) and *variance* (d = 1) for Trilogy™ and *variance* (d = 1) for TrueBeam™ consistently showed better performance than the conventional modulation indices, having higher values of r_s (with statistical significance) and higher values of AUC, except in the case of modulating parameters. However, even in this case, the r_s values of the textural features were higher than 0.86 for MLC errors, and 0.62 for gantry angle errors, indicating good correlations.

As mentioned above, *contrast* (d = 1) and *variance* (d = 1) for Trilogy™ and *variance* (d = 1) for TrueBeam™ showed strong correlations with the errors of MLC position and gantry angle. This result indicates that the textural features are able to predict the mechanical errors of MLCs ($r_s > 0.86$ with $p < 0.001$) and gantry rotation ($r_s > 0.62$ with $p < 0.001$) to some degree. However, most textural features, including *contrast*, *variance*, and conventional modulation indices, showed no correlations with the errors in MU. The small errors in MU (<0.23) seemed to be unrelated to the degree of modulation of VMAT plans. In the case of pretreatment QA results, the values of r_s for those textural features were greater than 0.6 in gamma evaluations at 1%/2 mm, whereas the remaining values were smaller than 0.6, indicating relatively weak correlations. Because the differences in modulating parameters were minimal, as shown in the results, the effect of modulating parameter differences on the passing rates of pretreatment QA might be negligible, resulting in relatively weak correlations. Moreover, the weaker correlations

could be partially caused by the insufficient resolution of the detector array, uncertainty of each detector, setup uncertainty of the device, or the limitations of 2D pretreatment QA.[5, 35, 36] To reveal the cause, pretreatment QA with various QA systems is needed; however, this is beyond the scope of this study. Further study utilizing various QA systems will be performed in the future.

Contrast (d = 1) and *variance* (d = 1) for Trilogy™ and *variance* (d = 1) for TrueBeam™ showed strong correlations with several dose-volumetric parameters of H&N plans. The *variance* (d = 1) for Trilogy™, in particular, was correlated with dose-volumetric parameters (with statistical significance) most frequently (*i.e.*, in 17 cases). Neither the textural features nor the conventional modulation indices were correlated with all differences in dose-volumetric parameters. A portion of the fluence map (*i.e.*, not the entire fluence map) is involved in a dose-volumetric parameter for a particular structure; therefore, a textural feature from a VMAT plan may or may not be correlated with a given difference in a dose-volumetric parameter. Although there was no single indicator correlated with all dose-volumetric parameters, *variance* (d = 1) for Trilogy™ had better performance than the others.

The results of pretreatment QA with various gamma criteria showed that the VMAT plans in this study were clinically acceptable in terms of plan deliverability. Consistent with the pretreatment QA results, the differences in modulating parameters for Trilgoy™ showed MLC positional errors of less than 0.8 mm, gantry angle errors of less than 0.4°, and MU differences of less than 0.2, on average; whereas those for TrueBeam™ were smaller, showing MLC positional errors of less than 0.08 mm, gantry angle errors of less than

0.04°, and MU differences of less than 0.01, on average. In addition, the dose-volumetric parameter differences for TrueBeam™ were also minimal for the given prescription dose. The differences in modulating parameters for two machines were calculated using each machine's log files, which have separate log recording systems. Because the dyanlog file of Trilogy™ requires a conversion factor to calculate the actual positions (by multiplying the values from the motor by the conversion factor), whereas the trajectory file for TrueBeam™ directly records the actual position, the accuracy of data acquisition increased. TrueBeam™ has been introduced with improvements in mechanical operation, which increase the accuracy of plan delivery. Gamma passing rates were affected by the spatial resolution of detectors and machine operation for measured dose distribution, and beam commissioning data for calculated dose distribution. As shown in Fig. 8, the gamma criteria of 1%/2 mm is suitable as a tolerance level for patient-specific QA for VMAT when using MapCHECK2 and Gafchromic® EBT3 film. The most stringent criterion in this study, 1%/1 mm, seemed inappropriate, because the original plan had already failed, with passing rates less than the required 90%.

Because no undeliverable VMAT plan was included in this study, we were unable to acquire absolute values of textural features, which indicates that the VMAT plan is undeliverable because of excessive modulation, which is a limitation of this study. The tolerance level of textural features for the detection of undeliverable VMAT plans will be acquired in future work with a larger sample size of VMAT plans, including undeliverable plans. Although the tolerance level was not provided in this study, the feasibility of textural

features as modulation indices for VMAT was identified, showing better performance than the conventional modulation indices. In this study, the values of *contrast* (d = 1) and *variance* (d = 1) for Trilogy™ and *variance* (d = 1) for TrueBeam™ were calculated from clinically acceptable VMAT plans, which ranged from 55 to 432, from 29 to 61, and from 27 to 60, respectively.

The correlations of conventional modulation indices (MCS_v and LTMCS) with pretreatment QA results found in this study showed weaker correlations with the plan deliverability than those of a feasibility study.[9] This result may be due to their different sample sizes, different correlation analysis methods, different TPS systems, different linac systems, or different pretreatment QA systems. In the feasibility study, a total of 142 VMAT plans were analyzed using the Pearson correlation coefficient. However, in this study, a smaller sample size of 40 VMAT plans was analyzed using the Spearman's rank correlation coefficient. The linac, TPS, and pretreatment QA system in the feasibility study were Elekta Synergy (Elekta, Crawley, U.K.), Oncentra MasterPlan VMAT module (ver. 4.1, Nucletron, Elekta, Crawley, U.K.), and Delta4 (Scandidos, Uppsala, Sweden), which are different from those used in this study.[9] Despite the small sample size of 40 VMAT plans, most of the textural features exhibited good correlation (with statistical significance) with the results of pretreatment QA, exhibiting better performance than the conventional modulation indices. As mentioned above, in the future, further analysis utilizing a larger sample of VMAT plans will be performed with various pretreatment QA systems.

In our feasibility study, the textural features were acquired as modulation

indices for only the VMAT plans. Even though the textural features were not applied to IMRT plans in this study, theoretically, there is no reason to restrict the application of texture analysis to the evaluation of modulation degree for IMRT plans, as IMRT also generates fluence maps. However, this analysis was not performed in this study; it will be performed in future work.

The correlations of *ASM* (d = 1) for both Trilogy™ and TrueBeam™ to the plan deliverability were generally weaker than the others, even though they still exhibited comparable correlations (with statistical significance) in some cases. No correlations were observed between *ASM* (d = 1) and the differences in dose-volumetric parameters between original treatment plans and plans reconstructed from log files. *ASM* (d = 1), which represents the overall homogeneity of the fluence map, seemed insensitive in its ability to predict plan deliverability in comparison with the other textural features. Textural features at d = 2 and 3 for TrueBeam™ did not show strong correlations with the plan deliverability, which means those values of d did not reflect the width of MLCs.

The textural features in this study were calculated from a single fluence map from each VMAT plan, which was generated by integrating spatial MU distributions defined by MLC apertures at each CP. Therefore, several small fields at different CPs could be summed, resulting in a large field. In this case, the effect of small fields on the textural features would vanish. Therefore, if we adopt methods to distinguish each of the small fields, the results might differ from those presented in this feasibility study. Although several small fields might smear out in a single fluence map, some textural features

including *contrast* (d = 1) and *variance* (d = 1) for Trilogy™ and *variance* (d = 1) for TrueBeam™ exhibited strong correlations with the plan deliverability in our feasibility study.

However, as mentioned above, the effect of several small or irregular fields on the values of textural features might be smeared out because every MU map was integrated to generate the fluence maps in our feasibility study. Therefore, we doubled the values of the pixels representing MLC tips in a fluence map to identify small or irregular fields in a single fluence map, and performed correlation analysis between the textural features calculated from that fluence map and VMAT delivery accuracy in this study. We generally found stronger correlations of *contrast* (d = 1) for Trilogy™ and *contrast* (d = 10) for TrueBeam™ to VMAT delivery accuracy than those of textural features (and conventional modulation indices) in our feasibility study. By enhancing the values in the region of MLC tips at each CP in a fluence map, we improved the performance of *contrast* (d = 1) for Trilogy™ and *contrast* (d = 10) for TrueBeam™ as a modulation index for VMAT.

As in our feasibility study, the values of *contrast* (d = 1) for Trilogy™ of lowly-modulated VMAT plans (prostate VMAT plans) were higher than those of highly-modulated VMAT plans (H&N VMAT plans).[28] Because of the enhancement of values in the region of MLC tips in this study, values of *contrast* (d = 1) of both prostate and H&N VMAT plans for Trilogy™ increased relative to those calculated with non-enhanced fluence maps. In the case of TrueBeam™, values of *contrast* (d = 10) increased compared to those calculated with non-enhanced fluence maps. The most noticeable

improvements of *contrast* (d = 1) for Trilogy™ and *contrast* (d = 10) for TrueBeam™ by edge-enhancement of fluence maps were observed in the number of statistically significant r_s values for the differences in dose-volumetric parameters (four cases with non-edge-enhancement vs. 11 cases with edge-enhancement).[28] Additionally, the performance improvements of *contrast* (d = 1) for Trilogy™ and *contrast* (d = 10) for TrueBeam™ caused by edge-enhancement were observed in both global and local gamma passing rates for every gamma criterion tested in this study and for all gantry angle errors. Although a lower value of r_s was observed between *contrast* (d = 1) for Trilogy™ and MLC errors by edge-enhancement of fluence maps (-0.853 for edge-enhanced fluence maps vs. -0.863 for non-edge-enhanced fluence maps), *contrast* (d = 1) still showed a strong correlation with MLC errors, with a value higher than 0.8 ($p < 0.001$). Comparing *contrast* (d = 1) with edge-enhancement to *variance* (d = 1) with non-edge-enhancement for Trilogy™, with the exception of correlation with global gamma passing rates at 2%/2 mm, *contrast* (d = 1) with enhancement had stronger correlations than did *variance* (d = 1) with non-enhancement for VMAT delivery accuracy verification.[28] In the case of TrueBeam™, *contrast* (d = 10) with enhancement had stronger correlations than did *variance* (d = 1) with non-enhancement for all methods of VMAT delivery accuracy verification, except for correlation with global gamma passing rates at 2%/1 mm. Because we quantified plan delivery accuracy using various verification methods and the results were not always consistent in this study, similar to the findings of Nelms *et al.* (data are not shown), neither *contrast* (d = 1) for Trilogy™ and *contrast* (d = 10) for

TrueBeam™ nor MI_t consistently showed stronger correlations with the results for all methods of plan delivery accuracy verification.[37] To determine which indicator is superior, further analysis by increasing sample size and collecting various types of samples (VMAT plans generated with various types of TPS, linacs, or treatment sites, and gamma evaluation with various types of detectors) should be performed. This analysis will be performed in future work.

We could not suggest a tolerance level for *contrast* (d = 1) for Trilogy™ and *contrast* (d = 10) for TrueBeam™ with edge-enhanced fluence maps in this study, because the sample size was only 40. Additionally, all of the VMAT plans in this study were clinically acceptable. Because no excessively-modulated VMAT plans that were clinically unacceptable were included in this study, we could not acquire tolerance levels for *contrast* (d = 1) for Trilogy™ and *contrast* (d = 10) for TrueBeam™ to identify clinically unacceptable VMAT plans. As mentioned above, in future work, by enriching samples with various types of VMAT plans and by the inclusion of excessively-modulated VMAT plans, a tolerance level for *contrast* (d = 1) for Trilogy™ and *contrast* (d = 10) for TrueBeam™ with edge-enhanced fluence maps will be created.

The global gamma passing rates with the 2%/2 mm criterion recommended by Heilemann *et al.* for VMAT pretreatment QA were (on average) 98.6% for prostate VMAT plans and 97.0% for H&N VMAT plans.[32] Within this small variation, *contrast* (d = 1) for Trilogy™ and *contrast* (d = 10) for TrueBeam™ with edge-enhanced fluence maps showed good correlations (with statistical

significance) with every type of verification method for VMAT delivery accuracy. Therefore, *contrast* (d = 1) for Trilogy™ and *contrast* (d = 10) for TrueBeam™ with edge-enhanced fluence maps could be used as a modulation index for VMAT; the method might allow the rejection of highly-modulated VMAT plans at the planning stage.

In this study, using the fluence maps calculated using summations of segments at sequential groups of CPs, we calculated the textural features of various fluence maps generated by the summation of sequences of various numbers of MU maps to obtain an optimal textural feature under optimal conditions, *i.e.*, that showing the highest correlation with the plan deliverability. As a result, we found four textural features that showed generally strong correlations (with statistical significance) with every type of plan deliverability, namely, *contrast* (d = 10) with 10 segments for Trilogy™ and *contrast* (d = 10) with 20 segments for TrueBeam™. Specifically, r_s values of the textural features for the MLC errors, which is known to be the most influential factor affecting the plan deliverability of VMAT, were always higher than 0.8 (all with $p < 0.001$).[14, 27, 32] Moreover, these cases showed statistically significant r_s values for the differences in the clinically relevant dose-volumetric parameters between original treatment plans and actual delivery in more than 12 parameters from a total of 35 tested parameters. Because the results of the three types of measurements of plan delivery accuracy were not consistent (as also demonstrated by Nelms *et al.*), it was not possible to suggest a single textural feature that consistently showed the highest correlations with every type of plan deliverability.[37] To review the

results comprehensively, *contrast* (d = 10) with 10 segments for Trilogy™ and *contrast* (d = 10) with 20 segments for TrueBeam™ showed strong correlations with every type of plan delivery accuracy, although they did not always show the highest values of r_s for every type of plan delivery accuracy. However, in the case of Trilogy™, *contrast* (d = 10) with 10 segments showed better performance than the previously suggested textural features, such as *contrast* (d = 1) and *variance* (d = 1) with 356 segments, and conventional modulation indices including MCS_v, LTMCS, and MI_{SPORT}.[28] *Contrast* (d = 10) with 20 segments for TrueBeam™ also showed better performance than the previously suggested textural features.

In this study, *contrast* (d = 10) with 10 and 20 segments and *entropy* (d = 10) with 5 and 10 segments generally showed good performance as modulation indices, as shown in Tables 34, 35, 36, and 37. Because *contrast* measures the local variations in an image, the degree of modulation of VMAT appears to be related to the local variations in the values of each beamlet, that is, MU variations. The prostate VMAT plans, which were low-modulation plans, showed higher values of contrast than did the H&N VMAT plans, which were highly-modulated plans. In addition, the r_s values of contrast with the gamma passing rates were positive values, whereas those to the MLC errors were negative values. As the modulation degree of VMAT increases, the gamma passing rates decrease, whereas MLC errors increase. Therefore, highly-modulated VMAT plans exhibit low local variations in the fluence maps. With the naked eye, the fluence maps of prostate VMAT plans had higher contrast images than were those of H&N VMAT plans (Fig. 13). The

optimal condition for the contrast to obtain the best performance was a *d* value of 10 with fluence maps generated by summations of 10 segments. As shown in Table 11, *contrast* showed generally good performance as a modulation index when it was calculated based on the fluence maps generated by summations of less than 20 segments. The summation of large numbers of MU maps to generate fluence maps, which makes the degree of local variations low (Fig. 5), was not good for predicting modulation degree of VMAT with *contrast*. In the case of *entropy*, although it had inferior performance to *contrast*, good correlations between *entropy* and the plan delivery accuracy were observed, as shown in Tables 8, 9, and 10. Moreover, *entropy* also showed generally better performance than the previously suggested modulation indices.[17] Because the *entropy* measures the randomness of images,[24] the modulation degree of VMAT plans is also related to the random variations of MU in a fluence. As the modulation degree of VMAT increased, the value of *entropy* also increased. The prostate VMAT plans had lower values of *entropy* (d = 10) with 5 and 10 segments than did H&N VMAT plans, with statistical significance ($p < 0.001$). The *entropy* also had better performance with fluence maps generated by summation of a small number of segments, similar to the results of *contrast*. In addition to *contrast* and *entropy*, the tendency of higher correlations of textural features that were calculated using fluence maps generated by summations of a small number of segments is clearly shown in the results of differences in dose-volumetric parameters between plan and delivery, as shown in Figs. 9 and 10. The total number of statistically significant dose-volumetric parameters with 5, 10, 20,

45, 90, 178, and 356 segments was 116, 121, 111, 32, 45, 46, and 54, respectively. Smearing out of certain textural characteristics in the fluence by increasing the number of segments might weaken the textural features' predictive power for modulation degree of VMAT. According to the results in this study, the threshold number of neighboring segments to be summed for the generation of fluence maps could be 20 for high sensitivity in the prediction of the plan delivery accuracy of VMAT.

In agreement with Nelms *et al.*,[37] no strong correlation was observed between gamma passing rates and the differences in clinically relevant dose-volumetric parameters. Consequently, various textural features sometimes showed strong correlations with the gamma passing rates while showing weak correlations with the differences in the dose-volumetric parameters or vice versa. However, several textural features such as *contrast* (d = 1 with 20 segments and d = 10 with 5, 10, and 20 segments) showed relatively strong correlations with both gamma passing rates and differences in dose-volumetric parameters. Moreover, these features showed strong correlations with the mechanical parameter differences, which are more direct indicators of plan delivery accuracy. Although a high score in a particular verification method for plan delivery accuracy does not guarantee a perfect match between plan and delivery, in the case of high conformity of planned and delivered plans, the score of plan delivery accuracy of each type of verification method should be high. In the same vein, if there is a VMAT plan that has a poor match between plan and delivery, the score of every type of verification method will be low. Therefore, if there is an ideal indicator that

could identify the plan delivery accuracy, it should show perfect correlations with the results of each method used to verify the plan delivery accuracy. In this study, *contrast* (d = 10) with 10 segments for Trilogy™ and *contrast* (d = 10) with 20 segments for TrueBeam™ showed strong correlations (with statistical significance) with all methods for verifying plan delivery accuracy.

We could not recommend a tolerance level for *contrast* (d = 10) with 10 segments for Trilogy™ and *contrast* (d = 10) with 20 segments for TrueBeam™ to identify clinically unacceptable VMAT plans, because no clinically unacceptable VMAT plans were included in the analyzed samples. In addition, the sample size of 40 was insufficient to recommend a tolerance level. Further study by utilizing more samples including heavily modulated and clinically unacceptable VMAT plans will be performed to obtain a tolerance level for *contrast* (d = 10) with 10 segments for Trilogy™ and *contrast* (d = 10) with 20 segments for TrueBeam™ in future work. To obtain a tolerance level, the study sample size must be increased, and investigation with various types of TPS, linacs, and measurement systems should be performed.

As mentioned above, the differences in dose distributions between plan and delivery of VMAT are caused by mechanical uncertainties in linac parts, especially in MLCs, and inaccurate calculation of small or irregular fields by commercial TPS.[14, 18, 27] Park *et al.* showed the correlations of drastic movement of MLCs with the plan delivery accuracy, suggesting MI_t, which was focused only on the mechanical uncertainty of linac parts during delivery.[27] However, texture analysis of fluence could simultaneously

consider both mechanical uncertainty and small or irregular field usage. If the size and shape of MU maps were small or irregular, the textural characteristics of fluence would be changed, resulting in changes in the values of textural features. In the case of mechanical uncertainty of MLCs, textural features could identify drastic movements of MLCs, as every beamlet represents an MU delivered by the MLC movements. If the variation in MU between adjacent beamlets increases, which means a drastic movement of MLCs occurred, the values of textural features would be changed.

In the clinic, in addition to routine periodic QA for linac performance, which is generally based on American Association of Physicists in Medicine (AAPM) Task Group (TG) 40[38] or TG-142 protocol[39], pretreatment QA is performed for each patient who is treated with IMRT or VMAT techniques. In this study, we suggested a textural feature, *contrast* (d = 10) with 10 segments for Trilogy™ and *contrast* (d = 10) with 20 segments for TrueBeam™, to quantify the modulation degree for VMAT. Because the mechanical performance of a linac is verified with periodic QA in the clinic, this indicator has the potential to be used as a substitute for pretreatment QA. Because *contrast* can be calculated immediately after plan generation, it could save the resources used to perform pretreatment QA. Furthermore, this technique could expedite the process of patient treatment. Because the VMAT plans in this study were all clinically acceptable plans, the variations in the values of the plan delivery accuracy were small. *contrast* (d = 10) with 10 segments for Trilogy™ and *contrast* (d = 10) with 20 segments for TrueBeam™ showed

strong correlations (with statistical significance) to all measurements of plan delivery accuracy.

CONCLUSIONS

In this study textural features were calculated with fluence maps generated from prostate and H&N VMAT plans to evaluate the degree of modulation of each plan. The performances of textural features as indicators for the modulation degree of VMAT plans were tested with Spearman's rank correlation analysis and compared to conventional modulation indices. For textural features calculated from a single fluence map, the *contrast* (d = 1) and *variance* (d = 1) for Trilogy™ and *variance* (d = 1) for TrueBeam™ showed considerable correlations with both the results of pretreatment QA, and the differences in dose-volumetric parameters between original plans and reconstructed plans using log files. These values showed higher correlations than the conventional modulation indices in every case. The sensitivity and specificity of the textural features with the pretreatment QA results were also better than those of the conventional modulation indices. It seems *contrast* (d = 1) and *variance* (d = 1) for Trilogy™ and *variance* (d = 1) for TrueBeam™ are promising modulation indices for VMAT plans in our feasibility study.

Contrast (d = 1) for Trilogy™ *contrast* (d = 10) for TrueBeam™ calculated from fluences with enhancement of values at the tips of MLCs to prevent potential smearing out of small or irregular fields showed considerable correlations with statistical significances to gamma passing rates, mechanical errors during delivery and differences in dose-volumetric parameters between plan and delivery of VMAT.

In this final study with textural features calculated from segmental fluence maps, we investigated textural features of fluence maps to search for a

modulation index showing strong correlations to the plan delivery accuracy of VMAT. *Contrast* (d = 10) with 10 segments for Trilogy™ and The *contrast* (d = 10) with 20 segments for TrueBeam™ showed strong correlations with statistical significances to all types of measured plan deliverability. *Contrast* (d = 10) with 10 segments for Trilogy™ and The *contrast* (d = 10) with 20 segments for TrueBeam™ showed higher correlations to the plan delivery accuracy than did conventional modulation indices for VMAT, including MCS_v, LTMCS and MI_{SPORT}, as well as *contrast* (d = 1) and *variance* (d = 1) for Trilogy™ and *variance* (d = 1) for TrueBeam™ with 356 segments, and *Contrast* (d = 1) for Trilogy™ *contrast* (d = 10) for TrueBeam™ with edge-enhancement, which were textural features suggested as modulation indices. It seems that *Contrast* (d = 10) with 10 segments for Trilogy™ and The *contrast* (d = 10) with 20 segments for TrueBeam™ has the potential to be used to verify VMAT delivery accuracy as a modulation index.

REFERENCES

[1]A. Brahme, J. E. Roos and I. Lax, "Solution of an integral equation e ncountered in rotation therapy," Physics in medicine and biology **27**, 12 21-1229 (1982).

[2]G. A. Ezzell, J. M. Galvin, D. Low, J. R. Palta, I. Rosen, M. B. Shar pe, P. Xia, Y. Xiao, L. Xing, C. X. Yu, I. subcommitte and A. R. T. committee, "Guidance document on delivery, treatment planning, and cli nical implementation of IMRT: report of the IMRT Subcommittee of th e AAPM Radiation Therapy Committee," Medical physics **30**, 2089-211 5 (2003).

[3]K. Otto, "Volumetric modulated arc therapy: IMRT in a single gantry arc," Medical physics **35**, 310-317 (2008).

[4]J. M. Park, J. I. Kim, C. Heon Choi, E. K. Chie, I. H. Kim and S. J. Ye, "Photon energy-modulated radiotherapy: Monte Carlo simulation an d treatment planning study," Medical physics **39**, 1265-1277 (2012).

[5]C. Wu, K. E. Hosier, K. E. Beck, M. B. Radevic, J. Lehmann, H. H. Zhang, A. Kroner, S. C. Dutton, S. A. Rosenthal, J. K. Bareng, M. D. Logsdon and D. R. Asche, "On using 3D gamma-analysis for IMRT a nd VMAT pretreatment plan QA," Medical physics **39**, 3051-3059 (201 2).

[6]M. Yu, H. S. Jang, D. M. Jeon, G. S. Cheon, H. C. Lee, M. J. Chun g, S. H. Kim and J. H. Lee, "Dosimetric evaluation of Tomotherapy an d four-box field conformal radiotherapy in locally advanced rectal cance r," Radiation oncology journal **31**, 252-259 (2013).

[7]N. Giorgia, F. Antonella, V. Eugenio, C. Alessandro, A. Filippo and C. Luca, "What is an acceptably smoothed fluence? Dosimetric and delive ry considerations for dynamic sliding window IMRT," Radiation oncolog y **2**, 42 (2007).

[8]R. Li and L. Xing, "An adaptive planning strategy for station paramete

r optimized radiation therapy (SPORT): Segmentally boosted VMAT," Medical physics **40**, 050701 (2013).

[9]L. Masi, R. Doro, V. Favuzza, S. Cipressi and L. Livi, "Impact of pla n parameters on the dosimetric accuracy of volumetric modulated arc th erapy," Medical physics **40**, 071718 (2013).

[10]C. K. McGarry, C. D. Chinneck, M. M. O'Toole, J. M. O'Sullivan, K. M. Prise and A. R. Hounsell, "Assessing software upgrades, plan prop erties and patient geometry using intensity modulated radiation therapy (IMRT) complexity metrics," Medical physics **38**, 2027-2034 (2011).

[11]A. L. McNiven, M. B. Sharpe and T. G. Purdie, "A new metric for a ssessing IMRT modulation complexity and plan deliverability," Medical physics **37**, 505-515 (2010).

[12]R. Mohan, M. Arnfield, S. Tong, Q. Wu and J. Siebers, "The impact of fluctuations in intensity patterns on the number of monitor units an d the quality and accuracy of intensity modulated radiotherapy," Medica l physics **27**, 1226-1237 (2000).

[13]M. Nauta, J. E. Villarreal-Barajas and M. Tambasco, "Fractal analysis for assessing the level of modulation of IMRT fields," Medical physics **38**, 5385-5393 (2011).

[14]G. Nicolini, A. Clivio, L. Cozzi, A. Fogliata and E. Vanetti, "On the impact of dose rate variation upon RapidArc implementation of volumet ric modulated are therapy," Medical physics **38**, 264-271 (2011).

[15]M. Tambasco, I. Nygren, E. Yorke-Slader and J. E. Villarreal-Barajas, "FracMod: a computational tool for assessing IMRT field modulation," Physica medica : PM : an international journal devoted to the applicati ons of physics to medicine and biology : official journal of the Italian Association of Biomedical Physics **29**, 537-544 (2013).

[16]S. Webb, "A simple method to control aspects of fluence modulation in IMRT planning," Physics in medicine and biology **46**, N187-195 (20 01).

[17]S. Webb, "Use of a quantitative index of beam modulation to characte rize dose conformality: illustration by a comparison of full beamlet IM

RT, few-segment IMRT (fsIMRT) and conformal unmodulated radiothera py," Physics in medicine and biology **48**, 2051-2062 (2003).

[18]W. Du, S. H. Cho, X. Zhang, K. E. Hoffman and R. J. Kudchadker, "Quantification of beam complexity in intensity-modulated radiation ther apy treatment plans," Medical physics **41**, 021716 (2014).

[19]J. Llacer, T. D. Solberg and C. Promberger, "Comparative behaviour o f the dynamically penalized likelihood algorithm in inverse radiation the rapy planning," Physics in medicine and biology **46**, 2637-2663 (2001).

[20]G. Nicolini, A. Fogliata and L. Cozzi, "IMRT with the sliding windo w: comparison of the static and dynamic methods. Dosimetric and spect ral analysis," Radiotherapy and oncology : journal of the European Soci ety for Therapeutic Radiology and Oncology **75**, 112-119 (2005).

[21]D. Assefa, H. Keller, C. Menard, N. Laperriere, R. J. Ferrari and I. Yeung, "Robust texture features for response monitoring of glioblastoma multiforme on T1-weighted and T2-FLAIR MR images: a preliminary i nvestigation in terms of identification and segmentation," Medical physic s **37**, 1722-1736 (2010).

[22]B. Ganeshan, K. A. Miles, R. C. Young and C. R. Chatwin, "Texture analysis in non-contrast enhanced CT: impact of malignancy on texture in apparently disease-free areas of the liver," European journal of radio logy **70**, 101-110 (2009).

[23]P. W. Huang and C. H. Lee, "Automatic classification for pathological prostate images based on fractal analysis," IEEE transactions on medic al imaging **28**, 1037-1050 (2009).

[24]E. Scalco, C. Fiorino, G. M. Cattaneo, G. Sanguineti and G. Rizzo, " Texture analysis for the assessment of structural changes in parotid glan ds induced by radiotherapy," Radiotherapy and oncology : journal of th e European Society for Therapeutic Radiology and Oncology **109**, 384-3 87 (2013).

[25]X. Yang, S. Tridandapani, J. J. Beitler, D. S. Yu, E. J. Yoshida, W. J. Curran and T. Liu, "Ultrasound GLCM texture analysis of radiation-i nduced parotid-gland injury in head-and-neck cancer radiotherapy: an in

vivo study of late toxicity," Medical physics **39**, 5732-5739 (2012).

[26]S. A. Mattonen, D. A. Palma, C. J. Haasbeek, S. Senan and A. D. Ward, "Early prediction of tumor recurrence based on CT texture chang es after stereotactic ablative radiotherapy (SABR) for lung cancer," Med ical physics **41**, 033502 (2014).

[27]J. M. Park, S. Y. Park, H. Kim, J. H. Kim, J. Carlson and S. J. Ye, "Modulation indices for volumetric modulated arc therapy," Physics in medicine and biology **59**, 7315-7340 (2014).

[28]S. Y. Park, I. H. Kim, S. J. Ye, J. Carlson and J. M. Park, "Texture analysis on the fluence map to evaluate the degree of modulation for volumetric modulated arc therapy," Medical physics **41**, 111718 (2014).

[29]E. Vanetti, G. Nicolini, J. Nord, J. Peltola, A. Clivio, A. Fogliata and L. Cozzi, "On the role of the optimization algorithm of RapidArc((R)) volumetric modulated arc therapy on plan quality and efficiency," Med ical physics **38**, 5844-5856 (2011).

[30]P. Gong, D. J. Marceau and P. J. Howarth, "A Comparison of Spatial Feature-Extraction Algorithms for Land-Use Classification with Spot Hr v Data," Remote Sens Environ **40**, 137-151 (1992).

[31]J. E. Rodgers, A. Niroomand-Rad and M. Lundsten, "Comment on cli nical implementation of the AAPM's Task Group-51 protocol for calibra tion of high-energy photon and electron beams," Medical physics **27**, 19 95-1996 (2000).

[32]G. Heilemann, B. Poppe and W. Laub, "On the sensitivity of common gamma-index evaluation methods to MLC misalignments in Rapidarc q uality assurance," Medical physics **40**, 031702 (2013).

[33]I. Iftimia, E. T. Cirino, L. Xiong and H. W. Mower, "Quality assuran ce methodology for Varian RapidArc treatment plans," Journal of applie d clinical medical physics / American College of Medical Physics **11**, 3 164 (2010).

[34]A. M. Gloi, R. E. Buchanan, C. L. Zuge and A. M. Goettler, "Rapid Arc quality assurance through MapCHECK," Journal of Applied Clinical Medical Physics **12**, 39-47 (2011).

[35]A. Fredh, J. B. Scherman, L. S. Fog and P. Munck af Rosenschold, " Patient QA systems for rotational radiation therapy: a comparative exper imental study with intentional errors," Medical physics **40**, 031716 (201 3).

[36]W. van Elmpt, S. Nijsten, B. Mijnheer, A. Dekker and P. Lambin, "T he next step in patient-specific QA: 3D dose verification of conformal and intensity-modulated RT based on EPID dosimetry and Monte Carlo dose calculations," Radiotherapy and oncology : journal of the Europea n Society for Therapeutic Radiology and Oncology **86**, 86-92 (2008).

[37]B. E. Nelms, H. Zhen and W. A. Tome, "Per-beam, planar IMRT QA passing rates do not predict clinically relevant patient dose errors," Me dical physics **38**, 1037-1044 (2011).

[38]G. J. Kutcher, L. Coia, M. Gillin, W. F. Hanson, S. Leibel, R. J. Mo rton, J. R. Palta, J. A. Purdy, L. E. Reinstein, G. K. Svensson and et al., "Comprehensive QA for radiation oncology: report of AAPM Radiat ion Therapy Committee Task Group 40," Medical physics **21**, 581-618 (1994).

[39]E. E. Klein, J. Hanley, J. Bayouth, F. F. Yin, W. Simon, S. Dresser, C. Serago, F. Aguirre, L. Ma, B. Arjomandy, C. Liu, C. Sandin and T. Holmes, "Task Group 142 report: quality assurance of medical accelera tors," Medical physics **36**, 4197-4212 (2009).

국문 초록

서론: 본 연구의 목표는 최신 방사선치료 기법인 용적변조회전 방사선치료(Volumetric modulated arc therapy, VMAT)에서, 환자치료 정확도를 플루언스 분포도의 질감분석(Texture analysis)을 통하여 검증하는 것이다.

방법: Millennium MLC 를 갖춘 Trilog^{TM} (Varian Medical Systems, Palo Alto, CA, USA) 에서 VMAT 을 받는 20 명의 전립선 암 환자와 20 명의 두경부 암 환자를 대상으로 선정되었다. 각 VMAT 에 대한 플루언스 분포도는 (1) 각 control point (CP) 에서 다엽콜리메이터 (Multi-leaf collimator, MLC)의 조사면에 의해 정의된 공간 monitor unit (MU) 분포를 통합하는 방법, (2) MLC 의 조사면 가장자리를 나타내는 MU 를 두 배로 하여 통합하는 방법 그리고 (3) CP 에 따라 플루언스 분포도를 분절시켜 통합하는 방법을 이용하여 얻어졌다. 각각의 플루언스 분포도를 이용하여 *angular second moment* (*ASM*), *inverse difference moment* (*IDM*), *contrast*, *variance*, *correlation*, *entropy* 라는 총 6 가지의 질감분석 파라미터를 계산하였다. 특정한 변위 거리 *d* (displacement distance) 1, 5, 10 에 대하여 각각의 질감분석 파라미터를 계산하였다. VMAT 의 환자치료 정확도를 평가하기 위해서 치료 전 정도관리 (Quality assurance, QA)의 지표인 gamma

passing rate 와 dynamic log file 과 VMAT 치료 계획 간의 MLC, gantry 각도, MU 와 같은 변조 파라미터 차이, dynamic log file 을 이용하여 복원된 치료 계획과 VMAT 치료 계획 간의 선량체적 파라미터 차이를 얻었다. VMAT 의 변조 정도에 대한 지표로 질감분석 파라미터의 성능을 테스트하기 위해, Spearman's rank correlation coefficients (r_s)를 계산 하였다. 비교를 위해, VMAT 의 기존 변조 지수인 MCS_v 와 LTMCS, MI_{SPORT} 를 계산하였고 각각의 상관 관계는 동일한 방식으로 분석 하였다.

Millennium MLC 를 갖춘 Trilog™ 에서 수행 된 동일한 20 명의 전립선 암 환자와 20 명의 두경부 암 환자에 대해서 High-definition MLC 를 갖춘 TrueBeam™ (Varian Medical Systems, Palo Alto, CA, USA)을 이용하여 VMAT 치료 계획을 세웠고 치료 전 QA 의 지표인 gamma passing rate 와 변조 파라미터 차이, 선량체적 파라미터 차이를 얻었다. 플루언스 분포도와 6 가지의 질감분석 파라미터를 다른 변위 거리 d 인 1, 2, 3, 5, 10 을 이용하여 계산하였고 각각의 상관 관계는 동일한 방식으로 분석 하였다.

결과: (1) 각 CP 에서 MLC 의 조사면에 의해 정의된 공간 MU 분포를 통합하는 방법을 이용한 단일 플루언스 분포도를 이용한 연구에서는 모든 환자치료 정확도와 항상 높은 상관 관계를 가지는 질감분석 파라미터는 없었다. 종합적으로 고려해본 결과, Trilogy™ 의 *contrast* (d = 1), *variance* (d = 1) 와 TrueBeam™ 의 *variance*

(d = 1)가 일반적으로 모든 환자치료 정확도 유형에 상당한 상관관계를 보였다. 이러한 질감분석 파라미터는 변조 파라미터 차이의 경우를 제외하고 기존 변조 지수보다 항상 더 좋은 성능을 나타내었다. 2%/2mm, 2%/1 mm, 1%/2 mm 의 기준을 가지는 global gamma passing rate 와 Trilogy™ 의 *contrast* (d = 1)의 r_s 는 0.563, 0.473, 0.718 이였다. Trilogy™의 *variance* (d = 1)의 r_s 는 각각 0.551, 0.481, 0.688 이였으며 TrueBeam™ 의 *variance* (d = 1)의 r_s는 각각 0.662, 0.740, 0.660 이였다. Local gamma passing rate 의 경우, Trilogy™ 의 *contrast* (d = 1)의 r_s 는 0.547, 0.578, 0.620 이였다. Trilogy™의 *variance* (d = 1)의 r_s 는 각각 0.519, 0.527, 0.569 이였으며 TrueBeam™ 의 *variance* (d = 1)의 r_s는 각각 0.403, 0.616, 0.443 이였다. 이러한 경우 모든 r_s 값은 통계적으로 유의하였다 (p < 0.004). MLC 오차에 대한 Trilogy™의 *contrast* (d = 1), *variance* (d = 1) 와 TrueBeam™ 의 *variance* (d = 1)의 r_s 는 각각 통계적 유의성 (p < 0.001)을 가지며 −0.863, −0.828, −0.822 이였다. 이 질감분석 파라미터는 통계적인 유의성을 보이며 선량체적 파라미터 차이에 대한 r_s 을 보였다.

(2) MLC 의 조사면 가장자리를 나타내는 MU 를 두 배로 하여 통합하는 방법을 이용한 윤곽 강조 플루언스 분포도를 이용한 연구에서는 Trilogy™ 의 *contrast* (d = 1)와 2%/2mm, 2%/1 mm,

1%/2 mm 의 기준을 가지는 global gamma passing rate 의 r_s 값은 각각 0.546 ($p < 0.001$), 0.487 ($p = 0.001$), 0.744 ($p < 0.001$) 이였고, TrueBeam™ 의 *contrast* ($d = 10$)의 r_s 값은 각각 0.705, 0.703 and 0.701 (모든 경우 $p < 0.001$)이였다. Trilogy™ 의 *contrast* ($d = 1$)와 local gamma passing rate 의 r_s 값은 각각 0.588, 0.644, 0.640 (모든 경우 $p < 0.001$) 이였고, TrueBeam™ 의 *contrast* ($d = 10$)의 r_s 값은 각각 0.459 ($p < 0.001$), 0.700 ($p < 0.001$) and 0.522 ($p = 0.001$)이였다. MLC 와 gantry 각도 차이에 대한 Trilogy™ 의 *contrast* ($d = 1$)의 r_s 값은 각각 −0.853, 0.655 이였고 (모든 경우 $p < 0.001$), TrueBeam™ 의 *contrast* ($d = 10$)의 r_s 값은 각각 were −0.722 ($p < 0.001$) and 0.333 ($p = 0.036$)이였다. Trilogy™ 의 *contrast* ($d = 1$)와 TrueBeam™ 의 *contrast* ($d = 10$)는 총 35 가지의 선량체적 파라미터 차이 중에 각각 11 개, 4 개로 유의한 r_s 값을 보였다. 그것은 기존 변조 지수뿐만 아니라 이전에 제안된 비 윤곽 강조 플루언스 분포도의 질감분석 파라미터 기능보다 환자치료 정확도와의 상관관계에서 더 나은 성능을 보여주었다.

(3) CP 에 따라 플루언스 분포도를 분절시켜 통합하는 방법을 이용한 윤곽 강조 플루언스 분포도를 이용한 연구에서는 Trilogy™ 의 *contrast* ($d = 1$) with 10 segments 와 1%/2 mm 의 기준을 가지는 global 과 local gamma passing rate 와의 r_s 값은 각각 0.692,

0.798 이였다 (모든 경우 $p < 0.001$). MLC 와 gantry 각도 차이에 대한 r_s 값 또한 각각 −0.895, 0.727 이였다 (모든 경우 $p < 0.001$). 선량체적 파라미터 차이에 대한 r_s 값의 개수 ($p < 0.05$)는 35 개의 선량체적 파라미터 합계 중에 14 개였다. TrueBeam™ 의 *contrast* ($d = 10$) with 20 segments 와 1%/2 mm 의 기준을 가지는 global 과 local gamma passing rate 와의 r_s 값은 각각 0.839, 0.738 이였다 (모든 경우 $p < 0.001$). MLC 와 gantry 각도 차이에 대한 r_s 값 또한 각각 −0.881, 0.569 이였다 (모든 경우 $p < 0.001$). 선량체적 파라미터 차이에 대한 r_s 값의 개수 ($p < 0.05$)는 35 개의 선량체적 파라미터 합계 중에 8 개였다.

결론: VMAT 의 분절된 플루언스 분포도에서 얻어진 Trilogy™ 의 *contrast* ($d = 1$) with 10 segments 와 TrueBeam™ 의 *contrast* ($d = 10$) with 20 segments 는 환자치료 정확도와의 상당한 상관관계를 보였고 이는 용적변조회전 방사선치료에서 환자치료 정확도를 평가하기 위한 지표로 사용될 수 있을 것이다.

주요어 : 질감 분석, 용적변조회전 방사선치료, 환자치료 정확도, 플루언스 분포도, 상관 관계 분석
학 번 : 2012-30574